
**ADDIS ABABA UNIVERSITY**

**ADDIS ABABA INSTITUTE OF TECHNOLOGY (AAiT)**

**SCHOOL OF CIVIL AND ENVIRONMENTAL ENGINEERING**

**Post Graduate Studies in Geodesy and Geomatics Engineering**

# Reconstruction of Digital 3D City Model Using Geomatics Technique. A Case Study in AAiT Campus of AAU.

**By:**

**Degu Tadesse Sendekie**

June 17, 2022

AAiT, Addis Ababa, Ethiopia

# Reconstruction of Digital 3D City Model Using Geomatics Technique. A Case Study in AAiT Campus of AAU.

By

Degu Tadesse Sendekie

(GSR/3885/12)

Supervised By: Dr. Getachew Tesfaye

Thesis Submitted to the School of Civil and Environmental Engineering – AAiT, Addis Ababa University, in partial fulfillment of the requirement for the degree of master of science in Geodesy and Geomatics Program, Specialization: Geomatics Engineering.

June 17, 2022

AAiT, Addis Ababa, Ethiopia

***This thesis work is dedicated to my parents, especially my father who was an unending source of inspiration and forever will be.***

# Approval Sheet

*Reconstruction of Digital 3D City Model Using Geomatics Technique. A Case Study in AAiT Campus of AAU*

## Approval Sheet

We the undersigned members have examined the thesis entitled "**Reconstruction of Digital 3D City Model Using Geomatics Technique. A Case Study in AAiT Campus of AAU.**" Presented by Degu Tadesse Sendekie. Therefore, it is certified that the thesis is worthy of acceptance in partial fulfillment of the requirement of Degree of Master of Science in Geodesy and Geomatics engineering.

Approved by Board of Examiners:

| | | |
|---|---|---|
| 1. Dr. Getachew Tesfaye<br>Advisor | Signature | 17/06/2022<br>Date |
| 2. DR. K. V. SURYABHAGAVAN<br>External Examiner | Signature | 13. 06. 2022<br>Date |
| 3. Sintayehu A.<br>Internal Examiner | Signature | 17/06/2022<br>Date |
| 4. _____<br>Chairman | _____<br>Signature | _____<br>Date |

Mebruk Mohammed (Dr.-Ing.)
Dean, School of Civil & Environmental Engineering

Director of Postgraduate Program
Addis Ababa University
Addis Ababa Institute of Technology

i

## Authorship Declaration

I declare that the research work titled "Reconstruction of Digital 3D City Model Using Geomatics Technique. A Case Study in AAiT Campus of AAU." has been prepared following academic rules and ethical conduct. This work is original except as indicated by reference in the text. No part of the dissertation has been submitted and examined for any other degree at any other University.

Author Name: Degu Tadesse Sendekie

Signature: _____ Date _____

This thesis has been prepared under my supervision and submitted for evaluation with my approval as well.

Name of Advisor: Dr. Getachew Tesfaye

Signature: _____ Date: _____

## Acknowledgments

First and foremost, kudos to God of Israel (JEHOVA) for all the blessings I've received as well as for enabling the completion of this work.

I would like to express my gratitude and thanks to my thesis mentor Dr. Getachew Tesfaye for his encouragement and willingness to help during the selection of this research topic, and later on for his valuable critical review, criticism, and advice during the process of writing this thesis. This research would not be in its current shape without his valuable comments.

Kudos to the Geospatial information institute of Ethiopia (GI2) for granting me a sponsorship to study this program and providing me with the required input dataset for this research work. My special thanks also extend to Addis Ababa Institute of Technology (AAiT), School of Civil and Environmental Engineering for their financial support which was pivotal to running this thesis work.

My many thanks to colleagues working at GI2, naming all here is not possible. Specifically, I wish to acknowledge the contribution of the photogrammetric processing and production working group, for their timely support and willingness to help during the research work.

I will be forever grateful to my family and family-in-law for all their support, encouragement, prayer, and everything they provided me throughout this journey.

Finally, I would like to acknowledge all my geodesy and Geomatics engineering instructors (crossed in both my BSC and MSc study), for their great contribution to developing my knowledge and skill that makes me competitive for future jobs and education.

Degu Tadesse Sendekie

2022 G.C.

# Table of Contents

# List of Tables

# List of Figures

# List of Abbreviation Terms

**2D** – 2Dimensional

**3D** – 3Dimensional

**3DCityDB** – 3-Dimensional City Database

**3DCM** – 3-Dimensional City Model

**AAiT** – Addis Ababa Institute of Technology

**AAT** – Automatic Aerial Triangulation

**AAU** – Addis Ababa University

**AGL** – Above Ground Level

**AMSL** – Above Mean Sea Level

**arc-min –** Arc Minute

**BIM** – Building Information Model

**CAD** – Computer-Aided Design

**CCD** – Charge Coupled Device

**CID** – Common Identification

**CityGML** – City Geography Markup Language

**CORS** – Continuously Operating Reference Stations

**DEM** – Digital Elevation Model

**DIM** – Dense Image Matching

**DOM** – Digital Orthophoto Map

**DSM** – Digital Surface Model

**DTM** – Digital Terrain Model

**EGM08** – Earth Gravity Model 2008

**EO** – Exterior Orientation

**FBM** – Feature-Based Matching

**FMS** – Flight Management Software

**GCP** – Ground Control Point

**GERD** – Great Ethiopian Renaissance Dam

**GI2** – Geospatial Information Institute

**GNSS** – Global Navigation Satellite System

**GPS** – Global Positioning System

**GSM** – Gyro Stabilization Mount

**IMU** – Inertial Measurement Unit

**IO** – Interior Orientation

**Lat** – Latitude

**LiDAR** – Light Detection and Ranging

**LOD** – Levels of Detail

**Lon** – Longitude

**LSM** – Least Square Matching

**M** – Meter

**NAV** – Navigation Message

**nDSM** – Normalized Digital Surface Model

**NIR** – Near-Infrared Region

**NVA** – Non-Vegetated Accuracy

**OGC** – Open Geospatial Consortium

**OPUS** – Online Positioning User Service

**OSM** – OpenStreetMap

**POS** – Position and Orientation

**POS AV** – Position and Orientation System for Airborne Vehicles

**POSPac MMS** – Position and Orientation System Postprocessing Package (POSPac™) Mobile Mapping Suite (MMS™)

**PPM** – Parts Per Million

**PPP** – Precise Point Positioning

**RGBI** – Red, Green, Blue, and Infrared

**RINEX** – Receiver Independent Exchange

**RMSE** – Root Mean Square Error

**SBET** – Smoothed Best Estimate of Trajectory

**UTC –** Universal Time Coordinated

**UTM –** Universal transverse Mercator

**XML –** Extensible Markup Language

# Abstract

Despite the real world we live in is considered to be represented by 3-dimension, 2D representations which neglect the third dimension were implemented to archive, plan, administer, analyze and describe the complex physical structure of the earth's surface. Thus, an extended representation technique that considers all the complexity such as 3D city modeling is emerged. A 3D city model (3DCM) is a georeferenced tridimensional digital model of the actual complex urban environment that animates all relevant urban spatial objects located above, on, or below the topographic surface integrated with their non-spatial information. The 3DCM is an important tool used in the domain of 3D cadastre, virtual reality, tridimensional spatial analyses, infrastructure planning, real-estate marketing, tourism, as well as for entertainment, and education. The 3DCM of the urban environment can be reconstructed by several technologies, the geomatics technique is there at the front of the queue. This research study is aimed to reconstruct a digital 3DCM using the geomatics technique specifically based on the photogrammetric techniques to be used as a data source as well as its data processing pipelines have been explored and tested. Thus, for this research direct georeferenced aerial photographs with aerial camera parameters with Ground control points were processed using the Inpho photogrammetry software tool that goes from automatic aerial triangulation, dense-image matching, and product generation. Thus, a photogrammetric point cloud with a density of 100 points/meter square, DTM, and a digital orthophoto map (DOM) were derived. Moreover, the accuracy of these photogrammetric products was assessed by independent checkpoints and hence obtained RMSE values in the range of a single-pixel for planimetric (x, y) dimension (aerial triangulation and DOM) and 2pixel vertical accuracy(z) that meets the standard error budget set by ASPRS for the highest accuracy geospatial data production, analysis and modeling purpose. Furthermore, File geodatabase has been developed to be used as a central data storage container and thus 2D features with their attribute information, normalized digital surface model (nDSM), DSM, DTM, DOM, and other available datasets were extracted and stored within it. From these datasets, the 3DCM at two levels of detail (LOD1 & LOD2) has been reconstructed. Consequently, this study showed that cost-effective reconstruction of 3DCM of the existing urban structure can be done from a couple of 2D nadir-looking photographs with a straightforward photogrammetric processing pipeline. The results are presented in the case of the 5-kilo (AAiT) campus area of AAU.


**Keywords**: **3D city model, Geomatics techniques, aerial photogrammetry, Levels of Detail (LODs), nDSM.**

# CHAPTER 1: INTRODUCTION

## 1.1 Background

In Geospatial science the real world we live in is agreed to be represented in 3-dimensions and spatial features on it exist in three dimensions described by their planimetric dimension (X or Easting, Y or Northing) and the vertical dimension (Z) which represent the elevation of an object or natural terrain above or below a certain reference datum. However, the archival, visualization, interpretation, and analysis of the 3D world, as well as surface objects on it have been done by 2D abstraction, which is inadequate contemporarily. Further, the acceleration of urban growth both in size and complexity (such as buildings with many stories, different roof geometry, material types, colors, etc.) and the inefficiency of the 2D map to accommodate these structures as well as its incapability to solve problems related to urbanism leads to a shift of focus to more extended modeling i.e., modeling of the above-ground and below-ground surfaces. In this sense, research interest for new context mapping (3D modeling) has raised significantly in recent years to develop a desirable system that meets the demand of the urban ecosystem and can store, handle, manipulate, and analyze urban spatial objects in a 3D environment, and hence 3D city modeling is emerged (Döllner et al., 2006).

A Three-dimensional city model (3DCM) is a computerized or digital, mathematically defined, and exact virtual copy (digital replica) of the existing spatial objects within the city(Nikola & Temenoujka, 2019; Stoter et al., 2021; Tunc et al., 2004). It could be a snapshot of the current city-state (Danilina et al., 2018) which can be used to present, manage, explore and analyze the urban geoinformation (Singla & Padia, 2020). The term 3D city model is composed of three keywords and can be described as; 3D refers to the representation of the three-dimensional world where objects are defined by their geographical 3D space; City refers to urban areas (ranging from a single building, universities, factories, and other landscapes); Model- refers to a graphical representation of object geometry. As a result, 3D city models are a georeferenced tri-dimensional model of the actual complex urban environment that animates all relevant urban objects located above (buildings; vegetation, lamp posts, etc.), on (terrain, streets, land use, etc.) or below (bridges, below the surface constructions, geology) topographic surface as well as their non-spatial information (Danilina et al., 2018; Döllner, Kolbe, et al., 2006; el Garouani et al., 2014). Hence, 3D city models are easier for a human to visualize, interpret and understand the spatial

relationships of these urban objects as well as to have a clear picture of the city as it appears (Jebur et al., 2017).

Furthermore, the 3D city model depicts the geometric, semantic, and radiometric properties of urban objects not only to be used for computer-based animation and visualization of imaginative virtual city models (Buyukdemircioglu et al., 2018; Zhu et al., 2009) but also to deal with sophisticated 3D spatial analysis, simulation and inquiries of the urban environment (CHIGBU et al., 2017; Danilina et al., 2018; Dewanto et al., 2020). Thus, the 3DCM is an important tool to solve numerous issues which modern cities confront, where researchers such as Döllner et al. (2006); el Garouani et al. (2014); Jovanovi´c et al., (2020); and Singla & Padia (2020) presented the application of the digital 3DCM in the domain of 3D cadastres, virtual reality, tridimensional spatial analyses (telecommunication, disaster management, and simulation, urban noise propagation mapping, estimating potential solar energy, vertical change detection, etc.), homeland security, infrastructure planning, real-estate marketing, tourism, as well as for entertainment and education. For such massive benefits of the 3DCM in a different domain application, the International Open Geospatial Consortium (OGC) adopted CityGML as the standard of production, storage, exchange, and modeling of the complex urban structure that integrate the geometric, thematic and semantic aspect of urban spatial objects.

The City Geography Markup Language (CityGML) is explained as an open data model used for the storage, representation, exchange as well as application of 3D city models (Gröger et al., 2012; Jovanovi´c et al., 2020). It is a general-purpose information model capable of handling multiple levels of representation, so-called Level of Detail (LOD) or degrees of realism based on accuracy and minimal dimensions of objects. The concept of level of details (LoD) in 3D modeling to reduce the size and geometrical complexity of a model without losing relevant information is used in a similar way scale used in 2D mapping to deal with the density of content depicted in the map (Stoter et al., 2021; Uyar & Ulugtekin, 2017). For example, for building object which is the most important, continuously changing, and complex structure of an urban system (Finlayson & Opitz, 2004; Ozdemir & Remondino, 2018), CityGML standards provides five level of details (LoD) considering their complexity and application purpose(Gröger et al., 2012; Ohori et al., 2018). Thus, the coarsest level is LOD0 where the 2D vector layer or aerial image is draped over DTM. LOD1 model is a prism model of the building with no roof detail. LOD2 manifests building models with

a detailed roof structure. LOD3 model is a 3D architectural element building model with photorealistic textures (wall) and opening details. LOD4 models are the most comprehensive level of representation which integrates LOD3 plus the indoor structure of the buildings. Furthermore, CityGML allows the visualization and also performs analysis of the same object at a different level of detail (LODs)(Buyukdemircioglu et al., 2018)

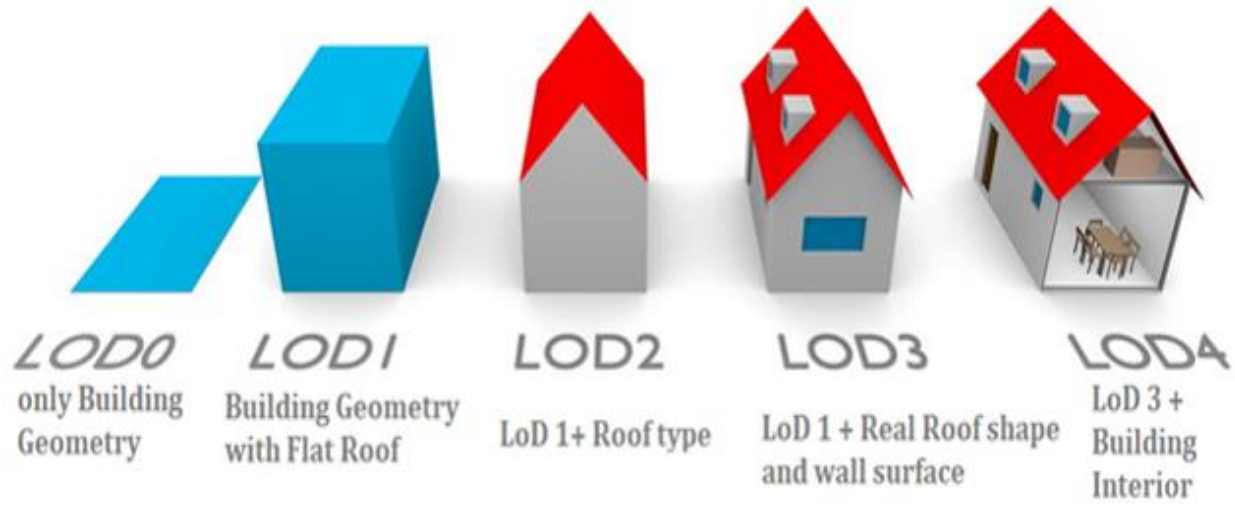


Figure 1.1: Levels of Detail (LODs) of a 3D building Model

(Source: Gröger et al., 2012)

A credible 3D city model that can be used for a variety of urban applications as well as for the representation of the urban scene can be satisfied by the advancement of the geomatics technique (Dewanto et al., 2020). Geomatics techniques are a technique of selecting appropriate technology and tools for data acquisition, retrieval, analysis, processing, modeling, and representation of spatially-referenced data obtained from comprised of disciplines such as Photogrammetry, Remote sensing, Geodetic Measurements, Cartography, and Geoinformatics(Gruen, 2013). Thus, the geomatic technique provides several approaches for the reconstruction of 3D city models based on the data source derived from those disciplines among which the photogrammetry and LiDAR-based 3D city modeling techniques are the most widely used approach (Singh et al., 2013b). Photogrammetry is an information extraction technique (i.e., 3D geodata, and other geometric information such as shape, orientation, size, etc.) of any target ground by making measurements on a pair of stereo images or photographs (Buyukdemircioglu et al., 2018; Jebur et al., 2017). The modern state-of-the-art photogrammetric technology supports automatic data processing and production techniques from overlapping aerial photographs through artificial intelligence and

object recognition with a minimum interaction of the operator. Thus, the photogrammetric derived datasets can be used for the generation of robust, fine resolution of details, and cost-effective 3DCM of the target scene(Toschi et al., 2019; Wu, 2021). Whereas the LiDAR technique is delivering a direct height data extraction technique from the laser light-emitting sensor to the targe and back. These height data consist of 3D mass points that store the geometric detail of the surface object including the third (Z)dimension. Thus, these point datasets can be directly used for the reconstruction of the 3D model of the target spatial object. Despite the high fidelity of the LiDAR data for 3D model representation, it requires a high cost of initial investment and data expensiveness, a huge volume of data, and tedious time consuming for data processing (Guo et al., 2021; Stal et al., 2012).

Given the aforementioned arguments, this research study explored the photogrammetric technique for data acquisition, processing, and derivation of required data input for the reconstruction of a digital 3D City model for two Levels of detail LOD1, and LOD2 as demonstrated in the Figure (1.1). The reconstruction was performed by taking the Addis Ababa Institute of Technology (AAiT) campus area of Addis Ababa University as a part of the larger investigation within the 3D city modeling concept from the data and technology that have at hand. The resultant 3D models are then transferred into a geographic information system (GIS) environment for virtual reality application and stored in a geospatial database and also can be published on the university website as well. Furthermore, the models can be accessible by the administration, visitors and students to be used for the map application and other different purposes left by 2D maps/plans like for web-based promotion/advertising, planning strategies, 3D visualization of the campus building pattern, virtual scene roaming and campus touring, walk-through applications, 3D spatial analysis, queries, etc.

## 1.2 Statement of the problem

The development of spatial data infrastructure is fundamental to establishing an urban spatial data framework. Based on the framework all types of information can be indexed and modeled together with attribute information(Li et al., 2013). In the context of the urban spatial framework, 2-dimensional maps charted from simple drawing, and traditional or modern surveying techniques have been used to abstract the physical realism including the urban areas for many years. Nowadays, the evolution of urbanization around the world both in terms of society and economy

is realized which in turn results in the introduction of complex urban infrastructure, rapid expansion, complex societal challenges, and other globalization effects in general (Tunc et al., 2004). Meanwhile, classical two-dimensional (2D) mapping abstracted as symbols, directions, and legend remains there to serve for monitoring, visualization, plan, analysis, and administration of the cities, while a rapid and continuous increase in urbanization, construction of high-rise buildings, condominiums (co-ownership of land), and other complex infrastructures occurs outside of it. Furthermore, the current 2-dimensions spatial representation is user-unfriendly due to the high level of abstraction (i.e., the man on the street cannot interpret the 2D map) as well as neglecting the third dimension (vertical dimension) of the spatial object is not any more accurate enough to provide the required service for proper presentation, handling, planning, manipulation, administration, and analysis of issues arising in the urban environment (Girindran et al., 2020). Thus, an advanced platform that considers the growing complexity of cities and also for better digital documentation of the existing city structure before it's too late (due to constant destruction) is becoming a necessity.

In Ethiopia, the utilization of the digital 3D city model in the area of the urban system, university campus, heritage sites, tourism, and others are very limited or not yet practiced. On the other hand, in recent times we have been familiar with watching the digital 3D model of various grand and flagship projects on the television screen such as the Mesqel square project, the '*Gebeta Lehager'* project (Wenchi, Gorgora, and koyesha), the Great Ethiopian Renaissance Dam (GERD) and others. However, those models are just CAD or purely graphical, mainly used for the presentation and visualization of the proposed project, and could not provide the capability to carry out 3D spatial analysis (e.g., vertical noise propagation, wind simulation, shadow estimation, etc.) to confirm their future for the nearby inhabitant. Following that limitation, this study proposes the method of reconstruction of 3D models of an urban spatial object that keeps its geographic location and is capable of various three-dimensional spatial applications. Meanwhile, the 3D City modeling concept needs to be applied in different sectors such as tourism/ heritage destinations (such as Lalibela, Axum, Gondar castle, etc.) for virtual tourism and heritage preservation, university campuses management, and promotion, and the likes other than the urban environment. Therefore, this research study is intended to develop a digital 3D city model of the 5 Kilo (AAIT) campus of Addis Ababa University. The campus system is part of the urban structure where one can find complex physical infrastructure that makes fresh students and visitors have a hard time orientating

themselves and finding the location of utility centers like registrar, café, dormitory, library, and more.

## 1.3 The objective of the Study

### 1.3.1 General objective

The General objective of this study is to explore the potential and implementation of the Geomatics technique specifically, the photogrammetric technology for the development of a digital 3D city model by taking the AAiT (5-kilo) campus of Addis Ababa University (AAU) as a case study.

### 1.3.2 Specific Objectives

- To explore the photogrammetric data processing pipeline, performance, and feasibility that can yield reliable results for further analysis and modeling.
- To develop campus geodatabase and 2D map of the campus system as well as extraction of the above-ground height of campus spatial feature.
- To reconstruct a geo-registered, interactive, and cost-effective digital 3D model of the 5-Kilo campus environment.

## 1.4 Research Questions

The research can be addressed the following questions:

- How applicable is using the geomatics technique specifically photogrammetric technology in producing data used for the effective representation of urban spatial objects?
- What are the approaches to managing spatial objects and their vertical height of the urban systems, university campus systems, heritage cites …etc. in a single storage location?
- What are the methodologies to be used for the effective rendering of a 3D model of the physically existing urban structure?

## 1.5 Significance of the study

The community's recognition of the urban built-up environment is no longer constrained to the conventional 2-dimensional planar representation or 2.5D topography surface world. Hence, an environment as identical as the real world should be necessary to visualize, simulate, analyze and interact with the 3D digital world in the same manner as one interacts with the real world - with the same physical constraints and dynamics. So, the present research work contributes the tools and techniques for the reconstruction of a spatially referenced digital copy of the existing complex

urban environment that provide numerous potentials application ranging from simple fly-through visualization to a comprehensive 3D environmental analysis and simulation. Furthermore, the methods and datasets adopted in this study give an insight for academia to carry out further similar research investigations as well as for government organizations and industry sectors to provide a cost-effective strategy for the production of georeferenced digital 3D city models of their region to support the nation's digitalization of its valuable infrastructure as well as to enable them to make faster, more informed and reliable decision making, smart governance and simplify their work processes.

## 1.6 Scope of the Study

The overall focus of this thesis is to generate a digital 3D campus model in the domain of 3D city model using geomatics technique specifically an exploration of the nadir photogrammetric technique for the production of DSM, DTM, orthophoto as well as for the extraction of the above-ground spatial feature height (nDSM) and store all these datasets at a single geodatabase location. Furthermore, this study mainly covers the utilization of these datasets for the generation of an interactive 3D city model that manifests only the ground and elevated spatial object of the campus system at two levels of detail (i.e., LOD1 and LOD2).

## 1.7 Limitation of the study

The major limitations encountered in the overall progress of this research but not limited to: -

- Considering the time constraints, this research study is only limited to the AAiT campus area
- Since the aerial/nadir photographs are meant to give tope view information of the target ground, the current research work falls short to reconstruct a 3D model higher than LOD2 from such dataset (no façade and interior structural information)
- In addition, the height of the generated 3D model of the spatial feature was not compared with the precise height of the respective feature obtained by other surveying methods, despite a comparison being carried out between the known standard height of the building with the obtained model vertical height.

## 1.8 Innovation in this work

Due to the exponential increment of urbanization across the world and the growing need of the population, expansion of infrastructure, environmental change, and other factors, reconstruction

of 3DCM was an important topic in the last two decades both in academia and industry. Meanwhile, this research explored the available techniques and tools used for developing a system of representation that considers the ongoing urban complexity and situation. Thus, this study investigated geomatics-based digital model reconstruction of AAiT campus spatial objects like buildings, trees, vegetation, playground, and others that is capable of 3D simulation and virtual touring, visualization as well as 3-dimensional spatial analysis. Thus, this study does not have a special novelty rather it could be considered as an initial start and hence all the adopted datasets, as well as methodologies, can be used as input in the process of digitalization of cities identical to its real-world context.

## 1.9 Target Group

The finding of this study is targeting audiences from academic institutions, business organizations, government sectors, and other industries who are engaging directly or indirectly using the geospatial data infrastructure for their analysis, decision making, business, and the like. To name the main audiences or target groups: city government, engineering, and construction industry, investment and business companies, tourism organizations, university campuses, disaster response, and rescue organizations.

## 1.10 Organization of the thesis

The thesis paper is organized into five chapters. Following the introductory portion of this section, the 2nd chapter conveys the review and discussions of earlier research papers to understand the current knowledge about the 3D city model, available modeling techniques and tools for data production, model reconstruction process, and also its use case in facilitating real-world problems. The 3$^{rd}$ chapter of the thesis presents the research project area, dataset description and software used, and an overview of the procedure followed for data processing, production, and reconstruction of digital 3D city models. The 4th chapter of the thesis has presented the obtained result and briefly discussed the result of the investigation from the inputted data source and the adopted methodology. The 5$^{th}$ Chapter is the last section of the research study where it briefly demonstrates the conclusion of the present research and also highlighted recommendations that require further future study.

# CHAPTER 2: LITERATURE REVIEW

## 2.1 Concepts of the 3D city model(3DCM)

As defined by Yalcin & Selcuk, (2015), 3D city models are digital descriptions of physical objects located at city quarters, cities, urban districts, university campuses, and other regions of the earth's environment as it exists in reality. It is a computerized model or digital copy of the city that contains the graphic representation of objects that exist in the real world(Singh et al., 2013b). It is a 3D representation of the surface features of a given area of interest or territory. The 3D city model contains the description of all the relevant urban spatial objects like buildings, vegetation cover, terrain, transportation infrastructure, waterbody, city furniture, and other land use spaces (Brenner & Haala, 1999; Buyukdemircioglu et al., 2018; Danilina et al., 2018; Ohori et al., 2018; Parthibanraja & Purushothaman, 2016).

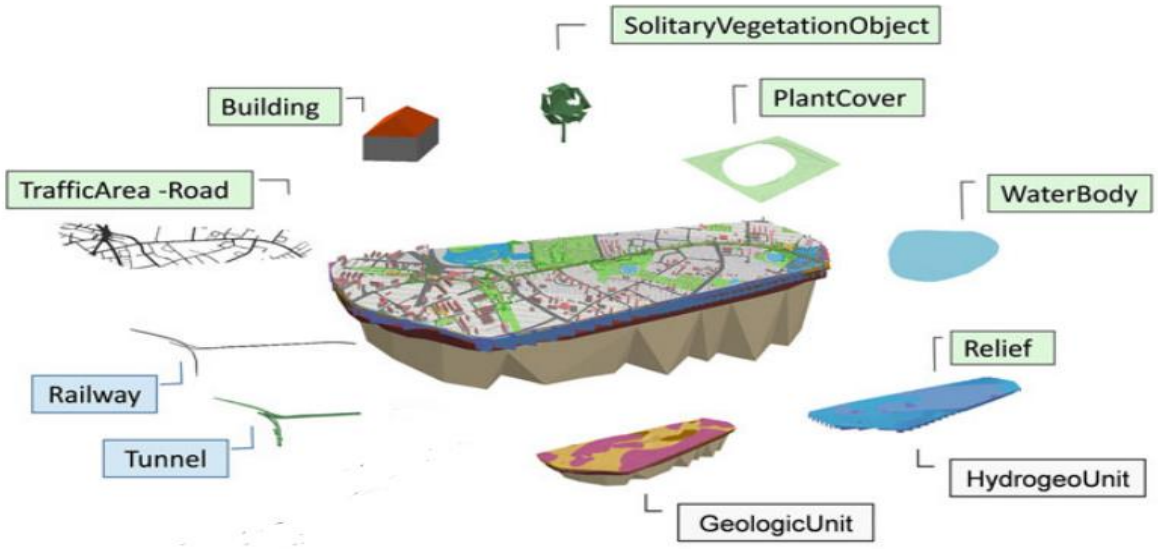


Figure 2.1: illustration of 3D city model

(Source: Kolbe & Donaubauer, (2021))

The 3D city models bring real-world context into a digital representation of the spatial object within the city, and they could be used for advanced and reality-based 3-dimensional GIS applications which are often difficult with 2-dimensional maps alone. In addition, it is the best way to transform the actual urban region into a smart city system for better analysis, visualization, and simulation of the urban environment as well as act as a platform to solve problems, share ideas and concepts with stakeholders, and the public(Kolbe & Donaubauer, 2021). Similar to 2-

dimensional representation that stores attribute information of the spatial object (i.e., parcel location, legal space, building name, story number, construction date, owners' name, etc.), the digital 3-dimensional city model is rich with such set of information in addition to the elevation and thematic information of the physical properties(Tunc et al., 2004). Thus, the 3DCM is of great importance to be used in different urban applications such as urban planning, 3D urban visualization, 3D cadastre, tourism, disaster management, environmental analysis and simulation, homeland security, 3D urban analysis, etc.(Alomía et al., 2021; Forlani et al., 2015; Ozdemir & Remondino, 2018; Parthibanraja & Purushothaman, 2016; Yalcin & Selcuk, 2015).

The 3D city model is covarying all spatial objects within the city, where a comprehensive standard of representation and development platform is required. Hence, an integrative standard like CityGML, accepted by the International Open Geospatial Consortium (OGC) to support geometry, semantics, and multiple representations of 3D landscapes, urban areas, territories, and city infrastructure objects, together with its application has been adopted (Buyukdemircioglu et al., 2018; Danilina et al., 2018; Gröger et al., 2012). City Geography Markup Language (CityGML) is an XML (Extensible Markup Language) based encoding standard for the representation, storage, and exchange of spatially referenced 3D city models (Kolbe & Donaubauer, 2021). CityGML is an open data model used as a standard geospatial model and platform for the implementation of the 3D models for smart city applications. The CityGML standard information model contains DTM (as raster, tin, mass point), building, vegetations, water bodies, transportation systems, city furniture, and others. As described by Gröger et al., (2012), CityGML provides five levels of details (LoD) to model each city object or group of city objects including their thematic properties, where LODs are used to describe the quality, level of complexity (details), and granularity of digital 3D city model given different data acquisition technique, processing methodology, and purpose of the city model required (Fan & Meng, 2009; Yalcin & Selcuk, 2015). In other words, the LOD describes how close the reconstructed 3D city model is to the existing real world. With the increase of LODs, the object models become more and more detailed in their geometric and thematic representation(Döllner et al., 2006). The five LODs defined by the CityGML standard are:

- LOD0 –2D vector data or aerial image to be draped on the terrain (DTM), the coarsest level

- LOD1 – Solid model of building with flat roofs (prismatic models), without wall openings and other detail
- LOD2 – city model with different roof structure and texture, but no wall details
- LOD3 – city model with detailed wall and roof structures and textures (outside architectural models)
- LOD4 – Completes the LOD3 model by adding interior structures like rooms, stairs, doors, and others.

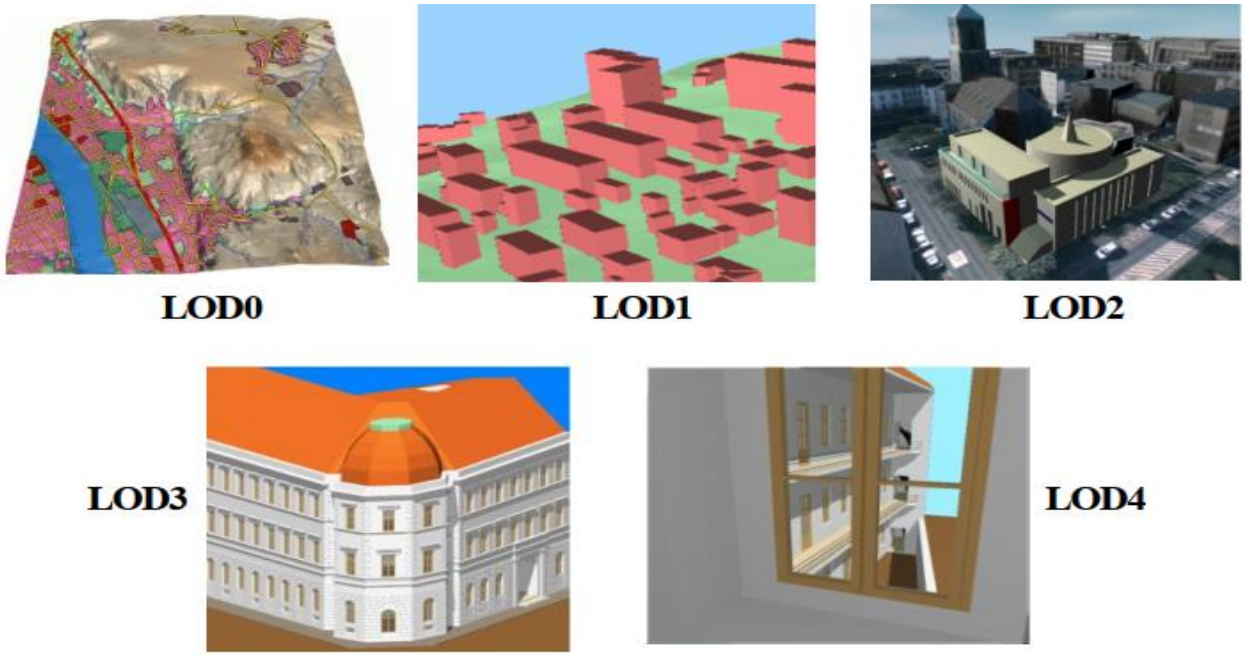


Figure 2.2: The Five Levels of detail (LOD) defined by CityGML for building objects

(Source: Gröger et al., (2012))

CityGML is to be seen as a framework that enables the graphical 3D representation of the spatial objects and also addresses the semantic, spatial, and thematic properties of the object (Döllner et al., 2006; Kolbe & Donaubauer, 2021; Singh et al., 2013b). Semantic properties are information about the objects attached to the building object's geometries, such as the materials it is made of, year of construction, number of stories, etc. Whereas, thematic properties are the thematic field of the model like DTM, building, vegetation, waterbody, transportation, city furniture, and more. Such a rich set of semantical and thematic information attached to 3D city models could be used for computer-based urban simulation, and analysis purposes, including the development of smart cities and digital twins(Fan & Meng, 2009).

With the constant development of modern technology, the growing need for 3D models, and 3D data acquisition techniques, the 3D modeling approach is constrained by the available data input method, target application, and modeling technique(Kobayashi, 2006). Some of the main 3D modeling approaches are Computer-Aided (CAD) based models only used for geometric and appearance modeling and visualization, the Building Information model (BIM) which is an architectural and engineering model, and real-world models (GIS model) that depicts topological and semantic properties of spatial objects (El-Mekawy et al., 2012; Saran et al., 2018). Both CAD-based models and BIM models are traditional and manual modeling techniques of 3D city modeling used for designing, space planning, and construction operations, which requires an enormous amount of time and manual work (El-Mekawy et al., 2012). However, in recent years the advancement in geomatics technology has become one of the core research areas to lead the representation of spatial objects in 3-dimensions (3D GIS) at multiple resolutions aimed at automatic generation of 3D city models and production time(Tunc et al., 2004). Moreover, the quality and accuracy of the 3D model have been greatly improved.

## 2.2 Geomatics Technique for 3D City Modeling

Although there are different approaches and methods developed to capture the human environment, the geomatics technique is there at the front of the queue to select appropriate technology, tools, and effort to collect, store, retrieve, analyze, transform, distribute and model spatially referenced data (Singh et al., 2013). Geomatics is an umbrella term constituting various mapping techniques such as Photogrammetry, Remote sensing, Geographical Information System (GIS), Global Positioning System (GPS), Light detection and ranging (LiDAR), Radargrammetry, etc. The geomatics technique supports the generation of 3D city models in a fully automatic, semi-automatic, and manual modeling approach depending on the input data source(Jebur et al., 2017). The manual 3D city modeling approach is a modeling approach where the operator creates city modes following an expensive procedure and time-consuming manner(Reljić & Dunder, 2019). The reconstruction of the 3D city model using the CAD method is a manual modeling approach. The semi-automatic modeling approach is the one in which the operators perform extraction, interpretation, and recognition of features manually with the support of automatic precise measurement and 3D model generation(Kaartinen et al., 2005). For example, the use of aerial images and satellite images for 3D city model generation uses a semi-automatic approach. The automatic modeling approach is the one that has been used to generate a 3D city model without

any interaction of the operator. The LiDAR point cloud data supports automatic 3D model generation using an automatic point segmentation algorithm (Kaartinen et al., 2005).

Among the many geomatics technologies, most researchers used the LiDAR point cloud data, aerial photographs, or a hybrid of both technologies with an existing 2D GIS map (Buyukdemircioglu et al., 2018; Kobayashi, 2006b; Loutfia et al., 2017; Uggla, 2015; Wu, 2021) as the most common data source techniques for the efficient and effective generation of the digital 3D city modeling.

### 2.1.1 Photogrammetry Based 3D City modeling

Photogrammetry is a measurement technology on a series of 2D photographs obtained from different camera sensors mounted on air, space, and ground-based platforms to derive photogrammetric products such as metric information, photo maps, target feature model, and other reliable information about the physical object which is used for detection, extraction and documentation, modeling, analysis and visualization of existing objects in urban areas and other target surfaces without contact(Alomía et al., 2021; Chen & Clarke, 2016; Forlani et al., 2015; Jebur et al., 2017; Reljić & Dunder, 2019; Wu, 2017, 2021).

In the modern-day, the continuous development of hardware and software technology intended for digital photogrammetry has been played important progress to acquire high resolution (i.e., a resolution of 0.1 m or better) with multiple bands of imagery (aerial, satellite, terrestrial) used for the production of large-scale topographic maps as well as for the recovery of the physical geometric structure and 3D virtual model of the spatial object(Georgopoulos, 2017). Parallel to the advancement of technologies used for data acquisition, the advancement of necessary sophisticated software tools equipped with cloud computing capability and artificial intelligence used for manipulation of these image data opens up untapped potential(Hopfstock et al., 2022). Such as automatic multi-stereo-dense image matching algorithm can perform a pixel-by-pixel correlation process between a couple of overlapping photographs taken at different vantage points. These capabilities of the software algorithms ease the generation of very dense 3D mass points capable of discriminating small detail of the target ground and other 3D geometric characteristics of the spatial object(McClune et al., 2014; Wu, 2017). The use of such photogrammetric product is a proven economic approach suited to extract the details of urban spatial objects like appearance, geometry, and scene of the region, required data components and hence facilitate the generation

of 3D city models in an automated approach using only a couple of overlapping (stereo) photographs (Saran et al., 2018). Thus, the photogrammetric technique based on stereo aerial photographs, satellite imagery, and other close-range photographs is the most convenient research direction used for the three-dimensional city modeling process (el Garouani et al., 2014).

The aerial photographs can be collected by an aerial camera sensor mounted on the airborne (controlled aircraft, and drone-based) platform so that acquisition of a geometrically corrected series of aerial photographs can be done based on the pre-defined flight plan with the assistance of airborne GPS, and inertial navigation sensors (Jebur et al., 2017). These datasets consisting of nadir-looking photographs along with their exterior orientation parameters (EO) and internal sensor parameter (IO) with additional ground control points (GCP) can be processed and delivered to photogrammetric products such as DSM, DTM, orthophoto, and other products. These all-photogrammetric derived datasets are required for the reconstruction of the geometric structure as well as dimension of the existing urban physical structure, where the DSM dataset is used to estimate the maximum height of the surface spatial object, DTM is used as the base elevation or standpoint of all elevated features and the orthophoto could be used for the detection and outline extraction of the spatial object as well as texturing of the model(3DCM) (Buyukdemircioglu et al., 2018; Toschi et al., 2017).

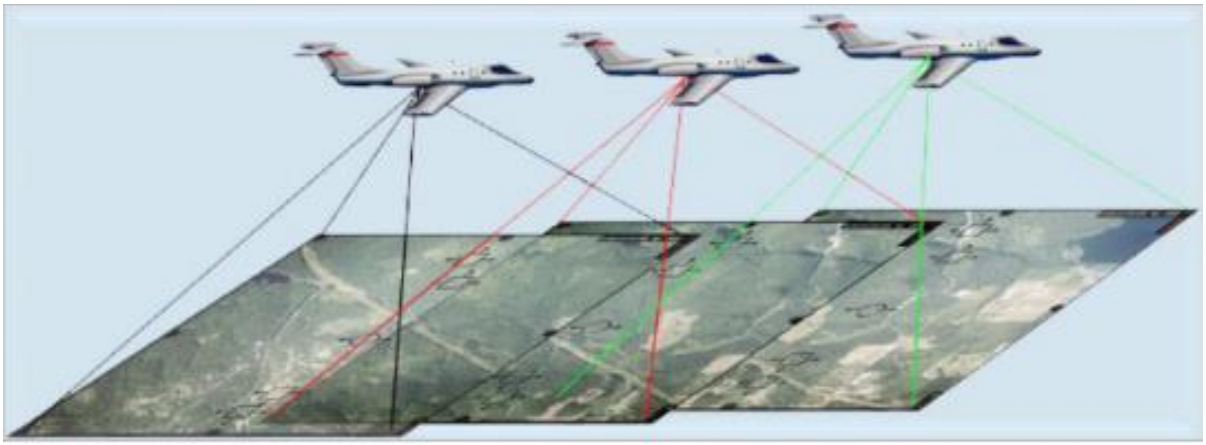

Figure 2.3: Illustration of aerial photogrammetry

(Source: Jebur et al., 2017)

However, different researchers employed different combinations of photogrammetric products with different 3D modeling software tools in the reconstruction of 3DCM. For example,

Buyukdemircioglu et al., (2018) used combinations of building vector footprint, DTM, and photogrammetric point cloud DSM data for semi-automatic reconstruction of LOD1 and LOD2 based 3DCM using BuildingReconstruction modeling software. The DSM cloud points were analyzed for roof edge geometry reconstruction. Based on the detected best-fit roof type the LOD2 building models were reconstructed and also these models were get textured from the nadir/close-range photograph. Finally, they converted the generated model into CityGML format for better utilization of the 3D city model in different applications.

Jebur et al., (2017), presented an automatic approach to reconstruct a 3D city model for two different areas in the city of Baghdad, Iraq, from a couple of stereo aerial photographs. The researcher used the LPS photogrammetric software and Agisoft Photo scan software to process the aerial photograph. Thus, the researcher generated a photogrammetric point cloud from both software. Further, the researcher made a comparison analysis between the point clouds generated from that software using statistical RMSE value, interpolation method, and other statistical assessments. So that they conclude that the point cloud generated from the Agisoft PhotoScan software was used for a fine resolution model reconstruction than the one generated from LPS software. Moreover, from both of the generated photogrammetric point clouds, the researcher reconstructed 3DCM of the two-area using ArcScene and google SketchUp software.

Furthermore, other researchers presented the methodology of generating a 3D city model from a combination of high-resolution stereo satellite imageries such as IKONOS and QuickBird(Kocaman et al., 2006), KONOS, and WorldView-2 (Gruen, 2013), Gaofen-2 and Sentinel-2(Y. Ying et al., 2019). The former researcher processed the satellite image with SAT-PP, (Satellite Image Precision Processing) and hence extracted outputs such as building geometries and DSM. From these datasets, they reconstructed a 3D city model in an automatic approach using CyberCity Modeler software. The later researcher processed the satellite imagery with homemade software and hence reconstructed the 3D models for the Little India district in Singapore. In addition, other scholars from India used high-resolution Indian Remote Sensing satellite images (Cartosat-1 and Cartosat-2S) for the production of digital elevation model (DEM as well as orthophoto map to integrate this output with open street map (OSM) data to generate virtual 3D city model of Ahmedabad city(Singla & Padia, 2020). The researcher employed the satellite photogrammetry technique to derive the feature height and ortho-imagery data. Thus, using QGIS

software the researcher attributed the height information for each OSM building boundary. Furthermore, 3D extrusion of the OSM building was performed with the ortho-imagery draped as a background or base layer for the generated 3D city model and served for realistic 3D visualization of the city landscape.

Additionally, 3D city modeling can be reconstructed using the terrestrial/close-range photogrammetric technique (Singh et al., 2013a). A terrestrial photogrammetry is a good option for 3D model generation by measuring photographs collected from a digital camera mounted on the ground-based platform to obtain lengths, shape, architecture details, façade information, and position of viewing objects from overlapping images taken at the different terrestrial shot position. For Example, Singh (2013), presented how researchers like Shashi and Jain (2007), generated 3D city models using close-range photogrammetry. The presented approach used normal digital hand-held cameras easily available at the market to take photographs of the building. Then, photographs were tied together and every edge of the building geometry was traced. From the traced building geometry, a photorealistic 3D model with good visual quality was generated. This realistic representation was then used for virtual reality applications where virtual interaction, 3D scene visualization, real-life navigation, and other application can be made by the public.

All the above reviews show the implementation of the photogrammetric technique for the reconstruction of the 3DCM used for different applications. Thus, researchers presented here and not, adopted the photogrammetric technique utilizing the close-range/oblique photograph, aerial/nadir photograph, and satellite imageries as a data source for the reconstruction of the 3DCM of the target urban center, university campuses, industrial ground, tourism site, or heritage location. Each of these photogrammetric techniques has their strength and weakness in terms of accuracy, cost, time, and safety. In this respect, the use of nadir aerial photogrammetry for 3D reconstruction is better as compared to the satellite that has less resolution and accuracy of the satellite image (satellite sensor is mounted at a high altitude (Kocaman et al., 2006; Uggla, 2015); also, better as compared to terrestrial/close range in term of cost, time and safety (time-consuming and manual field data collection) as well as a large amount of data (storage and data manipulation issue). Furthermore, oblique photogrammetry is a photogrammetric technology where slanted views photographs were overlaid for the reconstruction of a complete 3D model of the spatial object despite its very low image resolution and high geometric defects, non-trivial processing, and

occlusion issues as compared to the nadir aerial photogrammetry approach. Nevertheless, to get the best output of aerial photography, it should be processed with powerful software that employed sophisticated algorithms, one of the most famous state-of-the-art photogrammetric solution software is the INPHO photogrammetric software.

### I. INPHO

INPHO is one of the modern-day sophisticated and whole complete digital photogrammetric solution software which belongs to the Trimble Germany company. It is used to process images acquired from a helicopter, space shuttle, and UAV platforms equipped with different camera sensors for the delivery of all standard task photographic products(Darbas & Sužiedelytė-Visockienė, 2011). The INPHO software system contains several module software that is capable to perform straightforward and quick photogrammetric operation independently to deliver accurate and reliable results (Ma et al., 2011). The list of modules is MATCH-AT, MATCH-T DSM, DTMaster, OrthoMaster, OrthoVista, and so on.

**MATCH-AT**: is INPHO's aerial triangulation module software used for the definition of photogrammetric project blocks consisting of intrinsic parameter of the scanning camera sensor (IO), radiometrically adjusted image (aerial phototroph) data, perspective GNSS/IMU measurement (EO), and the ground control point (GCP) file. Further, the Match-AT software provides GCP measurements and image georeferencing tools in manual, semi-automatic, and automatic approaches with high precision and efficiency. Furthermore, it can be used to carry out automatic aerial triangulation (bundle adjustment) processing operations to perform adjustment of block information based on the ground point data as well as determination of absolute exterior information of points on the ground.

**MATCH-T DSM**: is INPHO module software explicitly intended for the automatic and precise extraction of digital surface models (DSM), digital terrain models (DTM), and dense point cloud data from digital stereo aerial photographs or satellites (Ackennann & Krzystek, 1991). It employed a robust multi-stereo dense image matching algorithm for the automatic generation of 3D surface information and quality control from overlapping photographs in different file structures such as las or point cloud, 3D mass point, grid, WINP, and more.

**DTMaster:** is a powerful terrain editing module software that can edit DSM data obtained from photogrammetry or LiDAR techniques (remove non-ground height information i.e., urban

structures, overpasses, and bridges) into ground surface information (DTM) quickly and accurately. Further, it is used to inspect the quality of the terrain data, filtering and classification as well as conversion of the digital terrain surface data into another format very easily.

**OrthoMaster:** is module software used to carry out high-quality automatic orthorectification operations for the correction of inclination and projection error present in the digital aerial/satellite image. The orthorectification process can be carried out utilizing the triangulation result with the project file, camera file, image data, and DTM data. Thus, this operation transforms the perspective characteristics of the image into the orthographic projection (true locations without relief displacements).

**OrthoVista:** is INPHO module software used to dodge and inlay each of the corrected images from OrthoMaster module software. such image-stitching and dodging tasks are performed to deliver a seamless single digital orthophoto map (DOM) of the region with consistent tone and color information.

### 2.1.2 LiDAR Based 3D City Modeling

Light Detecting and Ranging (LIDAR) is a modern active remote sensing technology used to capture information about the ground and non-ground (elevated) objects (Chang et al., 2008) in a way that the LiDAR sensor emits a laser beam to strike the target feature and return to the sensor, record the travel time, laser angle and signal at different levels of return depending on the object characteristics (Kobayashi, 2006; Sulaiman et al., 2010). This recorded information can be used as source data for post-analysis and computation of the range to the target based on the speed of light formula (using the time it takes to travel round trip to estimate the sensor position) as well as for determination of highly accurate vertical dimension of features(Jebur et al., 2017). As described by Uggla, (2015) the range/ distance between the LIDAR senor and the target surface can be calculated;

$$R = \frac{C * T}{2} \tag{2.1}$$

Where R is the range (distance), C is the speed of light ($3 * 10^8 m/s$) and T is the time it takes to travel the pulse and back.

The integration of the LiDAR sensor with GPS/IMU sensor technology eases the task of profiling and estimating the surface object's vertical placement precisely, which attracted to be implemented in different disciplines such as forestry, environmental research, urban 3D modeling and cadastral system, and remote sensing for production of high accuracy 3D spatial data (Hopfstock et al., 2022; Nath & Ramiya, 2016). Due to the level of detail the LiDAR data has, many researchers prominently used it for the reconstruction of the 3D city model of the existing urban structure used for a variety of applications such as urban planning, monitoring, environmental simulation, security, tourism, and the likes(Yastikli & Cetin, 2017). LiDAR data can be obtained from two types of acquisition approaches. The first approach is the airborne laser scanning approach where the scanning device is mounted on the aircraft or drone and hence provides nadir viewing information about the geometry of objects like buildings, trees, terrain structures, and others(Sulaiman et al., 2010). The second is the terrestrial laser scanning method where the device is mounted on a fixed ground-based platform (tripod, car, crane, etc.). This type of laser scanned data provides about the object's façade as well as interior structural information (wall, window, door, rooms, and more). Both of these data are used for the automatic generation of 3D city modeling purposes either independently or with integration.

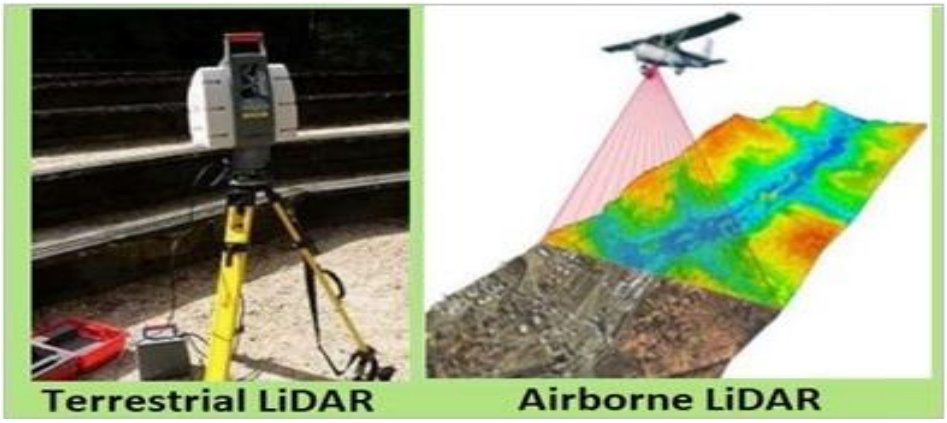


Figure 2.4: Illustration of the two types of Laser scanning

(Source: (Kumar, 2022))

The capability of the LiDAR point cloud dataset in providing high-accuracy 3D geographic position, color or intensity information of bare earth, as well as above-ground structure, makes it a standard geospatial data source for the generation of a 3D model of the target ground at semi-automatic and fully automatic modeling approach for different application purpose(Peeroo et al.,

2017). In this concern, Nath & Ramiya, (2016) has been adopted the LiDAR point cloud datasets for automatic and semiautomatic 3DCM reconstruction approach using the TerraScan module of Terrasolid software. They have tested those modeling approaches in two different areas with three different point cloud datasets having a density of 1point/square meter, 5 points/square meter, and 62 points/square meter which the first two datasets were tested at the same area/location. The researcher classified all the three-point cloud datasets into the ground and building class points and from the building class point 3D building geometry was reconstructed. In the building model generation process, a fully automatic building model vectorization was performed from 62points/ square meter data whereas semi-automatic building model extraction was performed from the 1point/square meter point cloud dataset. Further, both fully automatic and semi-automatic building modeling were performed from 5points/square meter point cloud data. Thus, based on the modeling results the researcher concludes that even though both approaches with different vectorization parameters deliver a good building model, the semi-automatic modeling approach is better to be adopted for datasets having a lesser point density despite the manual work required. Furthermore, those datasets with a lesser point density lost small details of the building geometry, especially for small buildings.

Another researcher, Yastikli & Cetin, (2017) has utilized LiDAR point cloud data for automatic 3D building models reconstruction of the Zekeriyakoy area, Istanbul. The researcher first classified the point cloud data into three meaningful object classes namely: unnecessary, ground, vegetation, and building from the automatic classifier by Terrascan software. Thus, from the building class point, a 3D model of the study area was successfully generated in an automatic approach. Thus, according to the researcher, the resultant 3D city model is capable to be used in different applications such as environmental analysis and simulation, navigation, and telecommunication.

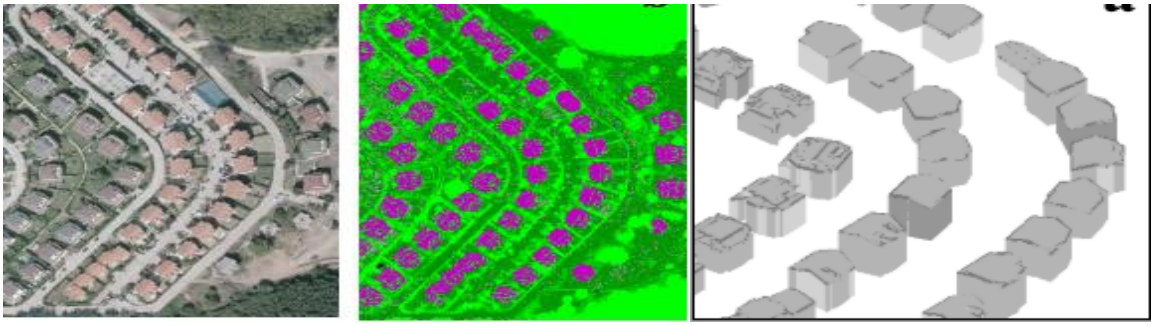

Figure 2.5. Ortho-image (left), classified point cloud(middle), the generated 3D model (right) (Source: Yastikli & Cetin, (2017))

Jovanovi´c et al., (2020) generated a virtual 3D city model of Novi Sad University, Serbia, from LiDAR point cloud data. The researchers developed 3DCM aimed to support smart city applications by integrating a different set of urban information that allows users to perform different types of analysis and visualization just by employing this model. Thus, the researchers have done a series of tasks in the process of 3D city model generation. They started from LiDAR and image data collection, processing these data, lidar data classification and grouping, 2D feature extraction from the image, and finally integrating the 2D feature with building class point cloud data for the generation of a 3D city model of the project area. Moreover, the researcher transformed the generated 3D city model into a CityGML model format to be able to employ the model for different applications.

I. TerraScan

The TerraScan software is a Terrasolid software family product fully integrated with the Bentley Microstation PowerDraft platform to mainly be designed to manipulate, process, and analyze billions of high-density 3D points obtained from different sources such as photogrammetric dense image matching ((DIM) operation, LiDAR scanning sensor, and others (Nath & Ramiya, 2016; Sulaiman et al., 2010). The Microstation-enabled Terrascan module software is like plugin software (Uggla, 2015), and employed a sophisticated algorithm that can be used to perform a wide range of tasks and processing operations like point cloud classification, feature detection, vectorization, filtering, 3D visualization, editing, and split up, feature extraction, conversion, and much more tasks in manual, semi-automatic and automatic approach. The Classification activity can be done based on some routines on points or routines used only in Macros to filter out unnecessary points in the dataset as well as to category points into where they should belong (meaningful classes such as default, ground, low vegetation, medium vegetation, high vegetation, building, etc.) like which points to the ground and off the ground. The classification operation can be performed either manually using a manual brushing tool or automatically based on given filtering parameters/ criteria like slope based (neighborhood points to be classified as ground and object points based on discrimination and comparison made in their position, height, and angle i.e., steepest slope information between points belong to non-ground point), surface-based (parametric region or buffer zone) or segmentation-based parameters. In such a way the classification algorithm determines all the points in the layer cloud dataset as ground or object or other particular meaningful categories. For example, the first iteration might be to identify ground

points and create terrain surface structures. Then all the other iterations can be processed based on their distance reference to the terrain. Additionally, the building vectorization tool of the TerraScan software can be used to detect geometrical faces based on the best fit points for the reconstruction of a 3D model of the building automatically. The automatic building vectorization tool is an efficient, robust, and predictable tool used to reconstruct tens of thousands of LOD2 3D building models automatically from building class points within a short time and without additional manual model editing needed depending on the quality of input point cloud dataset. Further, the TerraScan software provides model storing, export (e.g., KML, SketchUp, COLLADA, CAD, etc.), exchange, and publishing into 3D City Databases.

### 2.1.3 3D city modeling by a hybrid approach

3D city model can be generated from a combination of data sources mostly based on the integration of photogrammetry and LiDAR data to improve the planimetric as well as the vertical geometric accuracy of the model (Peeroo et al., 2017; Redpath, 2018; Uggla, 2015; Welter, 2021; Wu, 2021). The integration can be LiDAR data with aerial photographs or with satellite images(Toschi et al., 2019; Wu, 2021). In this concern, a study by Döllner et al., (2006) presented the 3D city model of Berlin city, Germany, aimed at the management, integration, and communication of the complex structure of the city. The researchers used hybrid technology of high-resolution stereo aerial imagery and LiDAR data as an input data source. The aerial photographs were analyzed to deliver a true orthophoto of the city whereas the LiDAR data were also used for precise DTM and DSM extraction. Furthermore, the cadastral footprints were extracted from the orthophoto and integrated with the height data for the automatic generation of the 3D city model of the city. In addition, for further geometric shape-ups, thematic enrichment, and texturing, the 3D Studio Max was employed as general-purpose 3D modeling software. The generated 3D city model preserved greater detail and consistency and hence converted into CityGML format to widen the applicability accessibility and interoperability of the model.

Kaartinen et al., (2005) adopted a hybrid technology for the reconstruction of 3D city modeling using a different set of modeling software such as TerraScan, CyberCity, and other software tools. The photogrammetric data is used for better extraction of the outline boundary of the building objects and length determination. Whereas the LiDAR point cloud data have been used for the precise determination of the building height information as well as detailed roof geometry. Thus,

by integrating the extracted building 2D outline with its respective height value, an automatic model reconstruction approach delivers a high-quality 3D city model.

Loutfia et al., (2017), has presented a simple and semi-automatic 3D city model reconstruction approach based on the fusion of orthorectified imagery with LiDAR data. The ortho-imagery was used to delineate the outline of the building boundary. They extracted the third dimension (absolute height) of the 2D building footprint from the LiDAR data by generating nDSM surface information where 2D height estimation was based on the statical mean of a set of random sample points within the independent boundary of each 2D building footprint. Thus, a 3D city model was generated from the automatic extrusion of the 2D building footprint to its maximum absolute height value. Moreover, many researchers have briefly explained that employing a hybrid technique for urban model reconstruction provides a much better modeling accuracy than each of the independent technology(Wu, 2017; Zheng et al., 2017).

### 2.1.4 GIS-Based 3D City modeling

Geographical Information Systems (GIS) is a comprised of hardware, software, and spatially referenced data massively designed for the digitalization of spatial features mostly based on the two-dimensional representation approach used for efficient management, 3D modeling, visualization, and analysis of the urban system (Alomía et al., 2021; Al-Rawabdeh et al., 2014; Buyukdemircioglu et al., 2018). However, recently, the use of GIS technology transforms its head into the three-dimensional representation of real-world features and widen its application, especially in the presentation of urban systems where the structure of spatial features has changed continuously(Uggla, 2015). In this sense, the GIS technology integrates various types of data sources such as existing 2D cadastral databases or ground plans (master plan) with DSM data obtained utilizing photogrammetry or LiDAR technique for 3D urban model generation(Suveg & Vosselman, 2004). The existing 2D database is used to define the outline of the model feature whereas the DSM can be used for the extraction of the above-ground height of these 2D outlines. The above-ground height of the 2D features can be obtained by the normalization operation between the DSM and DTM surface data, and hence the resultant surface is called Normalized Digital Surface Model(nDSM). The nDSM surface can be generated from the minus (difference) operation between DSM and DTM surface data(Burdeos et al., 2015; Hashemi, S.A.M., 2008; Peeroo et al., 2017). The DSM data stores the first echoes (maximum height) of the surface (ground

and non-ground information) and acts as the maximum elevation surfaces. On the other hand, the DSM data can be filtered out of its elevation information other than the ground/terrain level information and hence transformed to the bare earth model (DTM) which acted as the foundation of every elevated artificial feature. Then, based on the mathematical formula described by Hashemi, S.A. M., (2008) the nDSM Surface can be obtained by GIS software as follows:

$$nDSM = DSM - DTM \qquad (2.2)$$

Unlike the DSM and DTM surface that describes the elevation of features above/below mean sea level (AMSL) or ellipsoid, the nDSM surface represents the absolute height of artificial (non-ground) objects like building, trees, etc. relative to the ground terrain (Loutfia et al., 2017; Zheng et al., 2017).

The integration of existing 2D cadastral databases (vector polygon, ground plan, OSM), DTM data, and feature height information (cooked and attributed manually, or photogrammetric / LiDAR-based nDSM) for the reconstruction of realistic 3D city models have been widely used by GIS software. The fusion could be made in such a way that the 2D vector layer of the ground object (i.e., tree, building, road, etc.) is superimposed over the terrain model, and hence the 2D object footprint extruded into the height of the nDSM surface fitting. Depending on the type and quality of the desired 3D urban model and available data sources, different open source and commercial of the shelf GIS software tool such as ArcScene, SketchUp, Global mapper, Autodesk Revit, ESRI City Engine, QGIS, or a combination of software tools are used by different researchers for 3D model generation in an efficient, timely, and cost-effective manner(Dewanto et al., 2020; Xu et al., 2009). In this concern, Chigbu et al., (2017) adopted a combination of ArcGIS and SketchUp software tools for 3D modeling of the University Nigeria Enugu Campus (UNEC), Enugu, Nigeria. The reconstruction starts from the digitization of the feature's vector polygon from the aerial image using the ArcMap editing tool and approximates height attributes manually for each campus building. Then the vector data were called into ArcScene so that building features were extruded up to the height in their attribute. The extruded LOD1 model was converted into multipath features and then into a Trimble SketchUp compatible file format (*.skp). The Trimble SketchUp software is an easy-to-use three-dimensional modeling software with a reach set of tools used for 3D geometric modeling (push/ pull), measuring and scaling, texturing, etc. to be used in the field of mechanical, civil, architectural, and virtual gaming application (Banduthilaka et al.,

2013). Thus, the researchers used the SketchUp software to complete texturing of the extruded models from close-range photographs and textured the geometric detail of the building roof. Finally, the photorealistic 3D model of the campus was imported into ArcScene using the 3D editor tool while maintaining its spatial and non-spatial information.

Other researchers, S. Jain et al., (2017) have demonstrated the procedure of using the QGIS open-source software tool for the generation of a 3D city model for GIFT City, Gujarat, India, from existing master plan and Google Satellite image. The Google satellite image was used for the extraction of GCP data and hence used for georeferencing the scanned master plan. Thus, the researcher extracted 2D shapes of the building from the georeferenced master plan. Further, they obtained the height of each building from the urban department of the city. Finally, they generated the 3D model of the city by extruding the 2D boundary to its respective height.

Ramlee et al., (2019) developed a 3D model of University Technology Malaysia (UTM) that is capable of making 3D visualization, navigation, and query (spatial and non-spatial) operation about the campus environment. The researchers utilized freely available DEM and 2D geo-data from OpenStreetMap (OSM) together with its default height attribute and also QGIS open-source software for the generation of the model. From these datasets and software tools, the 3D model of the campus building was generated through the extrusion of a 2D vector polygon to a height in its attribute and the DEM acted as the foundation of the model. Finally, the generated 3D campus model was shared on the campus website for its intended application.

On the other hand, Alomía et al., (2021) presented a procedural 3D city modeling technique using ESRI City Engine software. The ESRI City Engine software is a GIS environment tool that has a full suite of tools to turn the 2D urban geospatial database and height information stored in it, into a complete 3D urban model based on a set of procedures that contains parameters and iterative custom rules (shape grammar-based model generation). The researchers used DSM resulting from a high-resolution stereo image matching process for 3D geometry reconstruction, an orthophoto map for 2D data extraction, and also a terrestrial photograph for facade texturing. From this dataset, the researcher generated a grammar-based 3D city model using City Engine software. The grammar rules are a well-established block of code that facilitates the generation of self-similar object modeling processes such as 3D extrusion of the 2D footprint, roof generation, street

definition, texturing (Roof and facade), and more. Thus, the created 3D city model provides various GIS analyses, for simulation of natural disasters and others.

The aforementioned discussion of articles conveyed information about the use of different geomatic technology for the generation of 3D city models from the photogrammetric, LiDAR, hybrid, and GIS techniques of the urban reality model reconstruction approach. Choosing an effective modeling technique should be based on the best compromise between cost, time, and fidelity. Thus, scholars such as Ahmed et al., (2011), and Stal et al., (2012) have conducted a comparative analysis of the photogrammetric and LiDAR techniques in terms of their vertical modeling accuracy, effectiveness, cost, and time. From their analysis, both researchers found out that the LiDAR technique produces an accurate 3DCM model despite it requires more time to process the point cloud data (bottlenecks in processing), difficult to understand (sophisticated and unstructured point cloud), and its expensiveness (both data and equipment) as compared to the photogrammetric technique that can achieve highly comparable accuracy (if high-resolution photographs used) of the 3DCM (both in structure and dimensions ) with quicker data acquisition and processing time, cost-efficient and visually understandable dataset. On the other hand, 3DCM reconstruction of the urban environment from the integration of existing 2D cadastral footprint, DTM and nDSM information using GIS software or a combination of these software technologies is a reliable approach to representing the real environment. However, the use of the existing database for 3DCM to use for various applications may potentially face actuality and incompleteness issues (Brenner & Haala, 1999). Given this argument, this research study will focus on the use of high-resolution aerial photogrammetric techniques for the generation of a 3D city model.

## 2.3 Use Case of 3D city model

Nowadays, the georeferenced 3-dimensional city models are getting popular, and hence many cities around the world have produced the digital 3D model of their cities to support their decision-making process as well as to utilize the model in a wide range of applications. As 3D city models are enriched with the semantic, geometrical, and appearance characteristics of the spatial object, their applications are manifold. Some of the high-level use cases of 3D city models studied in this research are discussed as follows.

### 2.3.1. Surface Preservation (Archival) and Documentation

In the world, an urban area is mostly a place where valuable assets such as historical buildings, Monuments, and other cultural heritage are left for the young generation(Georgopoulos, 2017). However, physical and structural changing occurs continuously and quickly, thus the implementation of the 3D city modeling technique for digital preservation of surface structure (geometric and appearance or texture) and landscape of the past, current, and future state of an existing urban area, historic site or an archaeological site and other structural remain models are a key to track changes, and also to present as a gift for future generations(Parthibanraja & Purushothaman, 2016). In this concern, researchers like el Garouani et al., (2014) have reconstructed a 3D city model of a UNESCO World Heritage historic medina Fez city, Morocco, for the preservation of historical complex building architecture and all infrastructure, aimed tourism purposes as well as for rehabilitation and conservation. Further, Nasir & Tahar (2017) has also reconstructed a 3D model of the historical mosque of Masjid Lama Nilai, Negeri Sembilan, Malaysia for the preservation of its geometric structure and appearance to track the change and also for maintenance and repair purpose. Such accurate documentation and archival of the urban structure (landscape, buildings, and other monuments) inside a geospatial database play an important role in the redevelopment of the historical structure, maintenance, and repair tasks in case of any destruction as well as it helps the feature generation to explore the historical, architectural and appearance information of their city at some time i.e., future-proof (Banduthilaka et al., 2013; Georgopoulos, 2017; Nicholls & Kruimel, 2017). Furthermore, the presence of such models can be used as a data source for experimentation and research study, tracking and analyzing the changes occurring in the city structure over time and others.

### 2.3.2. 3D Visualization and Navigation

The 3D visualization of an information model is the precondition for reconstructing it as well as using it in a more widely application(Xu et al., 2009). The 3-dimensional visualization can be carried out by using some kind of visualization software such as google earth, SketchUp, ESRI ArcScene and ArcGlobe, web visualization, etc. As the 3DCM is the virtual replica of the urban spaces that integrates buildings, parcels, blocks, and other land use spaces interconnected by streets, 3D visualization of such a topologically true digital urban environment from diverse viewpoints helps to gain insights into the city setup and structure (manmade and natural landscapes), assess regulatory height policies, visualize urban growth scenarios and properties of

urban spatial objects with its harmonization in the city and to better understand the location of objects in its 3D geometric context as well(Øyen-Eriksen, 2016). Such attainment of the mental model of the city supports the exploration of the existing city by tourists, strangers, navigators, etc. to make their way to the destination and virtual entertainment. The 3D fly-through visualization of the city on their digital model helps the user as well as the larger community to interpret their environment without ambiguity as the human brain naturally interprets the 3D scene in its true perspective. Furthermore, the 3D urban model is an important tool for the planning of optimal and safest route choices for people or vehicles based on the 3D fly-through derivation of information such as traffic flow, street conditions, temperature, and so on (Li et al., 2013; Øyen-Eriksen, 2016). Further, 3D city models are a priory platform built for the implementation of an intelligent transport system where autonomous unmanned vehicles can make their way through enhanced visual depiction, recognition of location, and interpreting the outdoor façade/ realistic display of the objects(Nicholls & Kruimel, 2017) as well it supports manual route navigation even when GPS service is available.

### 2.3.3. Business Development and Tourism

Tourism is an important part of economic growth. Thus, having the 3D model of such an asset has the biggest advantage for its mobility and business promotion which allows tourists from everywhere to get to know the historical site and tourism destinations through virtual flight. The 3DCM can be built to give a realistic impression of the existing unique architectural, historical value, and structural details of objects with their spatial location (destinations) where travel organizations can utilize the digital models to make awareness about the place to be visited, available for virtual touring before going to the location as well as to make remote visits in the time of crisis like covid-19 and also for web-based tourism marketing and advertisement. Furthermore, the 3DCM can be used in the business sector as a real-estate developer can get benefited from such a digital model to demonstrate the available property to the client without taking them to the site due to some reasons, or that the site is very far from sell office, this technique can be useful to show what the client exactly wants to buy.

### 2.3.4. Urban planning and Cadastral modeling

In modern-day, the 3D representation of the urban object is a widely recognized and appealing approach that opens a new level of understanding and brings high-quality standards of collaborative (government and community) urban design and planning(Kurakula & Kuffer, 2008;

Onyimbi et al., 2017). The 3D city modeling is an advanced technique for the simulation of the actual use of urban land with an unbiased and highly accurate representation of objects which is a critical tool for an urban specialist to assess the architectural and planning situation of the area to support future organizational and managerial decisions regarding sustainable development plans(Danilina et al., 2018). The city planners get benefits from the 3DCM to define the existing city condition, precisely evaluate the property characteristics and values (Cadastre), re-arrange the city set-up, introduce a new city look-out, simulate the future effect of the newly proposed planning, and so on with a more realism context. In this concern, the city governor can use the digital 3DCM to serve as a participation medium to involve its citizens in urban planning and administration where the community (both specialist and non-specialist) can be engaged with the digital environment to reflect their idea about the effect of the new development and share insights to what is best for them through making interactive visualization (el Garouani et al., 2014; Engman, 2016; Onyimbi et al., 2017; Uggla, 2015). Such a participatory urban planning strategy that integrates the community's interest with a designing perspective helps the city planner to avoid the introduction of design errors, and conflicts of interest in the implementation of the new project as well as improve the attractiveness of the city (S. Jain et al., 2017; Welter, 2021). Furthermore, the use of a 3D city model for urban planning operation helps the designer to consider the historical background, present state, and future urban scenarios in the design process to keep features and utilities in place according to tomorrow's requirements and suitable for the urban inhabitants (Jovanovi´c et al., 2020).

Moreover, the current use of parcel-based or 2-dimensional cadastral systems sketched from CAD tools or 2D spatial footprint is not adequate to deal with various aspects of land and property information (Li et al., 2021), and falls short of handling both the horizontal space (2D right) and vertical space (co-ownership: vertical configuration and volume of buildings structure) of cadastral objects(Y. Ying et al., 2019). Thus, 3DCM is an important development to meet a comprehensive and consistent land recording application based on an integrated representation of 3D space of cadastral objects such as building or building unites (e.g., Condominium), underground constructions, roads, parks, overcrossing structureless, etc. and links the spatial object's physical dimensions with their characteristics, their topological relationships and legal dimensions (rights, restrictions, and responsibilities on the properties) associated to the dynamic property rights to clarify the debate, and dispute between citizens (Li et al., 2021; Ying et al., 2012; Zhu et al., 2009).

These descriptions of the spatial object can be used as an inventory list of urban physical objects and can reveal objects that are not appropriately represented in the 2D cadastral map (e.g., missing or design change) which intern helps to minimize unfair distribution and unambiguous representation of urban land property (Kolbe & Donaubauer, 2021; Ying et al., 2012). Thus, 3DCM can be used as a multi-purpose cadastre for the management and administration of cadastral properties where the city government gets benefited from it to perform fiscal activities, property/housing valuation, legal activity (building height policy formulation), and minimize misinformation related to urban complex property (condominiums) rights.

### 2.3.5. Disaster risk management and Simulation

The importance of 3DCM is enormous where its third dimension plays a major role to perform a wide range of analyses and simulations in a multitude of domains. One of the most growing uses of the 3DCM is a vitality for the public safety organizations (e.g., firefighting departments, flood risk centers, and other rescue and emergency management organizations) for making a reality-based prediction, identification, and simulation of the possible urban disasters (e.g., earthquake, fire, explosions, flooding, urban blast and other physical processes) with less effort and time just by using the digital copy of the corresponding real-world environment(Welter, 2021). For example, flood protection centers can assess flooding incidents through 3D animation and virtual simulation at a different state, estimate the amount of damage or consequences of the disaster for a given area, and also safe evacuation ways through simulation in a 3D environment(Nikola & Temenoujka, 2019; Waser et al., 2018). Disaster simulation activity can be made in three phases time i.e., much before it arises, in the real-time, and post-disaster(Shoko & Gavu, 2021). The 3DCM are used for predictions of near realistic possible disasters with data-based sufficient argument to identify areas of risk at different what-if scenarios (Stoter et al., 2021) which helps decision-makers to locate and engineer mitigation measures to be taken, create contingency plans, evacuation space and humanitarian access and others before the problem raised. Whereas at the time when the disaster happens, 3DCM offers on-the-fly interaction and 3D visualization which is helpful to deal with real-time response to the disaster that can be useful to plan strategies to deal with the situation and resource mobilization as per the need, rescue operations, emergency management, and assisting evacuation routes and centers(Waser et al., 2018). On the other hand, the 3DCM can be used for visualization, investigation, and estimation of the volume of damage

(e.g., bombing, blast, etc.) as well as to plan for maintenance/recovery strategy for post-crisis effectively and remotely(Minds, 2021).

### 2.3.6. Other applications

The other important area of the 3D city model can be used to investigate the environmental phenomena in the vertical variations such as the demonstration of noise pollution in a particular area. Such presentation of environmental noise exposures from different noise sources (traffic flow, industry) requires the distance between the emission point and receptions (including the vertical geometry) to estimate the possible vertical noise propagation level at which the noise can affect the inhabitants(Kurakula & Kuffer, 2008). The noise status calculation and its mathematical model of 3D wave simulation can be done using parameters such as the building's façade information (transmissivity), traffic flow, road surface and size, heavy vehicle percentile, and road gradient. Thus, the 3D city model is a vital tool for presenting the audible noise level for the authorities and policymakers to protect the citizen from being exposed to unacceptable noise levels and to adopt noise limits. Further, the 3DCM is fundamental for military and security personnel to determine the suitable location of nodes or urban buildings for the installation of the surveillance control center to collect real-time data as well as to determine what points and areas are viewable and hence can estimate the coverage of visibility in planning realistic mission used for public safety, military operation and determination of potential threats Li et al., (2013). Moreover, the digital 3DCM can be used for the selection of suitable locations and installation of sensors to collect real-time data such as temperature, noise, speed and direction of moving objects, and potential rooftop solar energy (Dewanto et al., 2020). The 3DCM can be also used for education and training purposes where the student can quickly grasp the setup of the city situation and their technical staff. For example, a 3D city model can be used to train the pilot student to make simulated flies over the local known city of its corresponding digital model.

In this section of the study, the literature discussed the manifold application scenarios of geomatics-based digital 3DCM in the urban physical environment. In many of these application scenarios, they narrated the necessity to start implementing else adopt the digital 3DCM representation strategy of the existing urban environment to improve the quality of life for the urban inhabitant, modernize the property administration system, predict, prevent or mitigate possible hazards or disasters, and more.

# CHAPTER 3: MATERIAL AND METHODS

## 3.1 Study Area and Description

For this research project, the Addis Ababa Institute of Technology (AAiT) campus area is chosen to get firsthand experience in the process of digital 3D city model reconstruction of the urban environment. The AAiT campus is chosen due to its data availability and diverse infrastructure in the area as well as to help new students and inexperienced visitors orient themselves and recognize the geographical setting of the campus scene just by visualizing and exploring its digital model, and to lead by example for other universities at least to model their campus environments.

The AAiT is a branch of Addis Ababa University commonly known as the 5-Killo campus, was established around 1961 G.C and is one of the leading institutes of technology in Ethiopia. Currently, AAiT is executing technological teaching-learning tasks for over 5500 bachelor (undergraduate) and 4500 postgraduate (i.e., M.Sc. and Ph.D.) students enrolled in the various department programs of the Institute. The campus is specialized in teaching engineering and related technology disciplines such as Electrical and computer, Hydraulic, civil and environmental, agricultural, and biomedical sciences with many other specialties.

The campus is located on the downtown side of Addis Ababa city within the Arada sub-city covering an approximate area of 42482 square meters with Grid Coordinate ranging from 473817.332 to 474017.992 East (X) and from 999031.184 to 999259.334 North (Y). The campus scene is comprised of buildings with different heights (up to ground plus ten) and varied and complex geometries (such as a variety of roof shapes, installations, texture, etc.) surrounded by several trees utilized for a variety of purposes (i.e., administrative and staff, classrooms, Laboratory and workshop, Library, etc.), access roads (walk ways), green open spaces, and parking. The location map of the study area (i.e., AAiT) is shown in figure (3.1) below.

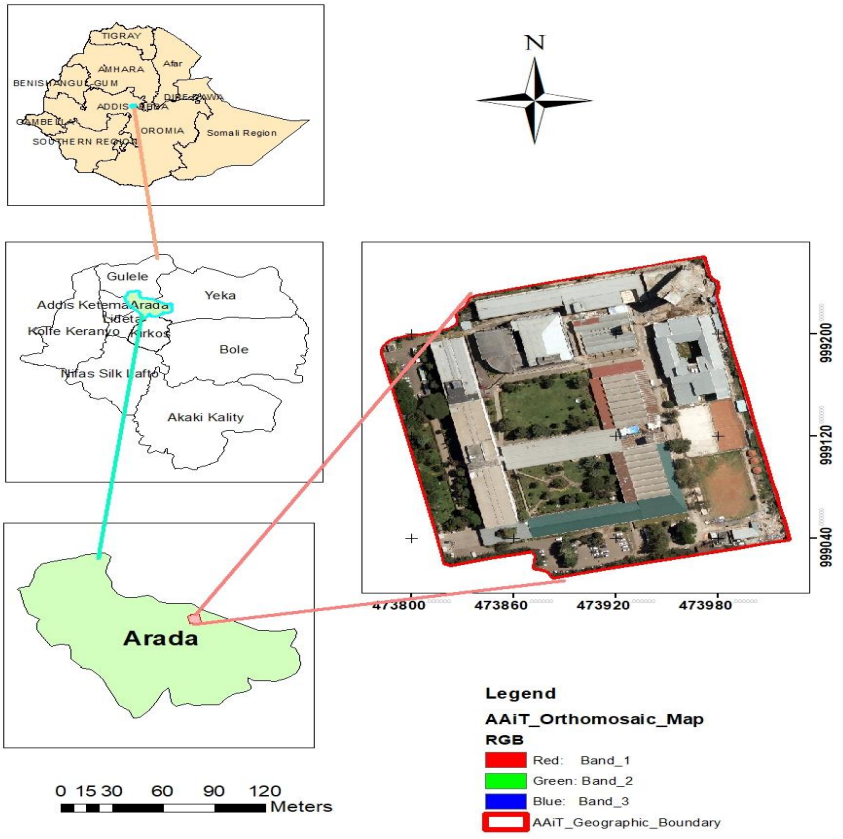


Figure 3.1: Addis Ababa institute of Technology campus location map

## 3.2 Materials

Different kinds of data input are used for the reconstruction of 3D city models. The data can be ranging from high-resolution remote sensing products (e.g., high-resolution aerial photographs (nadir & oblique) and satellite images) to high-precision LiDAR data. The kind of data input used can define the level of resolution for the extraction and representation of the 3D city model. Thus, to meet the described objective, the main available data input for this research study is high-resolution aerial photographs, ground control point (GCP) data, and other ancillary data that are used to enrich the derived information from the aerial photogrammetric process.

### 3.2.1 Aerial Photograph

The aerial photograph is a true picture of the ground that is captured from the air in such a way that aerial cameras are mounted on airborne platforms and hence scan parts of the ground under the camera view based on a predefined flight path. The aerial photograph provides a realistic-looking scene, used to extract information about the illuminated ground. The information extracted

from aerial photographs could range from the 3D coordinate (X, Y, and Z) of a particular point, dimension of planimetric features, digital photo maps, Terrain models, 3-dimensional models of the physical object, and more.

For this study, the aerial photograph was obtained from the Geospatial Information Institute (GI2) of Ethiopia. The GI2 is the only institution in Ethiopia that has the mandate to perform the acquisition, production, and dissemination of aerial photographic deliverable products to the end-user. To do so, GI2 has employed an ultra-large format aerial digital camera, UltraCam Eagle digital camera System from Vexcel Imaging, Graz, Austria, and a bunch of commercial photogrammetric software solutions to facilitate the photogrammetric processing operation. Hence, the institute used this sensor system equipped with sort of software and airborne platforms for the acquisition of high-resolution aerial imagery that can be used for a variety of projects such as cadastre application (urban and rural), highway/road design, irrigation, dams, etc. In this regard, the GI2 was agreed with the Addis Ababa city administration to perform the photographic project for the production of an orthophoto map for the entire Addis Ababa city. Hence, the GI2 has been carried out the acquisition of aerial photographs for the intended purpose. Indeed, from these acquired aerial photographs, photographs covering the 5 Killo campus and its surrounding area were used as the main data input for this research project. Moreover, for the success of every photogrammetric project, a series of tasks have to be performed i.e., the preparation of detailed flight mission planning and a good acquisition process.

#### 3.2.1.1 Flight Mission Planning for Aerial Photography

A flight mission plan is a navigation map that consists of a series of straight and parallel runs/strips or flight lines that show where the aerial photographs are to be taken and specifications about the aerial camera, photo scale, flying height, end lap, side lap, and tolerance parameters, and so on (Pepe et al., 2018). The preparation of a detailed flight mission plan is the first stage where the aerial photography stage begins. The quality of the flight mission influences the success of the photographic project where a well-designed mission plan played an important role to acquire the near accurate photographic acquisition of the project area. Hence, the preparation of flight mission planning for the photographic project requires careful consideration of planning parameters. So, during mission planning for this project, the project area of interest (AOI) with a known coordinate system, aerial sensor's parameter (focal length, sensor internal dimension, offsets, etc.), ground

sampling distance (GSD), overlaps between photographs (end lap and side lap), rough digital elevation model (DEM), tolerance level (crab/tilt, overlap, etc.) and other variables were carefully defined.

**Project Area of Interest (AOI):** As the aerial photographs used for this study were obtained from the Addis Ababa photography project, the closed polygon of Addis Ababa city defined by the World Geodetic System 1984 (WGS84) coordinate system with the UTM zone defined as zone 37 was used for flight mission preparation. The use of the WGS84 coordinate system for the AOI helps to avoid the coordinate disagreement between the onboard tracking GPS and the prepared flight missions during the acquisition of photographs.

**Aerial Camera:** The GI2 has employed one of the advanced mapping cameras, UltraCam Eagle, used for the acquisition of high-resolution aerial photographs where aerial images used for this research study were obtained. The UltraCam Eagle, the ultra-large format digital aerial camera is the product of Vexcel Imaging, Graz, Austria. It is a CCD (charge-coupled device) based multispectral sensor, used to capture nadir images from the airborne platform in four ranges of the electromagnetic spectrum (red, green, blue, and near-infrared (NIR)) as well as a panchromatic band (very high resolution black and white image)(Gruber et al., 2012).

The Vexcel's UltraCam Eagle (Calibrated) camera is equipped with 8 individual cameras(cones), where four of them are used to create the large-format panchromatic image at a size of 20,010 pixels across the track by 13,080 pixels along the track and the other four cones are responsible for taking the RGB (red, green and blue) and near-infrared image at pixels size of 6,670 by 4,360 (Figure 3.2).

The panchromatic part of the sensor combines 9 medium format CCD sensors to capture large format panchromatic images. Whereas each multispectral channel described above is supported by their respective four independent CCD sensors. The other constructive characteristics of the sensor such as a focal length of 100.5 mm, a frame rate of 1.8 frames per second, an option of aperture value, and shutter speed(Wiechert et al., 2011), and other details of the sensor are found in the appendices.

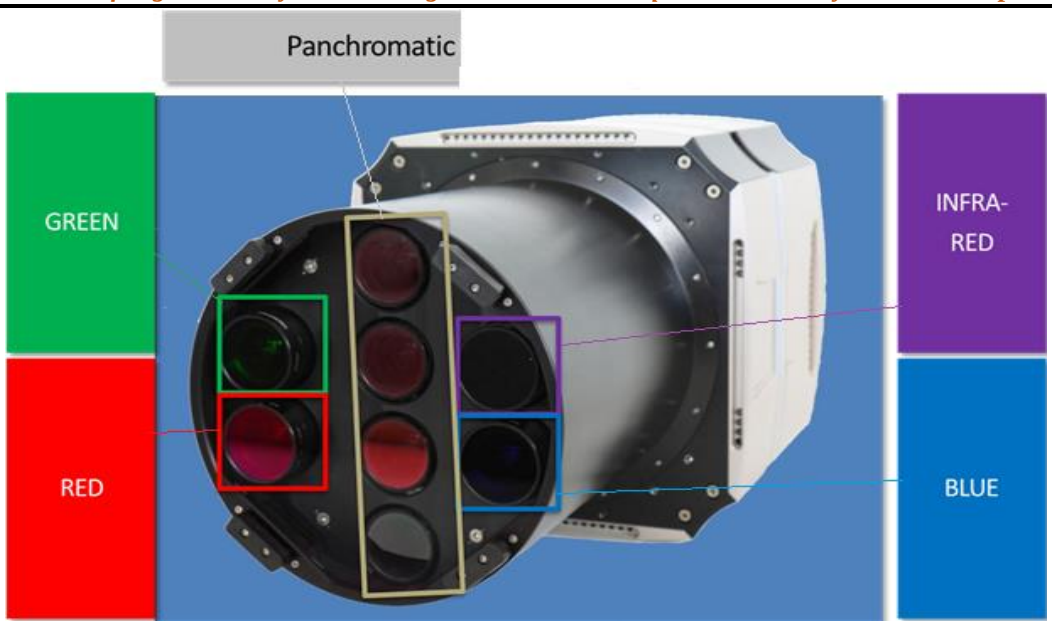


Figure 3.2: UltraCam Eagle digital image sensor unit

(Source: GI2)

**Ground Sampling Distance (GSD):** is the most important parameter for flight mission planning where it defines the distance between two successive pixel centers on the ground. It is an essential metric in determining the scale of the photographic mapping project. The selection of GSD value can be associated with the purpose of the aerial photography project (e.g., urban cadastre, rural cadaster, engineering project such as road, etc.), customer need, the accuracy of the final product required to achieve, the aircraft ceiling altitude, pixel size of the camera, and focal length of the sensor. Considering these factors, the Addis Ababa aerial photography project was set to be collected at a GSD of 10cm per pixel. In other words, each pixel in the aerial photograph represents 10 cm which equates to objects that have 10 cm on the ground are visible/mapped on the photograph. The GSD value can be calculated by the formula (Pepe et al., 2018):

$$GSD = \frac{H}{f} * Sensor\ pixel\ size \tag{3.1}$$

Where H is the above-ground flying height and f is the focal length of the aerial camera. The larger the GSD value of the photograph, the lesser the spatial resolution of that aerial photograph, and the limited/small detail the photograph provides.

**Overlaps:** aerial photography project requires making a series of exposures or shoots along each of the flight lines in the project boundary. The overlaps make sure to have stereoscopic coverage throughout the mission, the photographs must have an overlap. The overlap should be in two directions to guarantee the coverage of the whole project area i.e., along the flight line (forward overlap), and between adjacent flight lines (side lap). The forward overlap is a common image area on successive aerial photographs along a flight line which is fundamental to creating a three-dimensional effect (stereo model). The image forward overlap is necessary at the stage of photogrammetric post-processing operation to recover depth information based on the parallax effect of different image views. Whereas, the side overlap, is the overlapping areas of photographs between adjacent flight lines, which ensures no gaps in the three-dimensional coverage within the project. For the Addis Ababa city project, the aerial photography flight mission has been designed as per the ASPRS standard which is 80% end lap and 60% side lap for true orthophoto production purposes.

**Digital elevation model (DEM):** the DEM is a very important consideration for photography mission planning, used to fix the flight height above ground, which means the scale of the aerial photograph. The mission planning software, SNAP PLAN software module which is a product of Applanix Corporation fully supports downloading DEM for the project area directly from an internet-enabled computer. The DEM is then, involved to design each flight line according to the prescribed GSD(Scale) with keeping other planning parameters too.

**Tolerance level:** the scale and quality of the airborne data required cannot be achieved based on specified conditions due to a variety of factors such as variability of the terrain in the project area, and flight inaccuracies made by human and natural factors. So, the tolerance factor is a necessary value to define a safe minimum and maximum allowable range from the defined parameter. These allowable ranges were used to be considered in the calculation of flight detail calculation by the flight planning software (SNAP PLAN) and were well used during data acquisition. Hence, the aerial photography used for the current study was designed based on the tolerance level for GSD +10%, forward overlap ±5%, and side overlap ±10%.

Once all the required flight planning parameters were successfully organized and inputted into the dedicated software i.e., SNAP PLAN software module which is family to Track ‘Air software, belongs to Applanix corporation. Then, a detailed flight plan was prepared with some additional

manual parameters (such as the choice of flight direction mostly along the longer dimension of the AOI with consideration of local topography and orientation of the block as well as to the East-West direction, to minimize the effect of shadows and maintain uniform lighting). Flight planning parameters used for the Addis Ababa photography project are found in the Appendices. Thus, the generated detailed flight plan, the so-called flight guide map (figure 3.3), of the Addis Ababa project consists of pieces of information such as the numbers of flight lines required to cover the project boundary, the total number of photographs, estimated shot position (X, Y, Z), dimension of the photograph, both flight heights (above ground level (AGL) and above mean sea level (MSL)), Scale of the photograph, the total length of the flight lines, the number of photographs in a flight line and other important details. Finally, this flight map is exported to the airborne system to carry out aerial survey operations based on the predefined specification.

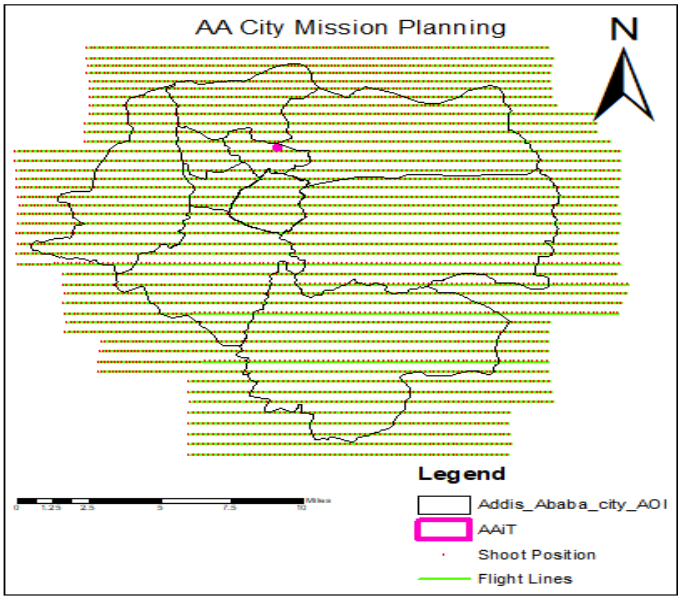


Figure 3.3: Flight plan map of Addis Ababa City

### 3.2.1.2 Acquisition of Aerial Photography

After successfully preparing a detailed photographic flight mission plan, the acquisition of good aerial photographs from a stable platform was the following step to go through in the photogrammetric process. However, to ensure the correct data acquisition, it is necessary to fix errors sourced from acquisitions such as acquisitions made during bad seasons and times of the day. The choice of an ideal acquisition season and time is the best way to maintain a good quality of the recorded photographs and avoid the extra cost of photography. Hence, the acquisition of

photography used for this research was done in May 2021, which is a relatively ideal season for aerial photography acquisition in Ethiopia, to get a clear picture of the ground. In the selected season, the lighting and weather conditions (clear sky) are acceptable for photographs in which aerial photographs are not subjected to haze, fog, smoke or dust, crosswinds, extreme vegetation, or cloud cover and the photographs are representing existing ground conditions. In addition to the season for aerial photography, choice of suitable time of the day is an important consideration, where often acquisition has been done between 9:00 am - 3:00 pm UTC when the solar altitude is above $30^0$. This helps to avoid possible long shadows by the objects and guarantees sufficient illumination of the surveyed scene(Pepe et al., 2018).

Once the choice of acquisition season and time has been confirmed, aerial survey operation was carried out using a Cessna Caravan manned airplane platform which is a fixed-wing single-engine airplane having a cruising speed of 343km/h and operated at an altitude of 15,000ft above mean sea level (AMSL). The airplane was equipped with an integrated airborne sensor system consisting of an Ultracam Eagle digital aerial camera, Gyro Stabilization Mount (GSM 4000 Stabilizer), Applanix Position, and Orientation System for Airborne Vehicles (POS AV) technology, and Flight Management Software (FMS) system. The UltraCam camera system is set on Gyro Stabilization Mount (GSM 4000 Stabilizer) so that the airborne sensor system is kept stable and vertical without the influence of the movements of the aircraft caused by atmospheric turbulence or arbitrary movement created by the aircraft itself and also ensure the near-vertical view of the ground. Additionally, the camera sensor is tightly integrated with POS AV technology to provide a direct geo-referencing task of the airborne camera data which is a highly precise time, position, orientation angle (roll, pitch, heading), velocity, rates (acceleration, angular rate) of the camera perspective center were recorded simultaneously in real-time or for post-processing solution(Hutton & Mostafa, 2005). The POS AV is a hardware and software system that uses the GPS receiver and IMU as its core navigation system to record the position and orientation of the aerial camera at the instant of exposure. These all systems are fully integrated and managed by a Flight Management Software (FMS), the so-called SNAPSHOT. The SNAPSHOT software module is a Track ‘Air software family which belongs to Applanix corporation, used for the management and control of the flight. During the flight, the SNAPSHOT provides the flight status and shows real-time flight information such as position, speed of aircraft, aircraft heading, the total number of photographs in a selected line (both recorded and left), and distances to the next shots,

etc. The FMS system provides a guide to the pilot to keep aligning the aircraft into flight lines, sends a pulse to the UltraCam Eagle camera to make an acquisition of image data following the predefined flight mission plan with a scheduled interval, and in turn records the time & position, in addition to other attribute information, for post-processing and also ensures up-to-date information about the mission progress for the flight crew. With this fully integrated airborne sensor system and with the correct acquisition setting (i.e., aperture, frame rate, time, image numbering, etc.), the Addis Ababa city aerial photography data acquisition was performed in such a way that, the aircraft follows a predetermined flight line as the UltraCam Eagle digital aerial camera automatically exposes successive overlapping vertical aerial photographs of the scene with the assistance of the airborne GPS and the flight management system when the aircraft reaches at shot locations as specified in the flight mission plan with a ground sampling distance (GSD) of 10-11cm, 80-85% forward overlap, 60-66% side overlap, photo scale ranging from 19235- 21159, and Tilt/drift/crab angle did not exceed ±2 degree. Following the successful acquisition of the aerial photographs in the field, the airborne data (aerial photographs and GNNS/IMU navigation data) were downloaded from a mass memory (airborne storage) onto a computer equipped with UltraMap software and a ground storage system (hard disk), a more accessible medium for further photogrammetric correction and processing.

### 3.2.2 Ground Control point (GCP)

The additional dataset used in this research study is the ground control point (GCP). The ground control points (GCPs) are points on the ground that are visible in the field with high contrast in shape and color compared to its surrounding (Redpath, 2018). The ground control point data are vital in supporting and maximizing the absolute accuracy of the aerial surveyed data. The points can be natural features of the scene but often deployed man-made physical objects with high contrast and a clearly defined centroid.

The ground control points used for this research study come from on-field GPS measurements at carefully selected point locations. The selection was performed after carefully studying the collected aerial photographs. The selected points were named Postmarks because the identification of a good photo control location was held months after the aerial photo was already acquired. Thus, for the current study area which is too small to consider the standard number of GCP points, only three easily identifiable and well-distributed ground points were selected surrounding the

study area. These postmark locations were chosen by considering multiple variables. Some of the considerations were that each aerial photo should have at least three points to full fill basic photogrammetry principle, points with sharp and visible edges that can be viewed on the image points that can be found easily when visiting to survey it, and points away from densely constructed and high buildings to minimize the multipath effect, and also points were placed in a suitable pattern connected each other to make a triangle shape to achieve high precision during processing. Of the selected three GCP points two of them were on the sidewalk corner and the other one is on the corner of the roundabout. Once the identification of a good photo control location was completed, three Leica Geo-office/GS10 dual-frequency receivers GPS instruments equipped with its tripod were taken to the selected postmark location and set up by centering the point. Then, each instrument's vertical bubble was adjusted to keep the instrument vertical. Furthermore, antenna heights were measured and inputted, IDs were created for each point, GPS data logging intervals were set to 5 seconds, mask angles were set to 10-degree, and storage location and other required settings were set. Once the required setting on each of the three GPS instruments was completed, the GPS receiver started to receive the Navigation Message (NAV) in static GPS surveying techniques. The NAV message is a GPS message which carries information the receivers need to determine positions, information about the precise location of the GPS satellites, clock corrections, health of the satellites in orbit, and information about the atmosphere (ionosphere) it passes through while its way to the receiver(van DIERENDONCK et al., 1978). The GPS data logging of each three points were lasts more than 2 hours with an instrument accuracy of 0.005m +0.5 ppm in all three dimensions and simultaneous data logging at each of the three points to maximize the accuracy of the measurement as the GPS receiver share similar satellites.

After successful completion of the GPS data measurement session, the data were copied to computers. The downloaded data was a binary data file so it was converted into a much more manageable, receiver independent exchange (RINEX) format. Further, the post-processing computations have been performed using a web-based(online) post-processing technique, Online Positioning User Service (OPUS). This is because the post-processing and adjustment of the measured data by local CORS reference stations (including ADIS and TANA stations) weren't possible as there was no active logging station at the time of observation. Even though there are other internet-based post-processing options, OPUS online postprocessing was chosen as it's the

most common post-processing solution to process statically measured GPS data[1]. The OPUS is a web-based processing tool that delivers a more reliable result from the processing of raw GPS measurements made by a dual-frequency GPS receiver in a static model(Nathanael, 2021). The processing has done in such a way that the RINEX data file was uploaded to the processing queues, antenna type LEIAS10 was selected, antenna height of each of the three instruments was filled, and UTM zone 37 and other output options were also filled. Then, OPUS computes the precise position of points from the submitted data relative to the best nearby base stations chosen by the system itself. The result of the OPUS processing solution was sent via an email address which depicts reference frame information, Lat/Long positions of points along with ellipsoidal height, overall positional accuracy, base station information used in the computation, and others. The processed solution reveals the planimetric and vertical positional information in a geographic coordinate system and ellipsoidal height system respectively, that needs to be converted into a local coordinate and orthometric height system for better utilization purposes. So, the Lat/Long geographic position was then converted into a local Adindan coordinate using Global mapper software. Whereas the conversion of the orthometric height of points to EGM08 was performed by an online geoid height converter[2] utilizing the Lat/long and ellipsoidal height information. This way, the horizontal and vertical positions (X, Y, and Z) of GCP points were obtained. These GSP values have been used to geo-reference the images in the bundle adjustment process and in the aerial-triangulation procedure to adjust the airborne GNNS/IMU data as well as for quality control of the derived photogrammetric product.

Table 3.1: The observed ground coordinate point data

| | **Geographic Coordinate** | | Ellipsoidal | **Adindan UTM zone 37** | | Orthometric | RMSE |
|---|---|---|---|---|---|---|---|
| Pt_ID | Lat (Deg) | Long (Deg) | Height(m) | Easting (m) | Northing, (m) | Height(m) | (95% confidence) |
| MAR_1 | 9.03693 | 38.76028 | 2444.646 | 473561.213 | 998737.152 | 2451.69 | ***0.024m*** |
| MAR_2 | 9.03801 | 38.76681 | 2439.154 | 474280.26 | 998856.23 | 2446.2 | ***0.022m*** |
| MAR_3 | 9.04351 | 38.76268 | 2469.378 | 473826.274 | 999464.189 | 2476.38 | ***0.023m*** |

*URL[1]:* *https://geodesy.noaa.gov/OPUS/*

*URL[2]:* https://observablehq.com/@cehanagan/geoid-height-calculator

### 3.2.3 Ancillary Data

Another type of dataset used in this research was ancillary data, it is an attribute and supportive data which provides information about campus objects such as buildings (names, stories, heights, areas, usages) and such details of other spatial objects within the study area. These supportive data were obtained from the AAiT facility management office.

Table 3.2: Summary of dataset adopted for the study

| Data type | Total number | Source/ Format | Coordinate system | | Remark |
|---|---|---|---|---|---|
| | | | Planimetric (X, Y) | Vertical(Z) | |
| Nadir aerial photograph | 12 | GII/Tiff | - | - | The aerial photographs have a GSD of 10 cm Overlap % (along/cross): 80/60 |
| Direct Georeferenced (EO) parameter | 12 | GII/Text | Datum: Adindan UTM_Zone_37N | Earth Gravity Model 2008 (EGM08) | The exterior orientation of each camera exposure consists of 3 coordinates (X, Y, Z) and 3 orientation angles (omega, phi, kappa) |
| GCP | 3 | Field survey/ Text | Datum: Adindan UTM_Zone_37N | | Each of the points was observed for more than 2-hours at simultaneously |
| Ancillary Data | - | AAiT facility management/ Text & CAD | - | - | This dataset is used for the enrichment of the campus features |

### 3.2.4 Software tools

For the success of the current study, several types of software tools were employed for data extraction, conversion, data processing, 3D modeling, analysis, and other wide range of purposes. The list of those software tools and their means of obtaining is compiled below, Table (3.3).

Table 3.3: List of Software tools adopted for this research study

| Software Name | Status | Owner/User | Function |
|---|---|---|---|
| ArcGIS 10.8.1(Arc Map, Arc Scene) | commercial | ESRI | used for data extraction, conversion, attribution, modeling, and analysis |
| Global Mapper | commercial | Hexagon | employed to coordinate conversion |
| Ultra-Map software | Commercial | Vexcel Imaging GmbH /GI2 | used for preprocessing of aerial imagery obtained from UltraCam Eagle aerial digital camera |
| POSPac MMS | Commercial | Applanix/GI2 | used to perform post-processing of airborne GNSS/IMU data |
| Inpho (MATCH-AT, MATCH-T_DSM, DTMaster, OrthoVista, OrthoMaster) | Commercial | Trimble/GI2 | employed to perform full photogrammetric processing and product derivation |
| Terrasolid (TerraScan) | Commercial | Terrasolid/GI2 | For manipulation of photogrammetric point cloud data and automatic building model vectorization from point data |
| SketchUp 2020 | cracked | Trimble/GI2 | For manual 3D model redrawing and texturing of the 3D model |

## 3.3 Methodology

In this section, a combination of methodologies followed to achieve the stated objectives has been described. The overall methodologies imposed involves photogrammetric data processing and 3D model reconstruction. The photogrammetric data processing was performed for the production of reliable information about the target surfaces and objects on them. Thus, the full photogrammetric strategies starting from pre-processing of the collected airborne data, automatic aerial triangulation, multi stereo-image matching, and 3D point cloud generation, DTM extraction, orthophoto production, and mosaicking steps were briefly conveyed. For photogrammetric processing and analysis, different commercial the shelf photogrammetric software has been utilized, which includes UltraMap software for image pre-processing and radiometric adjustment tasks, POSPac MMS software for airborne navigation data processing and EO extraction, Inpho software package to carry out fully automatic photogrammetric post-processing operation. Furthermore, the development of the campus geodatabase and 2D map, objects above ground height (nDSM) extraction, and the generation of 3D geometries of the spatial object from the photogrammetric dataset were briefly explained.

### 3.3.1 Photogrammetric Preprocessing

After the acquisition of aerial photography was completed, the collected aerial photography with GNSS IMU data was downloaded from aerial sensor storage into ground storage (Hard Disk) using workstation computers equipped with UltraMap software. The main data downloaded from the acquisition were aerial photographs and GNSS/IMU flight trajectory data. These data were raw data containing some sort of errors related to the imperfection of the acquisition process. Hence, both the downloaded data were undergone the pre-processing stage before using them as input for the photogrammetric post process.

#### 3.3.1.1 Image pre-Processing

Image preprocessing operations were performed on the collected raw image data to filter out unnecessarily recorded energy by the sensor during acquisitions. Such energy can be considered as noises to the image that are derived from the surrounding atmosphere (haze), platform (cone effect and image blurry), ground (fire smoke), and others. The preprocessing of the raw image data was carried out by the UltraMap software bundle, which is a distributed software suite for the complete processing of images recorded by the UltraCam sensor(Reitinger & Gruber, 2013;

Wiechert et al., 2011). By principle, the UltraCam images are captured as a separate band of CCD sensors (i.e., red, green, blue, panchromatic, and Nir) so that the collected raw imagery was stored in its respective channel. Hence, the first task was to perform fusion/merging of these separate band images read out from each CCD into single high-resolution four-band images (RGBI), the so-called Pan-sharpening operation. Pan-sharpening technique is a technique of making image fusion from a high spatial resolution panchromatic image with a lesser spatial resolution of the multispectral image to create a new high-resolution colored image with enhanced visual information by merging the color information of the multispectral image into a high-resolution panchromatic image(Agrafiotis et al., 2016). At this stage, the images were visualized and checked as if there was the existence of clouds, shadows, and other effects on the image to be filtered and corrected. Then, image radiometric adjustments and color balancing were performed to improve the visual quality of the aerial image by neutralizing effects such as image hotspots, shadows (cloud and terrain features), differences in illumination conditions, and different atmospheric effects on the images introduced during the aerial survey operation. The radiometric correction and color balancing was made by adjusting the absolute and relative level values (histogram statics), and gradation curve manually and also using an automatic high-level atmospheric correction model which removes haze and hotspot effects. Once the radiometric adjustment process has been completed, the final high resolution, pan-sharpened 8-bit true color (RGB) images were generated into uncompressed tiff Format.

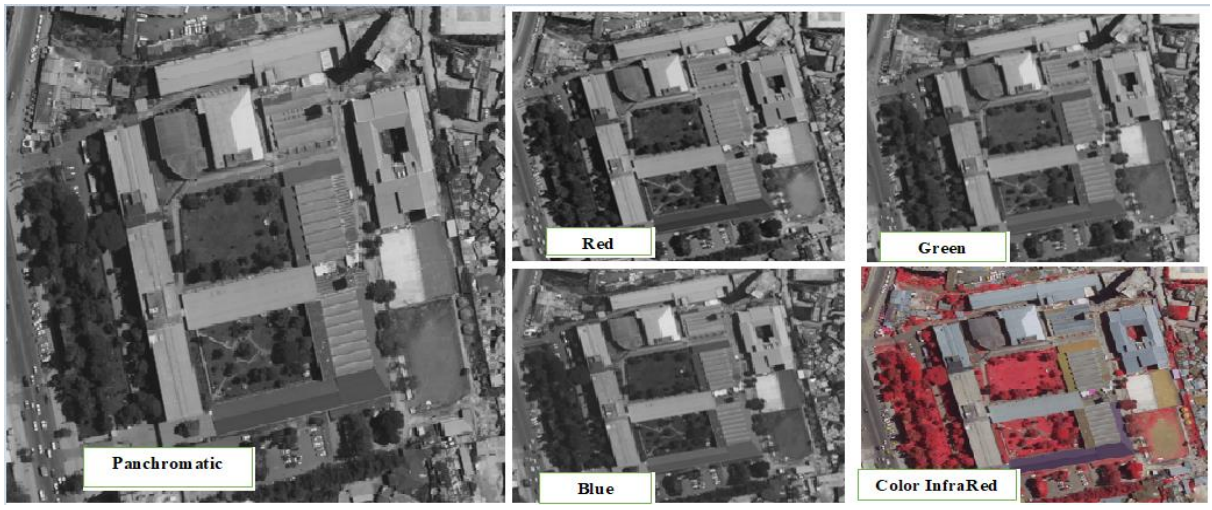


Figure 3.4: High-resolution Panchromatic Image(left) and four multispectral images(right) obtained from UltraCam Eagle aerial camera

### 3.3.1.2 Airborne GNNS/IMU data processing

The Position and Orientation (POS) data logged from navigation sensors such as a GNSS receiver and an inertial measurement unit (IMU) during aerial survey operation was just raw data collected from a moving aerial vehicle. These raw encoded data were undergone for post-processing operation to remove/ minimizae the alignment and observation errors, hence to yield an improved accuracy of the position, orientation, time, and velocity of the moving onboard GPS receiver. The Post-processing task was performed by employing the POSPac MMS software package from Applanix Corporation which is designed to import and process the data logged by POS AV technology. Thus, the raw POS data were imported into the POSPac MMS software and some of the important processing parameters such as offset values of lever arm and boresight misalignment information were filled before postprocessing. The Lever arm values are the misalignment distance in X, Y, and Z direction that the airborne GPS receiver mounted away (top of the aircraft) from the camera principal center (reference frame origin) which these shifts were obtained through manual tape measurement. Similarly, the boresight angles are misalignment angles between the camera perspective center and IMU sensor which were obtained through a separate calibration procedure made to be performed for this purpose and utilized for postprocessing too(Hutton & Mostafa, 2005). Thus, these two values were given to the processing software because even though the airborne sensor system is an integrated system, all the components mainly the GPS receiver, IMU sensor, and the camera principal center are not made to have the same origin (reference frame). Hence, these values were considered when computing the exterior orientation of the camera perspective center so that the camera, GPS receiver, and IMU sensor made to have the same origin, thus the computed position and orientation information referred to the camera projection center.

Once the required postprocessing parameters have been fulfilled, then from the POSPac MMS software, the GNSS-Inertial Processor tool was initialized and the precise point positioning (PPP) processing mode was selected to process the imported log data. For the PPP processing mode, the POSPac MMS software automatically searched and downloaded the available precise satellite final (14-day latency) ephemeris data via the internet. The downloaded precise ephemeris was then directly imported into the POSPac MMS software and the PPP processing was run so then the smoothed best estimate of the trajectory (SBET) was computed through automatic prediction and

update algorithm. The SBET is the optimal estimated trajectory of the moving aerial vehicle computed by removing the navigation sensors error(Hutton & Mostafa, 2005). Finally, from the resulted SBET, the exterior orientation information of each camera photo center was generated in local coordinate (Adindan datum, orthometric height(EGM08)) system given transformation parameters and orientation angles in decimal degree.

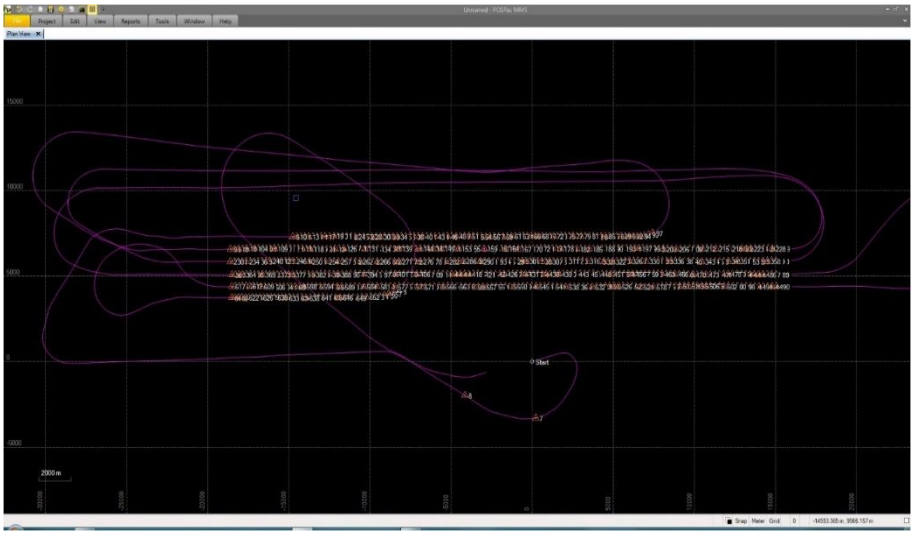

Figure 3.5: Real-Time flight Trajectory over AAiT campus (Addis Ababa project)

### 3.3.2 Photogrammetric postprocessing

#### 3.3.2.1 Project Definition and Automatic Aerial Triangulation (AAT)

For the current research study, the photogrammetric post-processing task was carried out using Inpho software bundles. The Inpho software bundle is a product of tremble Germany which has a sophisticated software algorithm to process aerial photographs and delivered products at higher precision. The INPHO software bundles consist of different software modules required to perform different photogrammetric processing tasks. Thus, project definition window, MACH-AT for automatic triangulation task; MATCH-T DSM for DSM generation task; DTMaster for DTM editing and generation task; Ortho-vista for orthorectification task and mosaicking.

The first task was to define a photogrammetric project block from a project definition window in such a way that a name was given to the photogrammetric block, the airborne camera model was selected and its intrinsic parameter (interior orientation) was defined based on the camera calibration report. Then, the radiometrically adjusted high-resolution images resulting from the image preprocessing were loaded to the defined photogrammetric project. Further, the approximate

post-processed position and orientation information (exterior orientation) of each camera projection center resulted from direct georeferencing technology was imported with their standard deviation value. Lastly, the field surveyed ground control point (GCP) data that define the coordinates of object space points were loaded to adjust and recalibrate the photogrammetric project. Thus, a block characterized by: 12 images with a GSD of 0.1m, lined up in two strips each containing six images, have an average overlap of 80/60 forward and side overlap respectively, and a similar number (12 with the aerial photographs) of EO information of the projection center where each EO tagged with its respective image, and three well-distributed GCP that form a triangle in the project area has been created (Figure 3.6).

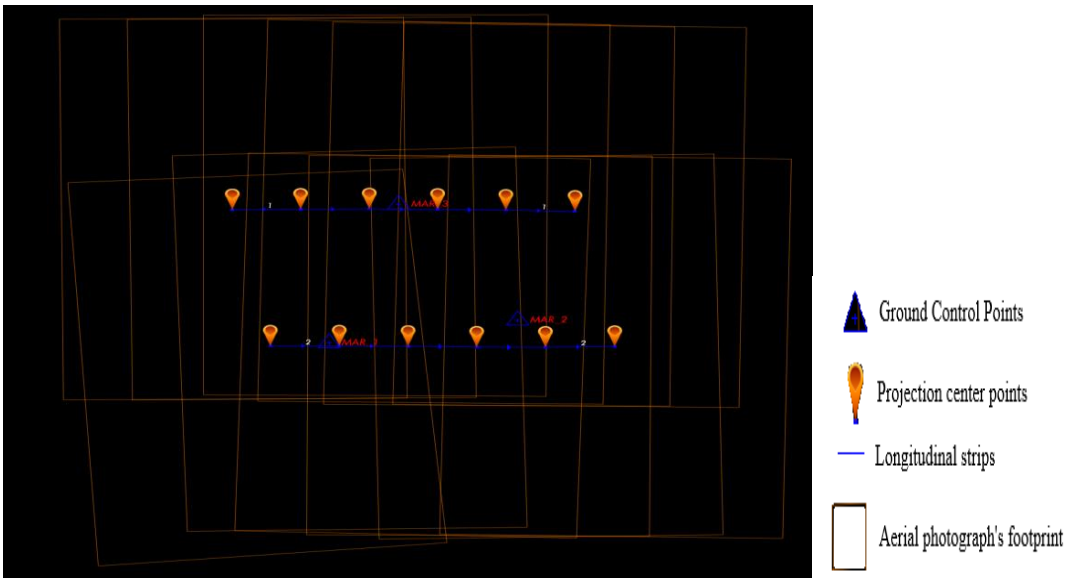


Figure 3.6: Defined photogrammetric block

Following the successful definition of the photogrammetric block project, an automatic aerial triangulation (AAT) operation was carried out to define the mathematical relationship between the 2D overlapping aerial photographs, the aerial camera sensor that obtained the photographs, and the ground coordinate as well as to improve the overall accuracy of the photogrammetric block. From the established relationship, the 3D position of the object points and exterior orientation information of all aerial photographs can be determined automatically from a photogrammetric triangulation software algorithm(Wu, 2017; Zomrawi et al., 2013). The software algorithm determines the 3D position of points in the real world through a collinearity equation. The collinearity equation is described as:

$$x - x0 = -f\left(\frac{m11(X-Xc)+ m12(Y-Yc)+ m13(Z-Zc)}{m31(X-Xc)+ m32(Y-Yc)+ m33(Z-Zc)}\right) \quad (3.2)$$

$$y - y0 = -f\left(\frac{m21(X-Xc)+ m22(Y-Yc)+ m23(Z-Zc)}{m31(X-Xc)+ m32(Y-Yc)+ m33(Z-Zc)}\right) \quad (3.3)$$

Where, f is the focal distance of the camera sensor, (x, y) is the image point coordinate, (X, Y, Z) are the 3D position of the object point, and (x0, y0) is the camera sensor principal point, (Xc, Yc, Zc) are the 3D coordinate of the camera projection center at the time of exposure, and mij are the elements of rotation matrix (ω, φ, k) in the direction of (X, Y, Z) respectively.

The AAT task started by performing block initialization using exterior orientation (EO) information of the aerial photograph to search for homologous points and hence well-distributed tie points in the overlapping photographs were generated. Tie points are points generated in the overlapping image area and recognizable in two or more aerial photographs (Jebur et al., 2017). The tie points were extracted automatically based on feature-based matching (FBM) and least square matching (LSM) algorithms. The FBM technique is used to identify the same feature across different photographs and create a series of homologous point features that could tie successive overlapping photographs using their image gray values (i.e., coarse point approximation)(Forlani et al., 2015). These tie points were then undergone for the refinement procedure based on the LSM algorithm using their location and orientation information up to the desired values in XYZ accuracy standards(Stal et al., 2012).

After the automatic tie point extraction, ground control point (GCP) measurement has been done at its exact location with high accuracy multi-photo measurement tool. The use of GCP helps to maximize the overall absolute accuracy of the photogrammetric block and also determines the ground coordinate of tie points. The GCP measurement was done on the photo coordinates of identifiable points in fully automatic measurement mode where multiple photographs were automatically registered to the measured GCP. From these measurements, postprocessing action was carried out to adjust the uncontrolled errors introduced in the exterior orientation parameter of the aerial photograph. Then, self-calibration was performed to enhance the camera parameters from the adjusted EO data and also for removing blunders through statistical analysis. These new enhanced camera parameters were then assigned to the defined photogrammetric block. Finally, the triangulation process was applied to the entire block, EO of each image, and the photogrammetric block was registered to the GCP for absolute orientation.

Once the automatic aerial triangulation processing operation was completed, the quality of the triangulation result was then checked. The assessment was performed visually as well as in an astroscopic environment. The stereoscopic assessment of the triangulation result ware performed in such a way that the triangulation result was imported into a stereo software tool, SMMIT EVOLUTION software and hence 3D measurement was made at the exact location of the GCP points using a 3D mouse and 3D stereoscopic glass. The coordinate value obtained from the 3D measurements and the actual GCP value were then compared and used to compute the root mean square error (RMSE) value of the AAT result. The RMSE is the square root of the mean squared differences between the coordinate values obtained from the triangulated dataset to be evaluated and the reference coordinate value obtained from an independent source with higher accuracy at the same location. These RMSE values are used to assess the quality of the resultant data as to the values observed, assuming all errors follow a normal statistical distribution (Chai & Draxler, 2014). Thus, the RMSE value of the automatic aerial triangulation result was calculated based on the following equations:

$$RMSEx = \sqrt[2]{\frac{\sum_{i=1}^{n}(Xri - Xmi)^2}{n}} \quad (3.4)$$

$$RMSEy = \sqrt[2]{\frac{\sum_{i=1}^{n}(Yri - Ymi)^2}{n}} \quad (3.5)$$

$$RMSEz = \sqrt[2]{\frac{\sum_{i=1}^{n}(Zri - Zmi)^2}{n}} \quad (3.6)$$

**Where** i is an integer ranging from 1 to N

n: Total number of points

*Xri, Yri,* and *Zri:* Reference GCP value in the X, Y, and Z positions, respectively

*Xmi, Ymi,* and *Zmi:* 3D measured coordinate value in the X, Y, and Z positions respectively

#### *3.3.2.2* Digital Surface Model (DSM) and Digital Terrain Model (DTM) Generation

Digital Surface Model (DSM) is a model that could tell the story of the earth's surface in three dimensions by capturing the elevation of both ground (land use, terrain) and non-ground features (i.e., buildings, trees, street lamps, etc.) of the environment(Brenner & Haala, 1999; el Garouani

et al., 2014). This 3D digital information of the earth can assist to develop the model of the feature used for a variety of applications such as smart urban planning and management, 3D city modeling, as well as heritage conservation, and more(Stal et al., 2012). Such 3D digital information of the existing earth's surface could be extracted using the concept of stereophotogrammetry, which uses a method of image matching principle utilizing the overlapping image information between successive aerial images. Thus, for the present study, the MATCH-T DSM software module was employed to retrieve a DSM of the study area from high-resolution aerial stereo imagery. The DSM extraction was performed in such a way that the aerial triangulation result (Inpho project file) was called into the MATCH-T DSM software and hence the software utilizes the calibrated sensor parameters, image overlaps, all control points (tie points and GCP), and other information in the photogrammetric block to constrain the matching process of feature points and edges. Then all the necessary DSM extraction parameters used by the multi-stereo-image matching algorithm like working boundary (AAiT boundary), generation type (DSM), area type (urban), mean terrain height (2495m), point density (1 pixel) output format (grid and point cloud), and others were properly specified. The multi-stereo dense image matching (DIM) algorithm is used to compute 3D points distributed across multilayered photographs depicting robust mutual information utilizing their image texture information and gray value, overlap information, AAT result, and others(Forlani et al., 2015; Haggag et al., 2018; Wu, 2021). Following the fulfillment of the control parameter, the MATCH-T DSM software carried out a pixel-by-pixel matching technique across multiple overlaid aerial photographs for the automatic generation of 3D information of the target surface. Thus, from this stereo view (algorithm to view the same terrain but from a different exposure station) aerial photographs, a high-density 3D point with a continuous topographical manifestation of an area, as well as the height of objects such as trees, buildings and other elevated features were determined.

Further, a copy of these generated photogrammetric DSM clouds data resulting from the automatic DIM process was then utilized for the extraction of digital terrain model (DTM) information of the working area and hence converted into the editing software compatible format (.dtm) file. Digital Terrain Model (DTM) is a digital bare-earth model (an elevation model) that contains elevations of natural terrain features such as barren ridgelines, peak/tops points, and river valleys (Sulaiman et al., 2010). The DTM was generated by digitally removing or filtering process of the above-ground elevations of surface features like vegetation, cultural features(buildings), and other

elevated features. The course of DTM generation for the present study was carried out by DTMaster terrain editing software where all the data files, aerial triangulation results, and the generated 3D point clouds (.dtm file) were called and then 3D relief perception environments have established on the digital photogrammetric workstation (DPW). Then, using the 3D immersive mouse and stereoscopic viewing (stereo eye glass) break lines were measured as a constraint of terrain filtering. Break lines are lines that tell the 3D analyst about the terrain surface level and they are traced on either side of elevated (above ground) features, and at the surface where sudden changes in terrain elevation and other discontinuities (like ridges, streams, and dams) were present(Ackennann & Krzystek, 1991; Ahmar et al., 1998). These break-lines are a good measure to ensure the automatic interpolation of the 3D surface point putting yields a fitted digital terrain model of the surface. The accuracy of the obtained DTM was then assessed through stereoscopic viewing as well as through the Global mapper point QC tool where the edited DTM as point cloud data and the selected three checkpoints were imported together into the Global mapper software. Then at the same location of strike between checkpoint and DTM data comparison was performed for each checkpoint's Z value and elevation of the DTM data from the LIDAR QC tool. Thus, the terrain elevation of edited DTM was automatically generated at the same position of each checkpoint. Finally, the RMSE value of the vertical dimension was calculated using equation (3.6).

#### 3.3.2.3 Orthorectification and Mosaicking

The ortho-rectification process has been carried out to remove/minimize the serious planimetric shift caused by the sensor effect, (e.g., tilting, perspective projection), platform (aircraft motion), and terrain effects to obtain a planimetrically corrected image(Ahmar et al., 1998; Haggag et al., 2018). The orthorectification process was carried out by OrthoMaster photogrammetric solution software. In the Trimble Ortho-Master software, necessary data files for the orthorectification process such as the block project file (Inpho project file), digital terrain model (previously edited DTM), and the study area as ortho-areas were imported. Then, orthophoto generation control parameters such as the defined pixel size (0.1m), output format (GeoTIFF), output datatype (8 bit), rectification method (exact or pixel-based), and others were specified. Based on these parameters, a fully automatic orthorectification process was then performed. Following a successful orthorectification process, ortho-mosaicking functions were carried out on the resultant orthophotos. The mosaicking function was employed to stitch the rectified photographs together to produce a single radiometrically homogenous digital orthophoto map (DOM) of the study area.

The ortho-mosaicking process was carried out by Trimble OrthoVista software tools. The OrthoVista software carried out a fully automatic ortho-mosaicking function through its automatic feature detection algorithm (urban area type) and hence generated a seamless and color-balanced mosaiced photo map. The resultant ortho-mosaic map was assessed for its planimetric positional accuracy using the ArcGIS accuracy assessment tools. The assessment has done in such a way that three selected independent checkpoints were imported as a reference layer and hence overlaid with a digital orthophoto (DOM) raster map (whose planimetric dimension going to be evaluated). Then, measurements were made on the orthophoto map at the same location of each checkpoint initially taken. Finally, the RMSE value of the produced ortho-mosaic image has been calculated automatically from the assessment tools utilizing the ortho-mosaic image as the data to be evaluated and the checkpoints as reference.

### 3.3.3 Geodatabase creation and 2-D Feature Extraction

For the present study, a data storage container was created as centralized scalable storage and management system. Thus, the ESRI file geodatabase was created using ArcMap 10.8.1 software to store spatial and attribute data. Following the successful creation of the ESRI file database, the previously generated high-resolution DOM was added to the ArcMap and the feature extraction process was then carried out using the ArcMap digitalization tool. The 2D shapefiles were extracted using the polygon tool, line tool, and point tool over the DOM through visualization of the feature's content such as color, texture, shape/region, position, and the edge of the features. The 2D feature extraction is about transforming features viewed in the image into a vector feature class stored in the geodatabase. To do so, empty 2D feature classes were created for each feature layer and added to the ArcMap window. Then, using a digitization tool with active snapping environment 2D vectorization of all AAiT campus features has been conducted. Parallelly, the attribution of each of these digitized features was also performed based on the ancillary data such as buildings names, number of floors, place names, and other formations collected from the campus facility department.

### 3.3.4 Normalized Digital Surface Model (nDSM) Extraction

The normalized Digital Surface Model (nDSM) is a raster surface where each cell has a value corresponding to the height of above-ground surface structures and vegetation(Hashemi, S.A.M., 2008). The raster surface is a continuous surface having a regularly spaced grid structure arranged

in rows and column elements (pixels or cells), which store its x/y coordinate as well as the third dimension (z) (Jebur et al., 2017; Parthibanraja & Purushothaman, 2016). The nDSM raster surface was derived by subtraction between the vertical information of DSM and DTM(Burdeos et al., 2015). The first step in obtaining the nDSM surface was the conversion of the previously produced 3D mass point data of DTM and DSM data into a continuous raster surface. The raster conversion of both DTM and DSM data was performed independently using ArcMap LAS Dataset to Raster conversion tool with conversion parameters. Thus, the DTM data conversion parameters were such as value field which was elevations, interpolation type which was triangulation with a natural neighbor interpolation method and the output raster cell size of 0.1m was used. Once all the required inputs have been given and parameters were filled up in the tool, a continuous elevation surface that manifests the bare earth was computed in such a way that the elevation of the un-sampled area was mathematically predicted from the nearby known mass surface points. Similarly, for the conversion tool, the DSM file (.las format) was given as input and parameters such as value field which was elevations, interpolation Type which is Binning with a cell assignment type maximum, along with a void filling method using natural neighbor interpolation, and the output raster cell size of 0.1m was set and hence raster surface of DSM data was generated as well.

After successfully creating both raster surfaces (bare earth surface (DTM) and DSM) as described, the MINUS function of the ArcGIS 3D Analyst tool was employed to perform the differencing operation between the two-raster surface. Here, the DTM raster surface was used as the base elevation surface layer whereas the DSM raster surface was used as the maximum elevation layer of the surface object.

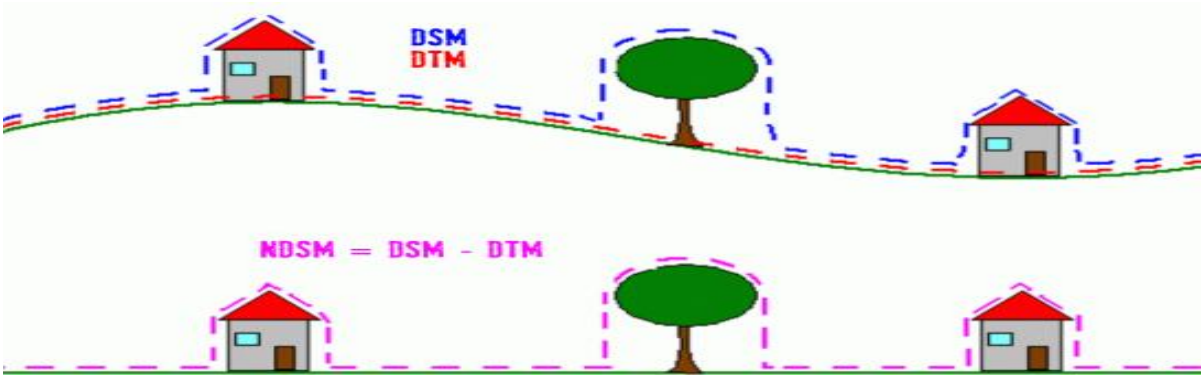


Figure 3.7: Illustration of the Normalized Digital Surface Model (nDSM)

(Source: Burdeos et al., (2015))

### 3.3.5 3D City Modelling (Campus Area)

In this section, the method of 3D model reconstruction at various levels of representation of the existing spatial feature within the study area has been presented. One of the first 3D models was about to create a plain or flat 3-dimensional model of the campus buildings, the so-called LOD1 model. Whereas the second type of model was the reconstruction of the 3D model of features that depicts a similar geometry as it exists in reality, especially the building roof shapes, which is said to be the LOD2 model.

#### 3.3.5.1 LOD1 Modeling

The LOD1 block model of the campus was rendered from the extracted 2D GIS vector features with the generated nDSM elevation surface. The modeling process has begun with the determination of each building element's height from the nDSM height layer by employing the ArcMap software. The determination of the elevation of each 2D building footprint has done by creating a set of random sample points from Create Random Points geoprocessing tool for each building boundary at a space of 1-pixel level (0.1 m) to march the resolution of the nDSM layer and to maximize the accuracy of the height information of the building.

Following the successful creation of a set of random sample points for each building boundary, the next step was to add nDSM surface elevation information to those points. Hence, the Add Surface information geoprocessing tool was employed to attribute the vertical information (Z value) of each generated random point from the nDSM surface layer. Then, the obtained height value of each random point was utilized by the ArcGIS Summary Statistics analysis tool to carry out the mean statistical calculation and hence to yield the average height of its respective building boundary. In the Summary Statistics tool, the Z value field was selected for calculation and the Common ID (CID) of the random points was used for grouping while the average height of each building boundary was calculated. As the obtained average elevation value of each building footprint was stored in a separate standalone table, the join operation was performed by the ArcGIS Join function. The joining function joins the table elements into each building vector feature using their common attribute (ID).

Unlike building features, the above-ground height information of the tree feature which is a point feature was not obtained through a statistical operation rather the added surface height value was directly used to determine the maximum height of the tree feature.

Following a successful determination of the above-ground height of building features and tree features, the LOD1 model reconstruction of each feature element has been carried out from the extrusion of 2D footprints into these height values. The ESRI ArcScene was employed for the generation of the LOD1 model utilizing three main ingredients: each feature (Building and tree) geometry, features height attributes, and extrusion commands. The building features have polygon geometry whereas the tree features have point geometry. The extrusion commands are instructed to use the height attribute field as the absolute elevation of each feature while performing extrusion. In this way, the 3-dimensional block model of the AAiT campus has been rendered.

#### 3.3.5.2 LOD2 Modeling

The LOD2 model is the 3D model of the existing physical structure that depicts all the external geometry of the feature including its complex roof shapes. The LOD2 model depicts all the specifications of the LOD1 model with detailed roof specifications. These LOD2 models could be reconstructed from very dense surface points where the generated photogrammetric dense point cloud was used as input for the reconstruction process of the LOD2 building models. The reconstruction process has been carried out by employing the Terrascan (Terrasolid) software with its user guide version 20 recommendations. Hence, the photogrammetric point cloud data (las format) were imported into the Terrascan software, and points were displayed as unclassified or zero class. However, for better manipulation of points, the imported point clouds were transformed into the default class (both object and ground surface points). Then, as these point clouds were randomly generated points from a dense image matching process, a sorting operation has been performed to sort each point into its continuous planimetric (x, y) position. From the sorted point dataset, a point cloud filtering operation has been carried out to remove noisy and outlier points. This is because the photogrammetric point cloud is usually suffered from the radiometric image quality (different illumination), presence of shadows, and object texture, and hence should be removed to reduce errors in the proceeding steps(Nex & Remondino, 2012). The identification and removal of these noisy points were done as if they were clearly below ground or in the air from their neighboring points by setting an absolute vertical distance (0.5m i.e., default value). Following the removal of unwanted/noisy points, the classification of points clouds has been done on the remaining active points. The classification of points on planar surfaces of any direction was performed to determine the category of each point that could smoothly fit the potential surface (model key points) of the scene. These categories of points were used to classify potential surfaces

such as default/unnecessary, ground, vegetation, and building surfaces. However, before classification, the active model key points were smoothened and thinned by point-to-point wise smoothing to modify points to their closest neighbors and hence reduce surface point thickness by keeping only the central points from the potential surface points (minimize the number of layered surface points on the same location). From the remaining thinned model key points, classification of the hard surface was performed to identify points that are extracted from the hard texture surface, potentially from the ground and building surface points. Hence, from the obtained hard surface points, points with the lowest elevation relative to their surroundings were classified as ground points. Once the ground points were successfully identified, the remained hard surface points with thinned model key points were grouped into the low vegetation class. Then, based on their relative vertical distance from the ground, low vegetation classes were classified into medium vegetation and high vegetation points (i.e., from 0.3-2 and 2-999 meters for medium and high vegetation classes respectively). Lastly, based on best fit geometry parameters such as minimum area (6 sq. meter), roof slopes (75 deg), height (2.5 m), visible band difference (color information), etc., building surface points were classified from medium and high vegetation class points. However, due to the noisy characteristics of the photogrammetric point cloud dataset, parametric automatic point classification was not sufficient to classify points into their true class. So, manual classification and modification of point classes (classify using a brush) have been performed.

Following the successful classification of the photogrammetric point cloud datasets into the ground, low vegetation, tree, and building class, the building class points were undergone for the reconstruction of the building model geometries. Thus, the TerraScan Vectorize buildings tool was employed to draw (vectorize) the best plane shape that fits a set of points of the building classes as well as based on the parametric details recommended by the TerraScan user guide (Version 20). The automatically drawn shape and reconstructed model of some building objects were not the same as it exists in the real world. In addition, the resultant model's constitute material was plain and untextured. Hence, the redrawing of some distorted shapes and edges of building objects as well as texturing of the roof of the building object from the orthophoto map were carried out manually by the Trimble SketchUp (version 2020) software. The general overall workflow adopted in this study has described in Figure (3.8).

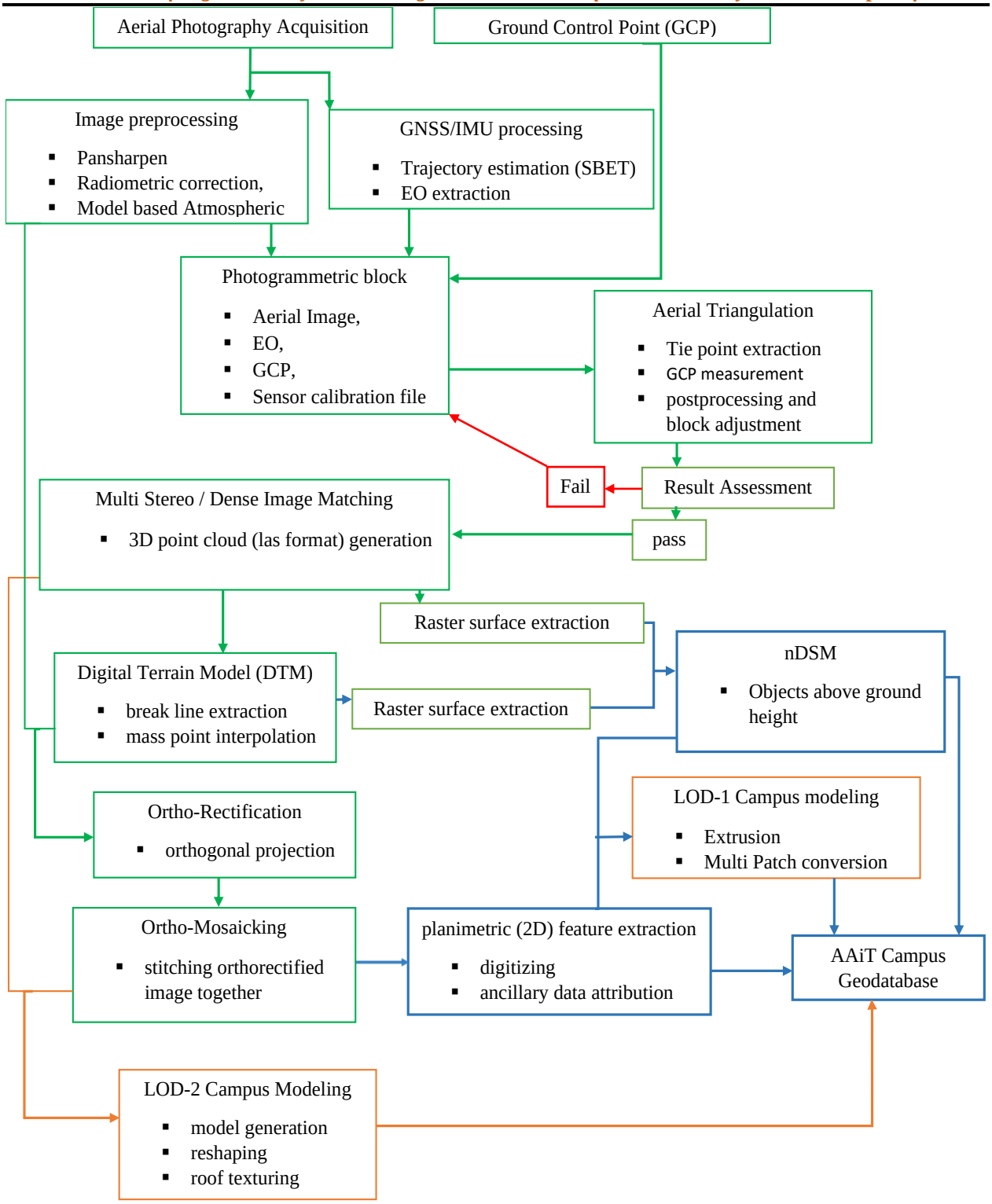


Figure 3.8: Overall workflow adopted in this study

# CHAPTER 4: RESULTS AND DISCUSSIONS

## 4.1 Results

This section of the research exhibits the results obtained from the adopted methodology in the previous chapter. Thus, the result of preprocessing of the aerial photographs and airborne GNSS/IMU data was briefly discussed. Further, the photogrammetric post-processing results such as the result of aerial triangulation with its quality assessment based on RMSE statistical value, the result of dense image matching operation and DTM production as well as orthorectification and orthophoto map production results were discussed. Furthermore, a campus geodatabases were developed and a 2D map of the study area was extracted, the height of the above-ground object was extracted and lastly, a 3D city model of the study area was reconstructed with two levels of representation (LOD1 and LOD2).

### 4.1.1 Data Preprocessing Result

The data resulting from the preprocessing stage were high-resolution aerial images and adjusted GNSS/IMU data. The resulted image data from preprocessing operation were a high spatial resolution (pan-sharpened) multispectral images resulting from the fusion of high-resolution panchromatic images with a lesser resolution of multispectral images. Furthermore, the resultant image is radiometrically adjusted from adjustments made to the image's histogram value. The resultant image color has also balanced and radiometric homogeneity across the overlapping imagery was maintained regardless of different illumination conditions, shadows, and others. Hence, a high-resolution aerial image with good visual quality and radiometric composition with a high coherency across multiple overlapping images and also high ground fidelity has resulted from the image preprocessing task. For the current study area, a total of Twelve (12) high-resolution pan-sharpened 8-bit RGB imagery, lined across two strips were generated in uncompressed tiff format.

Furthermore, from the processed airborne GNSS/IMU raw POS data, the real-time flight trajectory of the airborne vehicle was adjusted and get smoothed based on the precise satellite ephemeris data. The resultant smoothed and best-estimated trajectory (SBET) of the navigation data was obtained through the prediction and correction algorithm of the real-time navigation error by referencing the GPS satellite’s orbit and clock information. Thus, from the implementation of the lever arm values, boresight angles values as well as local coordinate transformation parameters,

the precise exterior orientation information of the camera center was extracted automatically in a local coordinate system (minimize the curvature effect) from the SBET. Thus, the generated EO depicts the precise direct georeferenced value containing the position and orientation of the airborne camera center at the time of acquisition. Considering the given transformation parameters for the software, the obtained EO referenced to the local Adindan datum, UTM Zone 37 North for X and Y position, orthometric height (EGM08) for vertical(Z) dimension, and also decimal degree for the 3-axis orientation angle (i.e., omega, phi, and kappa). The generated position and orientation data have an accuracy of 0.03m, 0.05m, and 0.05 in the X, Y, and Z positions respectively, as well as 0.008 arc-min for all orientation angles.

### 4.1.2 Automatic Aerial Triangulation (AAT) Result

The AAT was performed by Inpho MATCH-AT software, where little or no help from the operator (everything has done automatically), except GCP measurement. Before the AAT operation on the defined photogrammetric block, well-distributed tie points that connect each of the overlapping photographs were generated from the automatic feature-based matching (FBM) and least square matching (LSM) technique. The automatically generated tie points were completed across the block and tied all images of the block together using corresponding points and glued them to a mosaic. Moreover, the automatic registration of GCP points to the aerial photographs resulting that all the information in the photogrammetric block being calibrated or adjusted according to the ground surveyed value of object space coordinate reference value. Thus, from the resulted/adjusted exterior parameter information, a new camera model that has a new shift drift parameter was identified. These newly calibrated camera parameters (interior orientations) replaced the old sensor parameters and used with all of the information in the photogrammetric block for final bundle block adjustment which is resulted in the generation of absolute orientation parameters of each aerial image based on the GCP value. Thus, from the automatic aerial triangulation process, geometric inconsistencies were adjusted, an absolute orientation of the photogrammetric block with maximum accuracy was achieved, control points were densified (the ground coordinate of tie points was determined), and a photogrammetric block with undisturbed image orientations (different view positions of images to one reference, the GCP) have resulted for digital stereo image matching.

Following the aerial triangulation process, the obtained standard deviations of EO, ground control points, and overall accuracy of the entire block adjustment were checked visually from the triangulation report. Additionally, the RMSE of the triangulation result was calculated (Table 4.1) from the 3D measured value and the surveyed GCP value. Hence, the RMSE value of 0.0351m, 0.0662m, and 0.0858m in the X, Y, and Z coordinates respectively were obtained.

Table 4.1: The RMSE of automatic aerial triangulation (AAT) result

| ID | Surveyed GCP Value | | | 3D Measured Value | | |
|---|---|---|---|---|---|---|
| | X(m) | Y(m) | Z(m) | AT_X, (m) | AT_Y, (m) | AT_Z, (m) |
| MAR_1 | 473561.2 | 998737.2 | 2451.69 | 473561.3 | 998737.1 | 2451.755 |
| MAR_2 | 474280.3 | 998856.2 | 2446.2 | 474280.3 | 998856.3 | 2446.298 |
| MAR_3 | 473826.3 | 999464.2 | 2476.38 | 473826.3 | 999464.2 | 2476.471 |
| Mean square error in GCP (m) | | | | | | |
| **RMSE X= 0.0351m** | | **RMSE Y= 0.0662m** | | | **RMSE Z= 0.0858m** | |

### 4.1.3 Digital Surface Model (DSM) and Digital Terrain Model (DTM)

For the present study, the Digital Surface Model (DSM) which describes the means sea level (MSL) elevation information of natural terrain, and all reflective surface features such as the buildings, trees, and other elevated features were derived from multi-stereo image matching process carried on triangulated results. It has been obtained from an automatic pixel-based image matching algorithm that utilizes the level of similarity of objects on multi-layered aerial images carried out by MATCH-T DSM software. In the matching process, 3D surface points in the form of a point cloud were generated. The point cloud DSM data contains randomly distributed three-dimensional surface points that have LiDAR-like characteristics over the working area and hence it has stored as .las file format with only one return information. The extracted photogrammetric point cloud data has a density of 100 points per square meter (one 3D point per pixel), given an aerial photograph of 10cm (GSD), 80% forward overlap, and 60% side lap, and triangulation results. All objects (buildings, trees, ground,) found on the surface could be detected quite well from the resulted point cloud data, and also the discrimination between surface features (buildings, trees) could be done easily (Figure 4.1). Furthermore, the point cloud data have got colorized from

the color information of the stereo images they derived from and have a complete representation of digital surfaces.

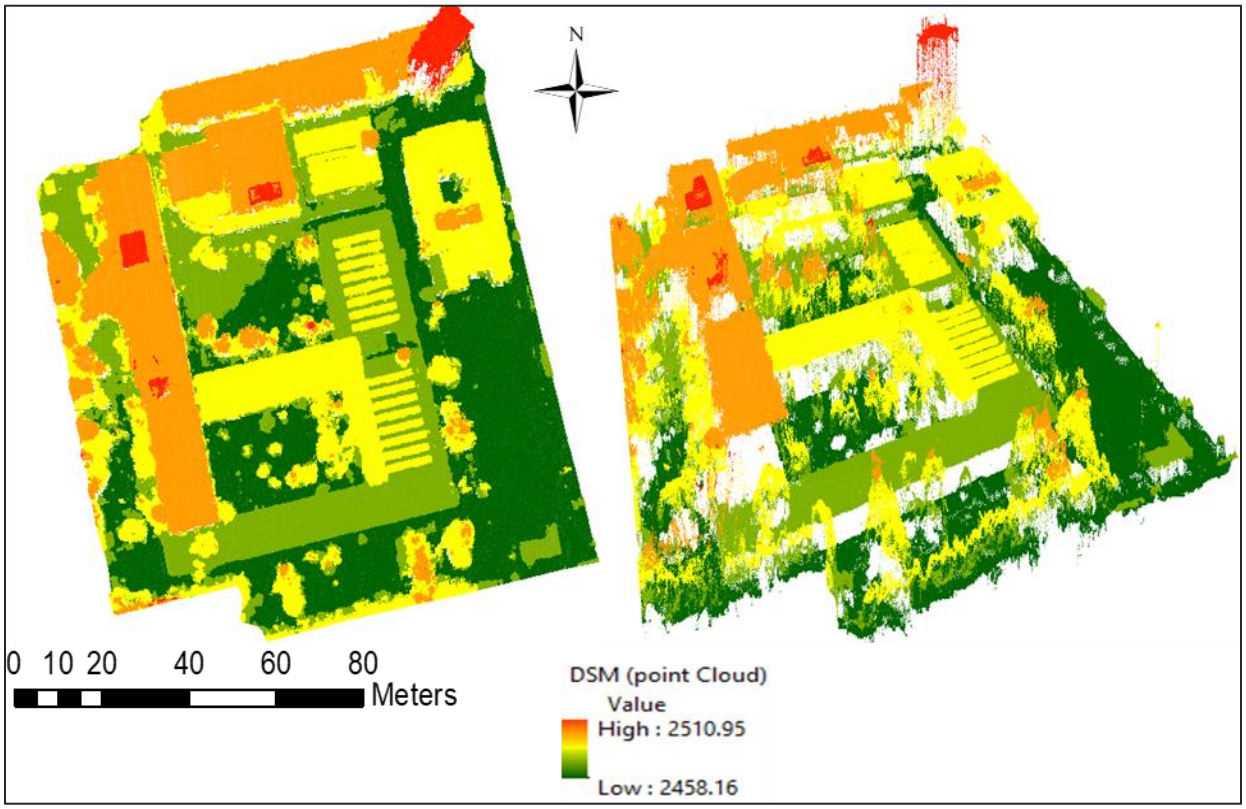


Figure 4.1: The Extracted Digital Surface Model (DSM): top view (left) and slant view(right)

The point cloud DSM was later used to extract the digital terrain model (DTM) data and also used to measure the three-dimensional metric information of important spatial features (buildings, trees, etc.), for the reconstruction of their digital 3D models and other applications. Thus, a copy of the generated photogrammetric point clouds was then further manipulated, and hence the bald earth model, the so-called digital terrain model (DTM) was extracted. The digital terrain model (DTM) of the present study was extracted from the removal of all non-ground objects from point cloud data using DTMaster stereo software tools. The removal of the elevated surface feature was performed by referring to the stereoscopically measured break-lines. The break-lines were extracted in a 3D relief perception environment by surrounding the elevated surface objects and at the place where there is a change in terrain slope. The measured break-lines acted as a filter and thus all the vertical heights of the surface object were set to take its terrain height through

mathematical morphology. Thus, a bare earth model (DTM) of the study area with minimum and maximum terrain heights of 2462.15 m and 2471.84 m, respectively has been obtained.

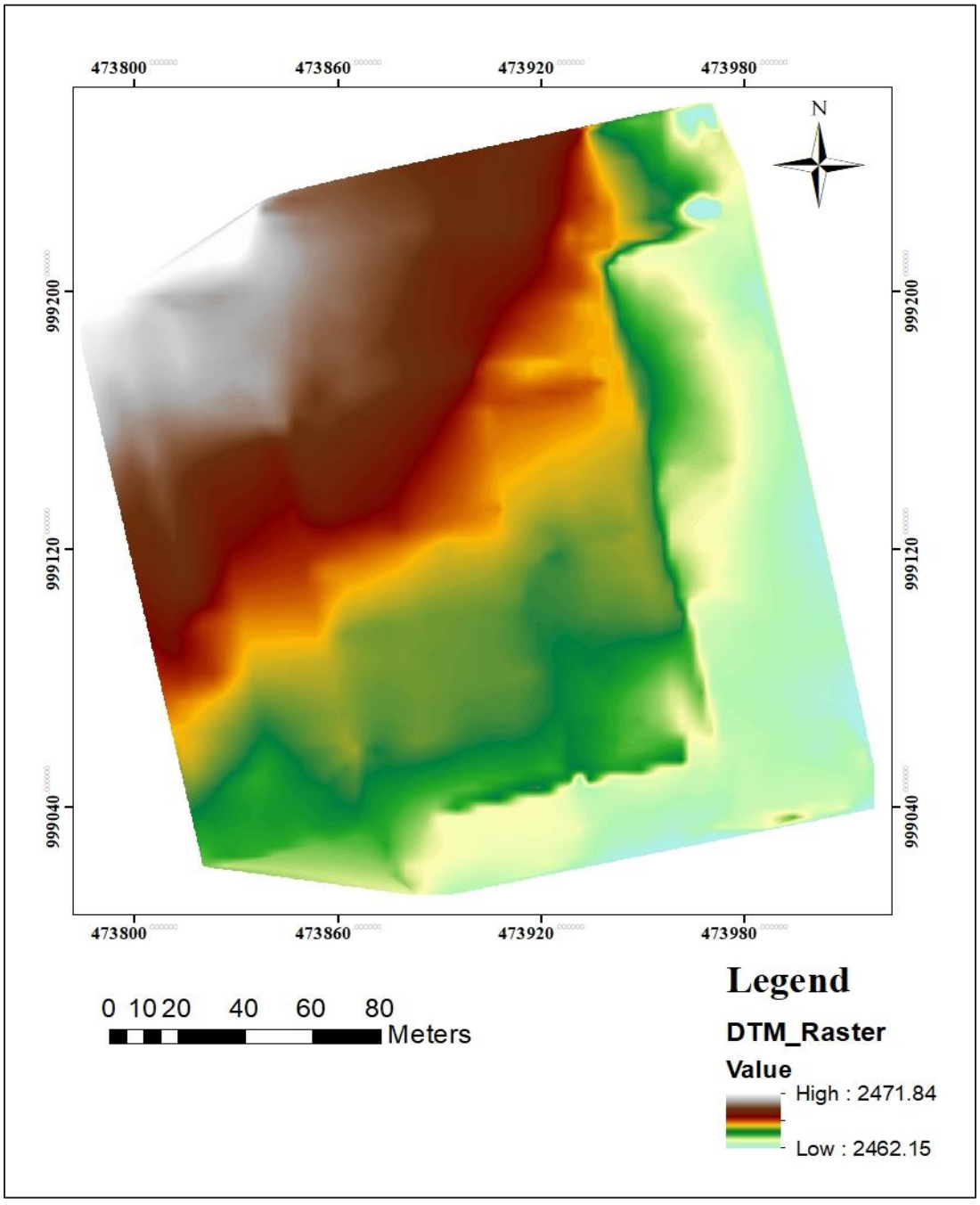


Figure 4.2: Digital Terrain Model (DTM) result of the AAiT campus area

The derived Digital Terrain Model (DTM) accuracy was assessed through stereo visualization and also it has been compared with independent reference data (checkpoints), thus the RMSE values

were calculated. The computed RMSE value between the DTM and checkpoints at the same location was 0.1615m in the Z coordinate (Table 4.2). This DTM was further used for the orthorectification process for the aerial images and also used as the base elevation on which objects such as building models, trees, and others are placed.

Table 4.2: The RMSE of the generated DTM (vertical dimension)

| Check Points | Checkpoint Coordinates | | | Edited DTM terrain Elevations (Z), (m) |
|---|---|---|---|---|
| | X (m) | Y(m) | Z (m) | |
| 1 | 473855.629 | 999140.989 | 2469.359 | 2469.148 |
| 2 | 473942.355 | 999212.67 | 2467.267 | 2467.126 |
| 3 | 473902.897 | 999024.285 | 2465.786 | 2465.668 |
| **RMSEz** | | | | **0.1615m** |

### 4.1.4 Orthophoto and Mosaicking

Orthophotos of the study area were produced from the automatic orthorectification process carried out on the triangulated aerial photographs with the camera calibration data and edited digital terrain model. The resultant orthophotos have resulted from the pixel-by-pixel basis rectification of each aerial photograph utilizing the digital terrain model (DTM) so that serious planimetric shifts were get removed or minimized. Hence, the produced orthophotos have a minimum or no relief displacement, and sensor tilt information which means physical features (e.g., buildings, vegetation) could be viewed straight down over anywhere in the photographs. Thus, each of the resultant two-dimensional ortho-rectified photographs has a true orthographic projection and also has a uniform scale similar to a planimetric map. The individually orthorectified overlapping photographs were then seamlessly mosaicking or stitched together into a single large colored image (DOM) covering the study area. This seamless digital orthophoto map (DOM) of the study area resulted from the automatic feature detection algorithm and hidden features/areas introduced by terrain or feature shadow in the orthoimage were filled from overlapping orthophotos. The generated ortho-mosaic map has a pixel size of 0.1m and all features are visible and represented in their true positions. The orthophoto map can be used as a reference map for realistic visualization as well as for spatial data extraction used for 2D city/regional planning.

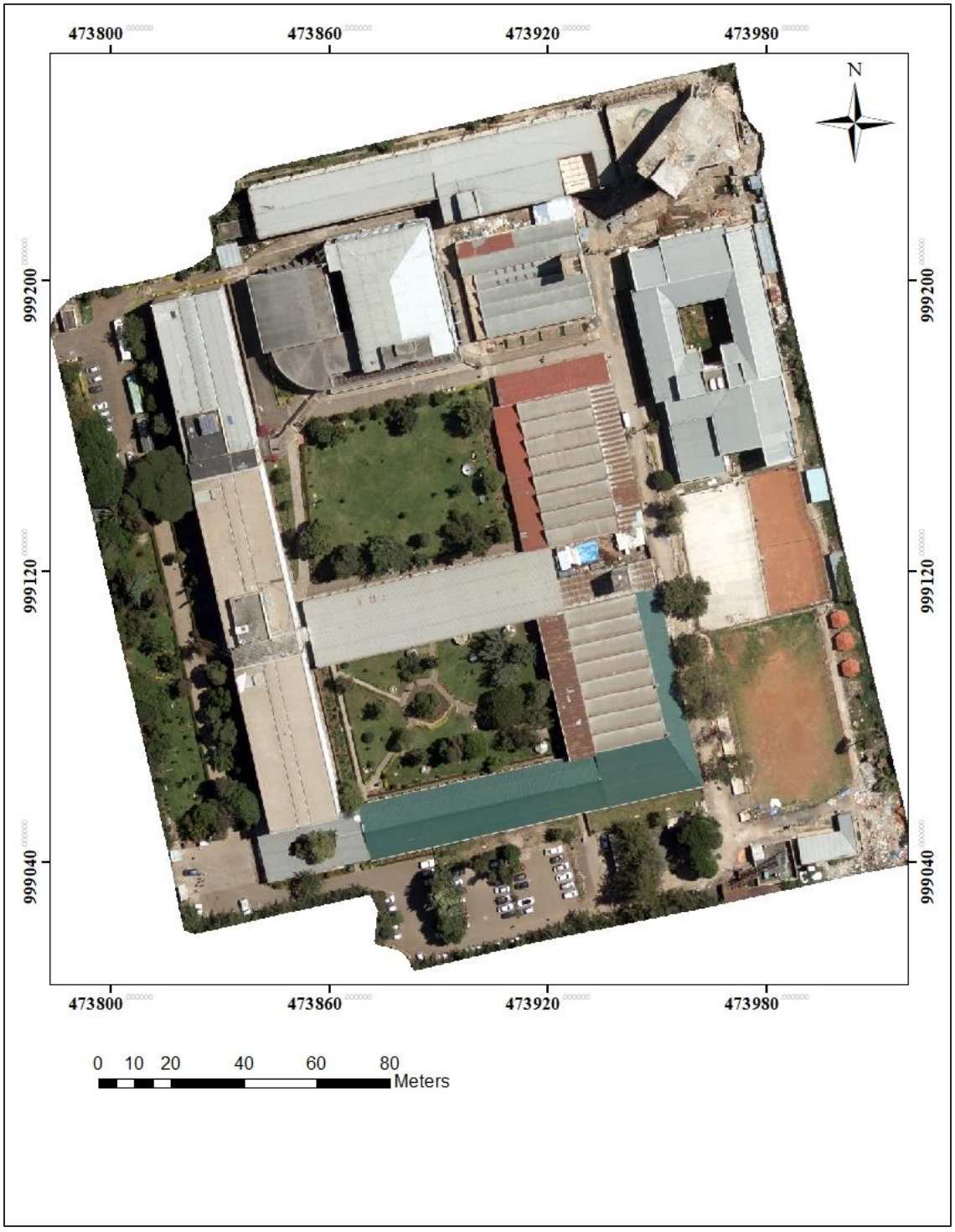


Figure 4.3: Digital Orthophoto (Orthomosaic) map (DOM) of the AAiT campus area

The accuracy of the resultant digital orthophoto map was assessed and its RSME was calculated by comparing it with the designed horizontal checkpoints. Hence, the automatically calculated

RMSE value was 0.0658m, and 0.0905m in the X and Y coordinate respectively (Table 4.3). The resultant ortho-mosaic map was utilized in GIS as a base map for the extraction of 2D information about the physical features present on the campus.

Table 4.3: The RMSE value of the planimetric dimension of the Orthophoto map

| Check Points | Checkpoint Coordinates | | | Orthophoto map Coordinates | | |
|---|---|---|---|---|---|---|
| | X | Y | Z | X | Y | Z Elev. |
| 1 | 473855.629 | 999140.989 | 2469.359 | 473855.7126 | 999140.859 | 0 |
| 2 | 473942.355 | 999212.67 | 2467.267 | 473942.2928 | 999212.583 | 0 |
| 3 | 473902.897 | 999024.285 | 2465.786 | 473902.9433 | 999024.2944 | 0 |
| **RMSEx = 0.065829767** | | | **RMSEy= 0.09048705** | | | |

### 4.1.5 Campus Geodatabase and 2D features

For the present study, ESRI file geodatabase was created and made to be a default storage location of spatial and attribute information of the AAiT campus feature. The file geodatabase provides better data integrity, backup, and security as well as ease of GIS operation carried out within the campus. Within this geodatabase feature classes (geographic features) were created and their geometry was extracted from the ArcMap onscreen digitization tool. Thus, from the backdropped high-resolution ortho-mosaic image (DOM), the two-dimensional outline of spatial features such as buildings, trees, open ditch, walkway, playground (basketball, football; and tennis field), parking, green area, open space, and reserved space layers of the campus was extracted. The ArcMap snapping environment ensured the geometric coincidence between extracted feature layers and hence the feature's edge and junction connectivity were maintained on the fly. As the digitization was performed on rectified 2D ortho-mosaic imagery, the extracted 2D vector features didn't contain any of the elevation (Z) values. However, each of the digitized features in the campus was made to join its respective attribute information collected from the campus facility management. Attribute information is the aggregate of information used to reflect the spatial characteristics of the objects and hence it can be used to present the object in graphs and diagrams. From the collective layers of all the digitized feature classes, a 2D map of the AAiT campus was developed (Figure 4.4). The maps describe the ground outline of the buildings and other features.

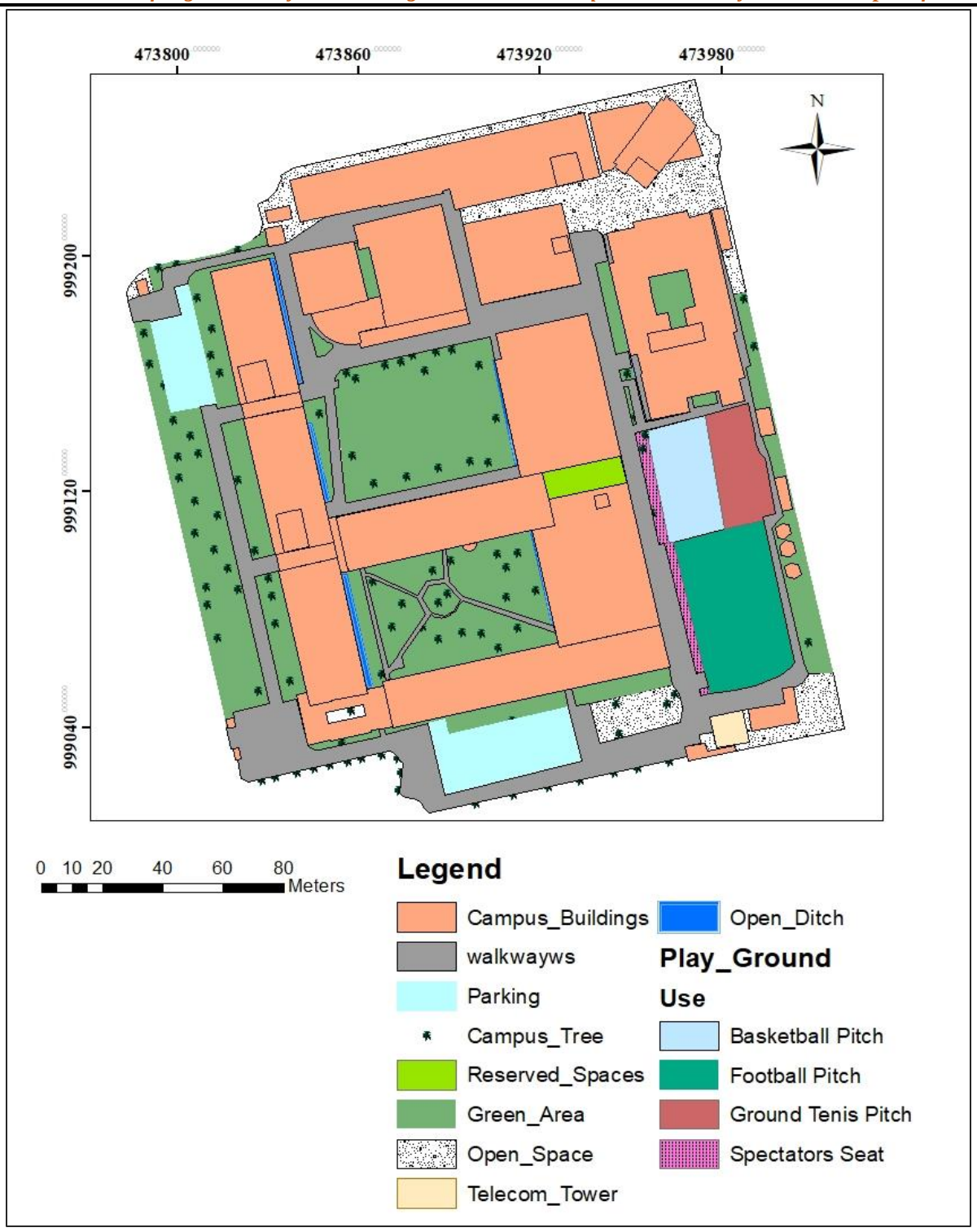


Figure 4.4: Two-dimensional (2D) map of the AAiT campus.

### 4.1.6 Normalized Digital Surface Model (nDSM)

The Normalized Digital Surface Model(nDSM) has resulted from the minus operation performed between the rasterized DTM and DSM data. As it can be shown below (Figure 4.5), the resulting nDSM is a continuous raster surface that contains absolute elevation information of the above-ground structures and vegetations relative to the terrain. The nDSM considers the ground terrain model (DTM) as a reference or base elevation while determining the height of the object. The resulted nDSM has a similar boundary extent to the inputted Raster DTM and DSM and also attains a similar cell size of 0.1m. The obtained elevation result reflects that the maximum above ground height within the campus is 44.23m while the minimum height is an underground ditch with a height of -6.9m. These height models were then used as a fundamental component in establishing the vertical placement of all the existing spatial objects without the influence of the terrain level which in this case the rooftop of each building element, and three feature classes.

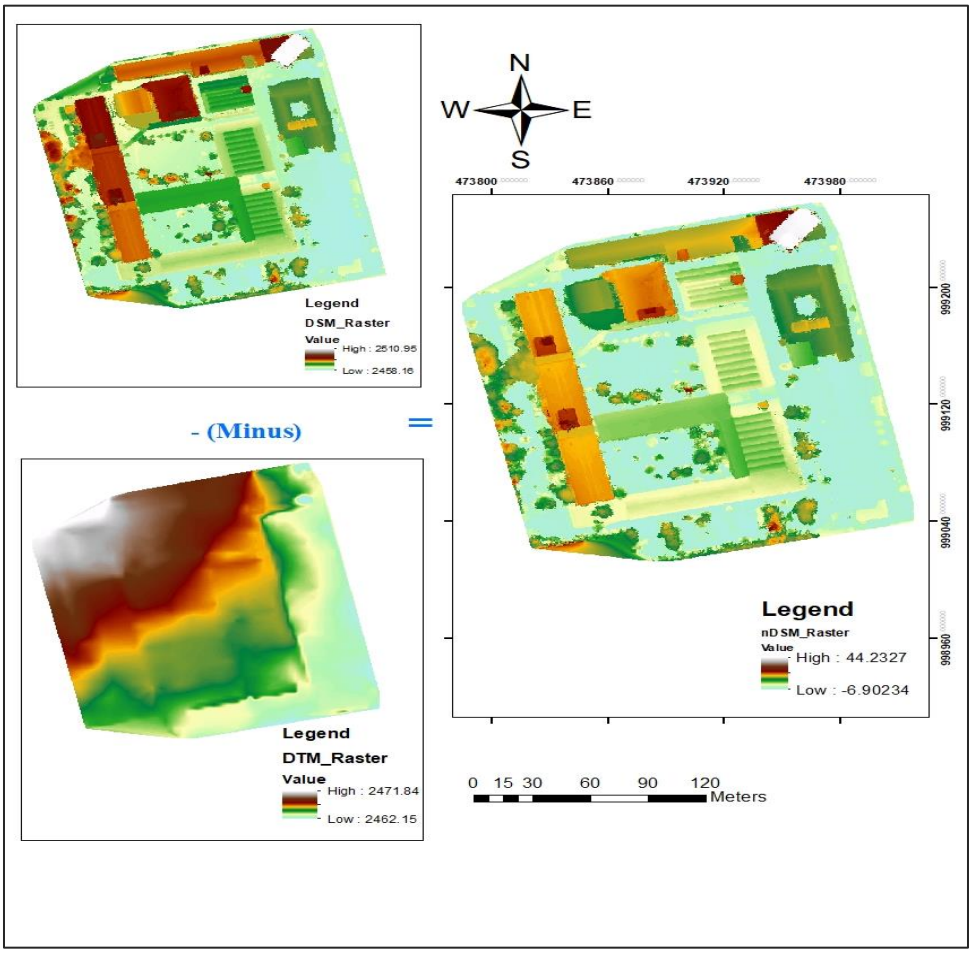


Figure 4.5: illustrates the nDSM of the AAiT Campus

### 4.1.7 3D city Model (AAiT Campus area)

#### *4.1.7.1* LOD1 Campus Model

From the reconstruction of the 3D modeling process, the present study produced two types of 3D models of the physical feature that existed in the study area. One of the generated models was a flat 3D model, the so-called LOD1 model of the scene that doesn't describe much detailed information about the model features. Such a block-wide 3D model of the campus was modeled based on the previously digitized 2D vector features (buildings and trees) and its average height value extracted from nDSM raster data. The average height value of each building has been obtained from the randomly generated sample points at a space of one pixel level for each building. The generated set of random sample points was lie inside of each building polygon boundary which later each random point took their elevation information at their right location from the nDSM surface. So then, from their belongingness in the building boundary (using their Common ID), a mean statistical operation was carried out, and hence average elevation of the respective building footprint was estimated. The output average height value of each building was generated in the form of an independent database table based on their respective Common ID. This resultant database table demonstrated the minimum and maximum average height of the building as 2.67m and 36.10m, respectively. The resultant average height of each building element was written into the buildings vector layer from the join operation utilizing their Common ID (CID) field. Similarly, the digitized 2D point tree features were involved in the generation of a 3D flat campus model from which the tree feature was taken its elevation from the nDSM raster surface and stored as the maximum height of the tree without being averaged.

From the estimated height attribute information stored in the building feature and tree feature attribute, the ESRI ArcScene extrusion command generated the 3D flat model of the campus. The vertical extrusion of features was made according to the estimated average height field of the building feature and the surface height value of the tree features derived from nDSM. The resultant LOD1 model of the campus was a flat/ box model that draped over the terrain with less detailed information specially the roof structure for building features and the models were stored as 3D multi-patch features for its suitability to perform 3D analysis.

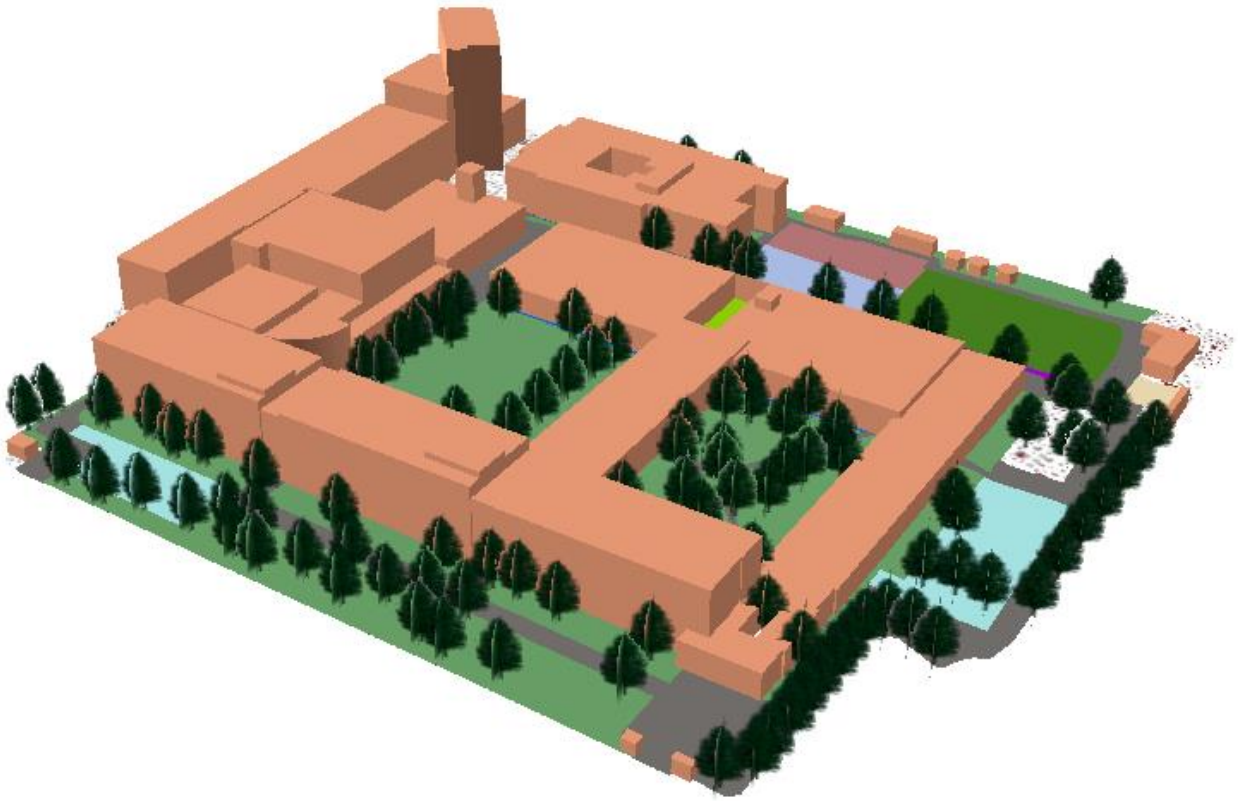

Figure 4.6: The 3D Block Model (LoD-1) of AAiT Campus (slant view from the main gate).

The resultant LOD1 model of the AAiT campus could be a more interactive tool for the campus system and capable to carry out 3D analysis, despite the lack of building roof details and texture materials.

#### 4.1.7.2 LOD2 Campus Model

The LOD2 model of the present study is the upgraded model of LOD1 that has been reconstructed based on the previously generated dense photogrammetric point cloud data. The photogrammetric Point cloud DSM which is composed of a 3D mass point where each point stored the X, Y, and Z position of ground and elevated features was utilized for automatic reconstruction of 3D building feature geometry from parametric command (Macro rule) of the TerraScan software. The photogrammetric point clouds were randomly generated from the image matching process and thus it has been rearranged or sorted into their planimetric (x, y) location for effective modeling and improved point cloud processing efficiency. From the sorted point cloud, the unnecessary and noisy points resulting from false image matching operations due to different image radiometry, texture, and shadow were identified and removed from the point cloud dataset. The removed noisy

points were points that were clearly below ground or in the air falls outside (isolated) a vertical distance greater than 0.5 m from their neighbor points, hence helping to remove the introduction of faulty geometry in the feature model. From the remained active points, potential surface points (model key points) that represent the real surface of the scene such as ground, vegetation, and building surface points were identified. These potential surface points were smoothened in their horizontal and vertical dimension and hence a more homogenous representation of surface points was obtained. Moreover, the thinned operation was performed and hence unnecessary density points were excluded so that the central potential surface points were kept and a cleaner surface was created from the potential surface points. From the thinned model key points, hard surface points that depict only ground surface points, and building surface points were identified. The hard surface points have been assessed based on their elevation value so that the points with the lowest elevation in their surroundings were permanently grouped into the ground surface point class. The remaining thinned model key points and remained hard surface points were classified into a low vegetation class where later this class of points with a height greater than 0.3m from the ground were classified into the tree (medium and high vegetation) class. Further, based on best fit geometry parameters such as minimum area, roof slopes, height, point color information, etc., the previously tree surface point classes were classified into building point class and tree. In the process of classification, each point in the cloud dataset was evaluated according to its properties as well as the used parameters and hence assigned to where it should belong.

Even though the automatic classifier of the TerraScan software performed very well assignment of points into where points should belong, some incorrectly classified points were manually brushed into its true point class. Hence, the imported photogrammetric point cloud was classified into multipoint feature classes such as noisy/unnecessary, ground, tree (medium and high vegetation), and building point classes. This classification of point clouds into their belonging is an important operation that supports the automatic extraction of feature geometry such as building model, tree model, road geometry, and other object information extraction.

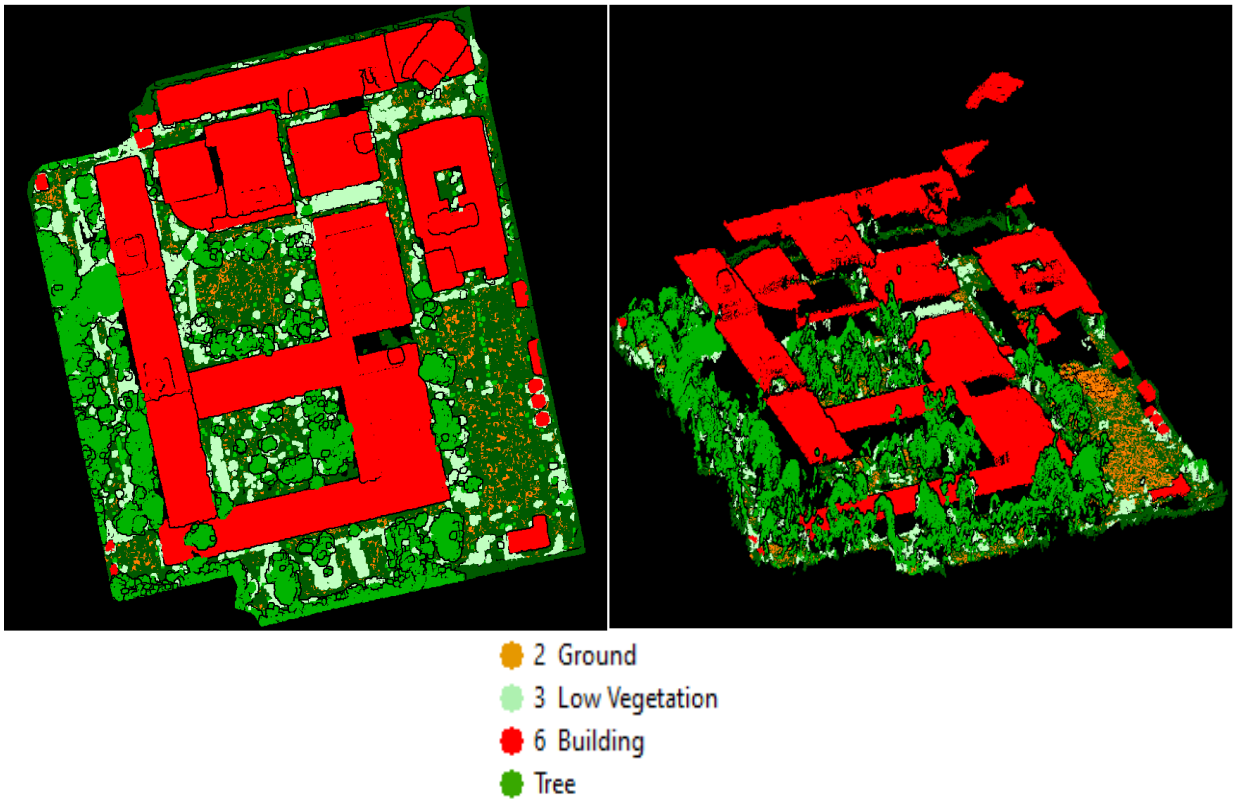


Figure 4.7: Classified photogrammetric point cloud; Top view(left); Slant view (right).

After the classification process, from the building class points, a wireframe 3D model of the building structure was successfully generated automatically from the building vectorization tool of the TerraScan software, and hence each part of the building face was drawn from the best fit points. A wireframe model is the 3-dimensional model of a building object or some other object represented by the number of vertices and edges. The automatically reconstructed wireframe model of the building was redrawn manually into its true geometry by SketchUp software so that the distorted corners and edges of the buildings were gone. Furthermore, the roof of the building models was manually textured from ortho-mosaic images. Texturing of the model gives a realistic impression of the building by making the 3D model more similar to a real object and more adequate for human perception and understanding. The reconstructed 3D model in this research shows a pretty good result and the model has walls starting above the ground, roofs with their texture, and other geometric details.

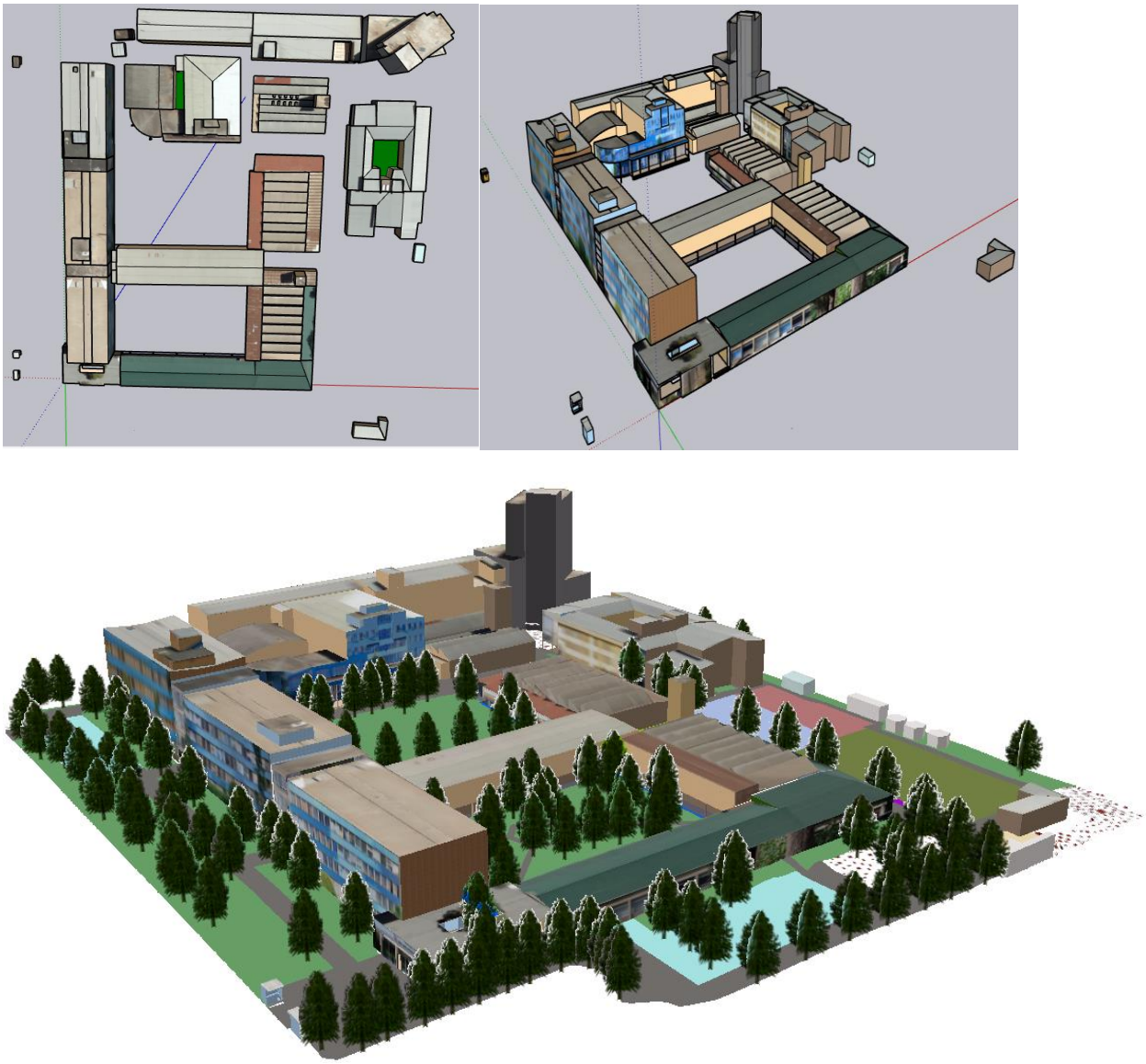

Figure 4.8: The Extracted LOD2 Building model of the AAiT Campus; top view (top left), Slant view (top right), and whole LOD2 Campus model (bottom).

The quality of the reconstructed 3D model was assessed on its vertical dimension (i.e., above-ground object height) and hence the RMSE value of the model's vertical dimension has been computed for the selected eight-building models having almost flat roof type (Figure 4.9) by comparing the photogrammetric based obtained building model height and the standard height (i.e., number of floors multiplied by 3m) of the physical building in reality. Thus, the resulted RMSE value was 0.545m in its above-ground vertical dimension (Table 4.4).

Table 4.4: Vertical accuracy assessment of the produced 3D model

| OID | Building Name | Usage | No_of Floor | Standard_Bldg Height (m) | Obtained_Bldg Height (m) | Difference (m) |
|---|---|---|---|---|---|---|
| 2 | | Water Tanker | 1 | 3 | 3.3787 | -0.3787 |
| 6 | G+10 Building | Installation | 12 | 36 | 36.1072 | -0.1073 |
| 7 | Sumsung Building | Installation | 4 | 12 | 11.3802 | 0.6197 |
| 12 | B-Block | Classrooms and Office | 5 | 15 | 15.5316 | -0.5317 |
| 16 | Bothy2 | | 1 | 3 | 3.0700 | -0.0701 |
| 23 | E-Block | Classrooms and Office | 2 | 6 | 7.0189 | -1.0189 |
| 25 | | Generator House | 1 | 3 | 3.2246 | -0.2246 |
| 26 | Workshop Building | Hydraulic, Civil, and Chemical Workshop | 3 | 9 | 9.6790 | -0.6791 |
| **RMSE** | | | | | | **0.5450 m** |

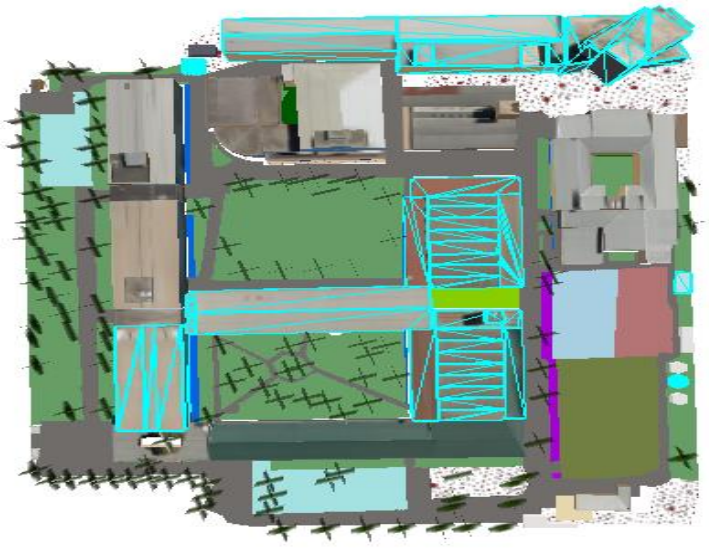

Figure 4.9: illustrates the Selected Building model for Vertical accuracy assessment

## 4.2 Discussions

This research work has investigated the approaches for the generation of digital 3D city models using the geomatics technique specifically the use of photogrammetric techniques has been studied. The 3D city model (3DCM) is not the firsthand product reconstructed by photogrammetric technique, rather it is the result of the complete workflow starting from photogrammetric processing operations, 2D/3D dataset production, footprint extraction, geodatabase creation, as well as 3D reality reconstruction.

The photogrammetric processing operation started from a defined photogrammetric block project containing an organization of required data sources such as radiometrically adjusted aerial images, estimated EO of the camera projection center, camera interior information, and GCPs for quality improvement. On the photogrammetric block, a fully automated aerial triangulation process was performed where an automatic algorithm recovers the precise 3D position and orientation of points in the image together with the new intrinsic parameter for the aerial camera, and object space coordinates of tie points were recovered(Darbas & Sužiedelytė-Visockienė, 2011). Thus, the result of the automatic aerial triangulation quality was assessed visually from the triangulation report and also the RMSE value was calculated for further demonstration of the triangulation result as well as to ensure and quantify the reliability of the result for further geospatial processing and production. Hence, an RMSE value of 0.0351m, 0.0662m, and 0.08580m in the dimension of X, Y, and Z respectively were obtained. These values are quite good where all are in the range of 1pixel and consistent with the standards set by ASPRS i.e., 0.5*RMSE of the map in all directions (X, Y, Z) for the same resolution of the data source (Abdullah et al., 2015). Thus, the AAT result meets the allowable accuracy to proceed further with geospatial data processing and production. This aerial triangulation result with other block information was used for the determination of the three-dimensional surface information (i.e., DSM) from a sophisticated multi-stereo-dense image matching algorithm. The algorithm performs an automatic pixel-based image surface interpretation and matching across sequences of multiple 2D aerial imageries and thus generated a 3D mass point dataset that depicts the precise three-dimensional coordinate information (X, Y, Z) of the terrain and physical objects. The currently produced 3D points are very dense that contain 100 3D surface points per square meter i.e., 3D point every 10 cm. As the extracted DSM points were at the pixel level, it provides a rich level of details and a good representation of the surface character of all objects (tree canopies, building roof structures, bald earth (topography) structure, etc.) located on

the target ground and also ensures to have a piece of complete surface information over the study area without any gap. In contrast, to point clouds obtained by other geomatics techniques such as the LiDAR technique, the produced photogrammetric point cloud density outperforms if not rivals those produced from typical LiDAR point density (Forlani et al., 2015; Guo et al., 2021; McClune et al., 2014; Nex & Remondino, 2012), despite the LiDAR technology is dedicated to providing high-density 3D point cloud at a high cost of sensor investments, a huge volume of data and high computational cost. Further, the generated photogrammetric 3D mass points were stored as a LiDAR-like structure (point cloud) consisting of only one return information, distributed uniformly over the surface. Yet again, this set of point cloud store color/spectral information to manifest every geometric detail of the area where feature discrimination detection and feature outline extraction from it is accurate as compared to the intensity image obtained from LiDAR point data that has a low spectral and radiometric resolution which is not quite suitable for feature extraction purposes(Kaartinen et al., 2005). The quality (geometric accuracy) of the generated photogrammetric point cloud defines the quality of the height of the 3D model to be generated from this point cloud.

Meanwhile, a copy of the photogrammetric point clouds was utilized for the extraction of the bald earth model (DTM). The DTM data were extracted in a 3D environment by measuring break-lines and form-lines to remove the elevated point to ground level point using an immersive 3D mouse and stereoscopic visualization. The measured break-line and form lines were used as a filter where 3D points located above or below these lines are mathematically interpolated into the level of these lines. Thus, a digital terrain model (DTM) that manifests the existing topography structure from mean sea level was produced and its vertical quality has been assessed based on independently selected vertical checkpoints (reference points). Hence, an RMSE value of 0.1615m at a 95 % confidence level in the vertical dimension (Z) was obtained. This vertical accuracy value of the DTM data was produced to meet the allowable vertical accuracy standards set by ASPRS in the non-vegetated accuracy (NVA) i.e., the allowable accuracy of DTM is 1.96* GSD of the source photographs (Abdullah et al., 2015). Thus, the extracted DTM surface manifests a good quality in its vertical dimension where the elevation information of macro-objects such as buildings, and vegetation was well detected and removed on the natural terrain surfaces. By taking this extracted DTM with other photogrammetric block information, the orthorectification process was performed. The orthorectification operation eliminates/ corrects every kind of distortion that the

aerial photographs suffered from and also transforms the aerial photographs from their original perspective/central projection into orthogonal projection where all features are uniformly viewed as the nadir. Thus, the ortho-rectified photographs have a fixed scale with all the characteristics of a 2D map and could be used in the same manner as a map. Furthermore, the orthorectified photographs were stitched or mosaicked together to give a single seamless, color balanced, and geometrically correct digital orthophoto map (DOM) of the project area. The quality of this DOM was assessed for its planimetric accuracy (x, y) with well-defined independent checkpoints selected from the triangulation solution, and hence an RMSE value of 0.0658m and 0.0905m in its x and y dimension respectively were computed. This value is better than the allowable error budget adopted by ASPRS for orthophoto accuracy which is 1*GSD of the source aerial photographs (Abdullah et al., 2015), which can be used for the highest accuracy mapping and renewal, reliable for city modernization, urban planning and management and so on(Ma et al., 2011).

Following completion of the photogrammetric processing operation, an ESRI file geodatabase was developed to be used as a data container to gather and store all the produced data at a single location. The ESRI File geodatabase was used as a central campus database for efficient integrity and storage of the campus datasets such as DSM, DTM, Orthophoto map, and others to be derived in the future. File geodatabase opted over personal geodatabase because, file geodatabase does not have a storage size limit and has better operational performance as compared to personal geodatabase (storage limited to 2GB only) (El-Mekawy et al., 2012). In the file geodatabase, 2D feature datasets were created to store 2-dimensional feature classes that have the same coordinate information. Thus, 2D feature classes were detected and extracted from the backdropped 2D digital orthophoto map (DOM) and hence the 2-dimensional campus map constitutes the outline of spatial features: building, walkways, trees, green spaces, parking, playground, reserved spaces as well as baren surfaces were developed keeping topological properties between features. The developed 2D map of the campus manifests the 2D cadastral map of the area in which all the spatial elements were represented at their ground level. Thereafter, the features above ground height (nDSM) were determined by differencing the conventional 2.5D (DTM and DSM surface) GIS raster dataset stored in the file geodatabase (Alomía et al., 2021). For the operation, the DTM surface acted as the base height whereas the DSM surface acted as the maximum feature height. The nDSM surface manifests the absolute height information of non-ground (artificial) features ranging from -6.90m to 44.23m which describes the height of excavated holes, buildings, trees, and so on.

From all these organizations of datasets stored in the campus file geodatabase; 3D model reconstruction tasks were performed. The 2D footprint of features was aligned over the DTM surface which acts as the foundation of 3D city models and ensures all objects are exactly located on the terrain. Thereafter, the associated above-ground height of these 2D footprints specifically the height of buildings and tree features was estimated and attributed to the feature from the nDSM surface. The height information assignment to the feature was performed by generating random points at each pixel level for each 2D polygon where these random points were made to take the surface information of the nDSM surface. Thus, the value of each random point was averaged based on their belongingness in the 2D boundary and hence the mean height value of the area was attributed/joined to the associated 2D feature. Thus, the 2D GIS data were extruded vertically to the limit of this height value and thus the LOD1 geometric model was quickly reconstructed. Since the automatic 3D extrusion command works to uplift every corner of the feature footprint to the same vertical level, a discrete LOD1 building model with a flat roof and a tree model of the same species type has resulted. Further, the LOD1 model manifests a solid geometrical model representation, in which the model's geometry described its boundary surfaces as a simple box/volume with no roof details and texture on it. Further, the LOD1 model demonstrates a building model represented by its boundary with a generalized shape defined by planar roof faces, nodes, and edges. These models were later transferred into a multi-patch feature class that consists of a set of triangles fused to form a multi-faceted feature that contains information of the terrain model, and objects model to represent a complete physical geometry model as well as to avoid spatial models floating over or sinking into the terrain (Vermeij & Zlatanova, 2001). Even though the developed LOD1 model is far from the existing realm in terms of its texture, it has higher visual perception and supports the distinction between features and visualization, simulation, 3D queries, and 3D analysis, and also it can be used for the presentation of the campus environment on the web. Furthermore, the LOD2 model which is one step higher than the LOD1 model was developed from the photogrammetric point cloud. The reconstruction process was not done directly from the photogrammetric point cloud, despite its being impressive in terms of completeness the points were unorganized, and also there were outlier points in the point cloud dataset as they suffered from the radiometric quality of the aerial photograph, photograph overlap, presence of shadows, and different object texture(Nex & Remondino, 2012). Thus, significant refinement of points for the removal of these outlier points (unwanted surface points) produced during dense image

matching has been done. Once the noisy point gets removed from the point cloud dataset, classification of points has been done on the remained points to categorize points into their real-world belonging using software recommended parameters (TerraScan) in conjunction with parameters determined by the researcher (considering the point density) such as vertical distance and angle, minimum details, slopes, and others. The categorization of points in the cloud dataset verifies the assignment of each 3D point into its meaningful object class as well as reduces the search limit of points to detect shapes in the automatic geometry reconstruction process(Yastikli & Cetin, 2017). Thus, the photogrammetric point cloud was classified into five classes namely unnecessary, ground, low vegetation, tree, and building class points. Further, the building classified were utilized to find the best fit points to detect the edge, corners, faces, and other geometric detail of the building and hence building models were fairly generated without any introduction of gaps and holes in the building part and also wall structures were generated from the edges of the roof to directly down till the lowest ground class points. The automatically generated LOD2 city mode manifests that the building model has a more faithful roof geometry, which is represented by more than one face, though building objects with complex roof shapes have suffered from unwanted/incorrect edges and surfaces due to the faulty points remaining in the cloud dataset. Thus, manual correction and redrawing of these faulty geometries and also texturing of the roof material from the orthophoto map enhanced the realism of the building model.

In general, the developed 3DCM (both LOD1 & LOD2) brought the current 3D geometric model of the most important objects i.e., buildings(Ozdemir & Remondino, 2018), of the study area into a digital reality by which any visualization, simulation, and interpretation made on the digital environment feels like in the physical scene. However, the LOD2 model looks more complete and better than the LOD1 model. For example, the LOD1 model is represented by its 3D outer boundary with vertical flat faces, sharp corners, flat tops, or bottoms which is less likely to attract all users equally and interpretation of this scene may not be easy for non-technical users. However, this model manifests the true impression of the height of the buildings and can be used by the users (freshmen, visitors, and the public) to easily recognize the geographical setting of the campus area by interacting with the digital view of the campus environment. In contrast, the LOD2 model has high variability in the geometry of building features (mainly building roof edges, vertices, and faces) that resembles realism and easy to communicate with users (even non-technical users can feel the sense of being there) because it has a greater visual fidelity of building roof structure with

its texture material as like as those exist in the real world. On the other hand, as the aerial photographs are only meant to show the textural description of the top structure, the reconstructed models (both LOD1 and LOD2) models do not contain any building façade and texture information, which such untextured 3D city models are not informative and considered as visually incomplete(Buyukdemircioglu et al., 2018). Thus, for the LOD1 model artificial textural descriptions were assigned to the face of the buildings. Whereas for the LOD2 model the issue has been tried to be compensated by the integration of photographs taken from manual terrestrial viewpoints. Both models can be stored on the computer, uploaded on the web, or converted to other formats and can be used for different applications ranging from visualization to 3D analysis (spatial and non-spatial), virtual roaming, updating process, and others. While users interact or communicate with the content of the model legend, direction and scale are not necessary for both LOD1 and LOD2 models, rather the user can communicate by a simple click action on the model which helps them to retrieve and display information about the model. Furthermore, the user can visualize by scrolling to a different viewpoint and can get clear information about the object's dimension just by "zoom-in" and "zoom-out" without the need for scale. Depending on the zoom level the user prefers, it's possible to interact with the model at different scales (campus, neighborhood, and, single building).

Figure 4.10. The LOD2 models are superimposed on the orthophoto: viewed at campus scale (top left), neighborhood-scale (top right), and building scale (bottom).

Similar to other technological products, the quality of the developed 3D city models was assessed to meet the completeness of production and metric quality. The assessment was made on the 3D model's vertical dimension and it directly related to the quality of the generated photogrammetric point cloud as the model's edge, corner, and face of the building were traced from the constitute point's X, Y, and Z coordinate information. However, as the quality of the vertical dimension up to the terrain level was already examined (DTM accuracy), this time the above-ground height information is assessed. Thus, the above-ground height information of the generated 3D model of the building was compared with the standard heights to be used for the building (i.e., 3m per floor), and hence the calculated RMSE value was 0.5450m which turned out in the range of five pixels for such rough estimation. On the other hand, (Jebur et al., 2017) assessed the above-ground height quality of the generated 3DCM and hence obtained an RMSE value of 0.3014m, despite the researcher having used the actual height of the building from precise surveying measurement and the building model height for comparison. Thus, the result of this study would have been better if the accurate measurement of the building height were used for comparison. This shows the performance and geometric fidelity of the photogrammetric techniques for extracting and detecting every geometric structure of the spatial object and how efficient this technique is for a precise model generation without additional cost.

# CHAPTER 5: CONCLUSION AND RECOMMENDATION

## 5.1 Conclusions

As the title of this paper has already implicated, this research study demonstrated the feasibility of digital 3D city model reconstruction by taking the AAiT campus area of Addis Ababa University as a pilot project area. The methodology adopted for the research was the use of the geomatics technique specifically highlighted the digital photogrammetric data production technique required for the modeling process. Thus, this research study has shown the complete process of the photogrammetric workflow started from the collection and preprocessing of high-resolution aerial photography that has a GSD of 10cm with 80% forward overlap and 60 % side overlap acquired from a stable manned aircraft and then post-processed with a digital photogrammetric solution software equipped with artificial intelligence (AI) and machine learning technique for automatic (limited manual intervention) processing operations such as aerial triangulation (with self-calibration) followed by multi-stereo-dense image matching and product generation. Thus, the automatic aerial triangulation operation determines the absolute 3D coordinates of points in the aerial photograph, as well as tie-points object space coordinates. Further, from a well-established state of the art photogrammetric multi-stereo dense image matching algorithm, the exceptional quality of photogrammetric point cloud which has100 points per square meter (point/pixel or 10cm) point density is quite higher than the density of point cloud obtained from a practical LiDAR project has been generated. Furthermore, other photogrammetric derivable like DTM, and orthorectified photo maps were produced. Thus, this study mainly covered three parts: i) exploring the workflow and performance of the photogrammetric technique, ii) database development and feature height extraction, and iii) reconstruction of the 3D city model.

In the 1st part of the study, it has learned that how the current state of photogrammetric technique where direct georeferencing technology on the line, less ground control required, is well-established itself with straightforward and fully automatic data processing and extraction procedure which all these efforts give a significant boost for 3D geometric extraction and modeling of the target spatial features. Furthermore, from a thorough investigation of the photogrammetric workflow, this study is worth witnessing that the output dataset such as AAT, DTM/DSM, and orthophoto map was achieved the benchmark set by ASPRS for the allowable error budget within the dataset that can be used for reliable spatial data extraction, modeling, and analysis purpose.

The 2nd part of the study was the development of a centralized and scalable geodatabase system that can store a variety of datasets like 2D features,3D models, raster data structure as well as other statistical tables in one place for a particular target geographical ground. Thus, ESRI file geodatabase was found effective to be used as the default data container to store all the available spatial and non-spatial datasets i.e., 2D features (Building, tree, green space, walkways, etc.), raster surfaces, database tables, reconstructed 3D models of the structure as a multi-patch feature (3D building, 3D tree, etc.), 4D spatial-temporal information, and other information of the organizations in a single location and ease the integration of this dataset for advanced GIS analysis through accessing them from a scalable and central storage unit. Furthermore, the above-ground height of spatial features (nDSM) was extracted and transferred into the respective feature through the surface-to-feature strategy. This height surface has been estimated from the difference operation made between DSM and DTM (i.e., a surface extracted by removing all elevated surfaces of the DSM data) surface. Thus, this study showed that the photogrammetric DSM delivered the precise absolute above ground height of physical/spatial features that can be used for model generation as well as other 3D metric analyses.

In the 3rd part of the study, the reconstruction of the 3D city model of the study area was performed at two different levels of representation. The first one was the LOD1 model which is a 3D flat model of the pilot area, generated from a combination of 2D vector boundaries extracted from an orthophoto map and nDSM height surface. The LOD1 model may not be attractive as they don't contain details of the object but gives a demonstration for sectors to transform their existing 2D cadastral databases or ground plans into a 3D city model with the addition of estimated object height (nDSM data) for quick, reliable and economic volumetric 3DCM generation for better management of their environment. The model is capable of 3D visualization, simulation, 3D measurement, 3D analysis, and other applications without fear of blown error. The second LOD2 model was well established from the photogrammetric point cloud data where the point cloud data were sorted, filtered, and classified into their real-world belongings so that the building class points were used for model reconstruction through automatic detection of edges, corners, and faces of the building object. Thus, the resultant LOD2 model was reconstructed quite accurately which demonstrates details of the roof geometry of the building model well with only some minor redrawing and roof material texturing from the orthophoto map. This shows the potential of the photogrammetric technique where a couple of nadir-looking stereo aerial images provide reliable

point cloud data that is easy to deal with the 3D geometric characteristics of the target urban object at a remarkable resolution, accuracy, and fidelity. Nevertheless, the photogrammetric-based point cloud may provide an unnecessary edge, face, or any geometry in the 3D model of the spatial object due to the inherent artifacts (e.g., noise) in the aerial photographs resulting from too much sunlight, shadows, surrounding environment (e.g., building partly covered by trees), occlusions and poor contrast that affects the point cloud quality which in turn introduce incorrect geometries in the model. Thus, to fix these problems, visual checks and manual redrawing of the model have been required.

In general, the model reconstruction process showed that from a couple of 2D nadir-looking photographs, a significant digital copy of the real-world model (3D city model) with different levels of representation (i.e., LOD1 and LOD-2) was effectively reconstructed. These models contain the integration of elevated surface objects (building, trees, etc.) and on-surface objects (terrain model, parcel, and land use). While tree features and vegetation details were not usually represented in traditional or standard databases, these urban features are relevant for different analyses and well represented in the 3D city model to bring a realistic landscape character. Furthermore, the vertical accuracy of the 3D model is good, it is worthy to mention that the photogrammetric technique is the well-suited economic acquisition of the planimetric and vertical information of the target physical structure at reasonable quality. However, it has to be acknowledged that the developed models look still visually incomplete as each model does not contain the façade details, texture information, and indoor space structure due to the inability of the nadir photographs to show building interfaces and facades. Thus, the integration of terrestrial or oblique photographs with indoor mapping techniques is mandatory for higher LOD development and realism. Nevertheless, the reconstructed 3D city model is a concrete manifestation of the reliable 3D digital campus model where it is sufficient to be used as a platform for the development of a smart campus system to improve the quality of education, preservation of campus structure for maintenance and rebuilding, web animation/promotion, and campus tourism, simulation of present and future development within the campus area and others.

To conclude, this study pointed out the significance of geomatics techniques in developing a digital system that considers the growing complexity of the urban environment. Specifically, the photogrammetric technique where 2D high-resolution aerial photographs were obtained from large

format digital aerial camera with direct georeferencing technology of the navigation sensors on the line, few numbers of GCP and process these datasets by one of commercial of the shelf digital photogrammetric solution software were sufficient for this work to reconstruct a functional and comprehensive 3d city model of the target physical environment with quite straight-forward and automatic processing procedure. This means the straightforward processing and modeling technique helps to reduce a significant amount of time whereas the automatic process delivers more accurate object representation by reducing human intervention (possible error). These benefits of the photogrammetric technique make it a viable and fairly economical (cost-effective) strategy for transforming the entire existing city structure into an identical digital 3D model which combines its location, attribute (i.e., cadastral information), and vertical information of spatial objects efficiently, where such 3D spatial information model is the foundation for digital transformation, smart city implementation, urban environmental studies, emergency response and simulation, security and surveillance, storage of urban databases and other rich sets of intelligent and evidence-based solutions for governments and end-users. Otherwise, cities that do not forge ahead to use such innovative technology and governance model, those that do not follow the current trend of technology and smartness, will fall behind with negative consequences.

## 5.2 Recommendation

This study presented the 3D city model reconstruction techniques that can replace the incompetency of the current 2D maps in their representation, management, analysis, and prediction of the urban environment. However, further work is geared towards the reconstruction of a 3D city model that's capable to handle most urban-related topics. Thus, future work and research are recommended to be are carried out in the following area:

- Feature research should be encouraged for the integration of terrestrial or oblique photogrammetric techniques with aerial photogrammetry to reconstruct true digital 3DCM at a higher level of detail (LOD3 and LOD4) that are higher informative by fulfilling all required semantic information (i.e., wall surface, outer floor surface, indoor surfaces and structures, windows, rooms and so on.), and façade details. Furthermore, it is recommended to include indoor space structures and subsurface objects like the basement, underground rail systems, tunnels, underground sewerage lines, etc. within the 3D city model.
- the current research work has focused only on the photogrammetric approach for the reconstruction of 3DCM. However, further research is recommended to develop 3D city models based on photogrammetric and other geomatics techniques such as LiDAR techniques, for the same target ground so that one can confirm which technique to use in the future implementation through comparative analysis.
- As such digital model development of the existing physical structure does not need a piece of special technological equipment and tools other than the currently used data source (aerial photograph, GPS data,) and software tools, thus, it is recommended that public institutions, businesses organizations, government sectors, and others should seek for the reconstruction of affordable digital 3D model of their respective environment to benefit themselves from this innovative tool for supporting their decision-making process and to meet their customer need and requirement.

# 6 Reference

Abdullah, Q., Maune, D., Smith, D., & Heidemann, H. K. (2015). New standard for new era: Overview of the 2015 ASPRS positional accuracy standards for digital geospatial data. *Photogrammetric Engineering and Remote Sensing*, *81*(3), 173–176. https://doi.org/10.14358/PERS.81.3.173

Ackennann, F., & Krzystek, P. (1991). MATCH-T: Automatic mensuration of digital elevation models. *In Proceedings of Technical Seminar of the Sociedad Espanola de Cartografia Fotogrammetria y Teledeteccion, April 12*, (pp. 67-73).

Agrafiotis, P., Georgopoulos, A., & Karantzalos, K. (2016). The effect of pansharpening algorithms on the resulting orthoimagery. *International Archives of the Photogrammetry, Remote Sensing and Spatial Information Sciences - ISPRS Archives*, *41*(June), 625–630. https://doi.org/10.5194/isprsarchives-XLI-B7-625-2016

Ahmar, F., Jansa, J., & Ries, C. (1998). the Generation of True Orthophotos Using a 3D Building Model in Conjunction with a Conventional Dtm. *Iaprs*, *32*, 16–22.

Alomía, G., Loaiza, D., Zúñiga, C., Luo, X., & Asorey-Cacheda, R. (2021). Procedural modeling applied to the 3D city model of bogota: a case study. *Virtual Reality and Intelligent Hardware*, *3*(5), 423–433. https://doi.org/10.1016/j.vrih.2021.06.002

Al-Rawabdeh, A., Al-Ansari, N., Attya, H., & Knutsson, S. (2014). GIS Applications for Building 3D Campus, Utilities and Implementation Mapping Aspects for University Planning Purposes. *Journal of Civil Engineering and Architecture*, *8*(74), 19–28.

Banduthilaka, B. M. S., Kariyawasam, C., & Alagiyawanna, A. M. N. (2013). Building 3D Models using the Data stored in a Relational Database. *International Journal of Education and Research*, *1*(11), 197–207.

Brenner, C., & Haala, N. (1999). Rapid production of virtual reality city models. *Geo-Informations-System*, *12*(2), 22–28.

Burdeos, M. D. A., Makinano-Santillan, M., & Amora, A. M. (2015). Automated building footprints extraction from DTM and DSM in ArcGIS. *ACRS 2015 - 36th Asian Conference on Remote Sensing: Fostering Resilient Growth in Asia, Proceedings*, *6*(Acrs), 4797–4802.

Buyukdemircioglu, M., Kocaman, S., & Isikdag, U. (2018). Semi-automatic 3D city model generation from large-format aerial images. *ISPRS International Journal of Geo-Information*, *7*(9). https://doi.org/10.3390/ijgi7090339

Chai, T., & Draxler, R. R. (2014). Root mean square error (RMSE) or mean absolute error (MAE)? -Arguments against avoiding RMSE in the literature. *Geoscientific Model Development*, *7*(3), 1247–1250. https://doi.org/10.5194/gmd-7-1247-2014

Chang, Y.-C., F. Habib, A., Lee, D., & Yom, J.-H. (2008). Automatic classification of lidar data into ground and non-ground points. *International Archives of Photogrammetry and Remote*

*Sensing*, *37*, 463--468. http://citeseerx.ist.psu.edu/viewdoc/download?doi=10.1.1.158.6234&rep=rep1&type=pdf

Chen, J., & Clarke, K. C. (2016). Rapid 3d modeling using photogrammetry applied to google earth. *The 19th International Research Symposium on Computer-Based Cartography Albuquerque*, 14–16.

CHIGBU, Njike., OKEZIE, Maduabughichi., & OKOYE, V. U. (2017). Realization of a Functional Photorealistic 3D City Geographic Information Realization of a Functional Photo-Realistic 3D City Geographic Information System (3D GIS), the Place of Google Earth and Arc Scene. *FIG Working Week 2017*, *8757*. https://www.fig.net/resources/proceedings/fig_proceedings/fig2017/papers/ts05e/TS05E_chigbu_okezie_et_al_8757.pdf

Danilina, N., Slepnev, M., & Chebotarev, S. (2018). Smart city: automatic reconstruction of 3D building models to support urban development and planning. *MATEC Web of Conferences 251*, *03047*, 1–8.

Darbas, B. magistro, & Sužiedelytė-Visockienė, J. (2011). *PROCESSING OF THE DIGITAL IMAGES USING PHOTOGRAMMETRY SYSTEMS. Master's thesis in VILNIAUS GEDIMINO TECHNIKOS UNIVERSITETAS*.

Dewanto, B. G., Novitasari, D., Tan, Y. C., Puruhito, D. D., Fikriyadi, Z. A., & Aliyah, F. (2020). Application of Web 3D GIS to Display Urban Model and Solar Energy Analysis using the Unmanned Aerial Vehicle (UAV) Data (Case Study: National Cheng Kung University Buildings). *IOP Conference Series: Earth and Environmental Science*, *520*(1). https://doi.org/10.1088/1755-1315/520/1/012017

Döllner, J., H. Kolbe, T., Liecke, F., Sgouros, T., & Teichmann, K. (2006). THE VIRTUAL 3D CITY MODEL OF BERLIN - MANAGING, INTEGRATING AND COMMUNICATING COMPLEX URBAN INFORMATION. *In Proceedings of the 25th International Symposium, urban data management UDMS in Aalborg, Denmark*, 15–17.

el Garouani, Abdelkader., Alobeid, Abdalla., & el Garouani, Said. (2014). Digital surface model based on aerial image stereo pairs for 3D building. *International Journal of Sustainable Built Environment*, *3*(1), 119–126. https://doi.org/10.1016/j.ijsbe.2014.06.004

El-Mekawy, M., Östman, A., & Hijazi, I. (2012). A unified building model for 3D urban GIS. *ISPRS International Journal of Geo-Information*, *1*(2), 120–145. https://doi.org/10.3390/ijgi1020120

Engman, H. (2016). Examples and critical success factors - Web-based 3D in Urban Planning. *GIM International*, *Figure 1*, 3–4. https://www.gim-international.com/content/article/web-based-3d-in-urban-planning

Fan, H., & Meng, L. (2009). Automatic Derivation of Different Levels of Detail for 3D Buildings Modeled by CityGML. *In 24th International Cartography Conference, Santiago, Chile*, (pp. 15-21).

Finlayson, C., & Opitz, D. W. (2004). A Complete Building Extraction System from Elevation Data. *Proc., Int. User Conf., ESRI, San Diego*.

Forlani, G., Roncella, R., & Nardinocchi, C. (2015). Where is photogrammetry heading to? State of the art and trends. *Rendiconti Lincei*, *26*, 85–96. https://doi.org/10.1007/s12210-015-0381-x

Georgopoulos, A. (2017). Preserving the Past Using Geomatics. *GIM International*. https://www.gim-international.com/content/article/preserving-the-past-using-geomatics?sid=139206&utm_campaign=Newsletter %7C GIM %7C 26-05-2022 &utm_medium=email&utm_source=newsletter?output=pdf

Girindran, R., Boyd, D. S., Rosser, J., Vijayan, D., Long, G., & Robinson, D. (2020). On the Reliable Generation of 3D City Models from Open Data. *Urban Science*, *4*(4), 47. https://doi.org/10.3390/urbansci4040047

Gröger, Gerhard., Kolbe, T. H., Nagel, C., & Häfele, K.-H. (2012). *OGC City Geography Markup Language (CityGML) En- coding Standard*.

Gruber, M., Ponticelli, M., Bernögger, S., Reitinger, B., Hegenbarth, H., Cosic, Z., & Wiechert, A. (2012). UltraCam Eagle, understanding the new sensor. *American Society for Photogrammetry and Remote Sensing Annual Conference 2012, ASPRS 2012*, 203–208.

Gruen, A. (2013). NEXT GENERATION SMART CITIES - THE ROLE OF GEOMATICS. *Firesearchgate: International Workshop on "Global Geospatial Information*, 25–41. https://www.researchgate.net/publication/259292496_Next_generation_Smart_Cities_-_the_role_of_Geomatics

Guo, L., Deng, X., Liu, Y., He, H., Lin, H., Qiu, G., & Yang, W. (2021). Extraction of Dense Urban Buildings from Photogrammetric and LiDAR Point Clouds. *IEEE Access*, *9*, 111823–111832. https://doi.org/10.1109/ACCESS.2021.3102632

Haggag, M., Zahran, M., & Salah, M. (2018). Towards Automated Generation of True Orthoimages for Urban Areas. *American Journal of Geographic Information System*, *7*(2), 67–74. https://doi.org/10.5923/j.ajgis.20180702.03

Hashemi, S.A.M. (2008). Automatic peaks extraction from Normalized Digital Surface Model (NDSM). *The International Archives of Photogrammetry, Remote Sensing and Spatial Information Sciences., XXXVII, Beijing*.

Hopfstock, A., Hovenbitzer, M., Lindl, F., & Knöfel, P. (2022). Building a Digital Twin for Germany. *GIM International*, 1–23.

Hutton, J., & Mostafa, M. M. R. (2005). 10 years of Direct Georeferencing for airborne photogrammetry. *Geo-Informations-System*, *2005*(11), 33–41.

Jebur, A., Abed, F. M., & Mohammed, M. U. (2017). 3D City Modelling by Photogrammetric Techniques. *Research Gate, July 2019*. https://doi.org/10.13140/RG.2.2.11494.06722

Jovanovi´c, D., Milovanov, S., Ruskovski, I., Govedarica, M., Sladi´c, D., Radulovi´c, A., & Paji´c, V. (2020). Building Virtual 3D City Model for Smart Cities Applications: A Case Study on Campus Area of the University of Novi Sad. *International Journal of Geo-Information*.

Kaartinen, H., Hyyppä, J., Gülch, E., Vosselman, G., Hyyppä, H., Matikainen, L., Hofmann, A. D., Mäder, U., Persson, Å., Söderman, U., Elmqvist, M., Ruiz, A., Dragoja, M., Flamanc, D., Maillet, G., Kersten, T., Carl, J., Hau, R., Wild, E., … Vester, K. (2005). ACCURACY OF 3D CITY MODELS: EuroSDR comparison (muito importante). *ISPRS WG III/3, III/4, V/3 Workshop "Laser Scanning 2005", Enschede, the Netherlands, September 12-14, 20, January*, 227–232.

Kobayashi, Y. (2006). Photogrammetry and 3D city modelling. *WIT Transactions on the Built Environment, 90*, 209–218. https://doi.org/10.2495/DARC060211

Kocaman, S., Zhang, L., Gruen, A., & Poli, D. (2006). 3D city modeling from high-resolution satellite images. *Proceedings of ISPRS Workshop on Topographic Mapping from Space, Ankara, Turkey, 14-16 Feb., 1*, Volume XXXVI-1/W41. https://www.semanticscholar.org/paper/3-D-City-Modeling-from-High-resolution-Satellite-Kocaman-Zhang/15af229565f5044fe3242a6d72460fd78a079472%0Ahttp://www.p.igp.ethz.ch/p02/general/persons/sultan_pub/kocaman_zhang_gruen_poli_Ankara_06.pdf

Kolbe, T. H., & Donaubauer, A. (2021). Semantic 3D City Modeling and BIM. In *Urban Book Series*. Springer Singapore. https://doi.org/10.1007/978-981-15-8983-6_34

Kumar, P. (2022). *What is LiDAR technology? How does LiDAR help in depth measurement?* E-Con Systems. https://www.e-consystems.com/blog/camera/technology/what-is-lidar-technology-how-does-lidar-help-in-depth-measurement/

Kurakula, V. K., & Kuffer, M. (2008). 3D Noise Modeling for Urban Environmental Planning and Management Vinay Kumar KURAKULA and Monika KUFFER. *Real Corp 008, 2*, 517–523.

Li, D., Shan, J., Shao, Z., Zhou, X., & Yao, Y. (2013). Geomatics for smart cities - concept, key techniques, and applications. *Geo-Spatial Information Science, 16*(1), 13–24. https://doi.org/10.1080/10095020.2013.772803

Li, L., Guo, R., Ying, S., Zhu, H., Wu, J., & Liu, C. (2021). 3D Modeling of the Cadastre and the Spatial Representation of Property. In *Urban Book Series*. Springer Singapore. https://doi.org/10.1007/978-981-15-8983-6_33

Loutfia, E., Mahmoud, H., Amr, A., & Mahmoud, S. (2017). 3D model reconstruction from aerial ortho-imagery and LiDAR data. *Journal of Geomatics, 11*(1).

Ma, D., Cui, J., & Ding, N. (2011). The making of Digital Orthophoto Map based on INPHO. *Applied Mechanics and Materials, 90–93*, 2818–2821. https://doi.org/10.4028/www.scientific.net/AMM.90-93.2818

McClune, A. P., Miller, P. E., Mills, J. P., & Holland, D. (2014). Automatic urban 3D building reconstruction from multi-ray photogrammetry. *International Archives of the Photogrammetry, Remote Sensing and Spatial Information Sciences - ISPRS Archives*, *40*(3), 219–226. https://doi.org/10.5194/isprsarchives-XL-3-219-2014

Minds, G. (2021). The Beirut Explosion: UAV Mapping as a First Step to Recovery. *GIM International*, 2–3.

Nath, A. R., & Ramiya, A. M. (2016). 3D Reconstruction of Buildings from Classified LiDAR Point. *International Journal of Earth Sciences and Engineering*, *9*(1), 162–166.

Nathanael, M. (2021). *POSITIONAL ACCURACY ASSESSMENT OF ORTHOPHOTO AND DIGITAL ELEVATION MODEL: A CASE STUDY IN DIRE DAWA CITY, ETHIOPIA Unpublished Master's thesis Addis Ababa University*. *September*. http://etd.aau.edu.et/handle/123456789/27960

Nex, F., & Remondino, F. (2012). AUTOMATIC ROOF OUTLINES RECONSTRUCTION from PHOTOGRAMMETRIC DSM. *ISPRS Annals of the Photogrammetry, Remote Sensing and Spatial Information Sciences*, *1*, 257–262. https://doi.org/10.5194/isprsannals-I-3-257-2012

Nicholls, B., & Kruimel, D. (2017). UNDERPINNED BY A 3D NATIONAL Singapore: Towards a Smart Nation. *GIM International*.

Nikola, Y., & Temenoujka, B. (2019). 3d Maps – Cartographical Aspects. *Proceedings, 7th International Conference on Cartography and GIS, June 2018*.

Ohori, K. A., Biljecki, F., Kumar, K., Ledoux, H., & Stoter, J. (2018). Modelling cities and landscapes in 3D with CityGML. *Building Information Modeling: Technology Foundations and Industry Practice*, 1–584. https://doi.org/10.1007/978-3-319-92862-3

Onyimbi, J. R., Koeva, M. N., & Flacke, J. (2017). Public participation using 3D city models: e-participation opportunities in Kenya. *GIM International*, *31*(7), 29–31. https://ezproxy2.utwente.nl/login?url=https://webapps.itc.utwente.nl/library/2017/scie/koeva_pub.pdf

Øyen-Eriksen, K. (2016). New 3D map solution: Covering Norway. *GIM International*, *30*(6), 34–35. https://www.gim-international.com/content/article/new-3d-map-solution-covering-norway

Ozdemir, E., & Remondino, F. (2018). Segmentation of 3D photogrammetric point cloud for 3D building modeling. *International Archives of the Photogrammetry, Remote Sensing and Spatial Information Sciences - ISPRS Archives*, *42*(4/W10), 135–142. https://doi.org/10.5194/isprs-archives-XLII-4-W10-135-2018

Parthibanraja, .A, & Purushothaman, B. M. (2016). Digital Elevation Model Based on Aerial Image for 3D Building. *International Journal of Science and Research (IJSR) ISSN (Online*

*Index Copernicus Value Impact Factor*, *57*(3), 2319–7064. https://doi.org/10.21275/ART20181007

Peeroo, U., Idrees, M. O., & Saeidi, V. (2017). Building extraction for 3D city modelling using airborne laser scanning data and high-resolution aerial photo. *South African Journal of Geomatics*, *6*(3), 363. https://doi.org/10.4314/sajg.v6i3.7

Pepe, M., Fregonese, L., & Scaioni, M. (2018). Planning airborne photogrammetry and remote-sensing missions with modern platforms and sensors. *European Journal of Remote Sensing*, *51*(1), 412–435. https://doi.org/10.1080/22797254.2018.1444945

Redpath, D. (2018). 3D Modelling for Construction. *GIM International*, 3–4. https://content.geomares-marketing.com/webmail/704093/79373529/19c10bcfdf8cca97bba5d1e1a4673f0f30136359729407e31b8cdb86d63b5538

Reitinger, B., & Gruber, M. (2013). UltraMap - Details and results from the digital photogrammetric workflow. *American Society for Photogrammetry and Remote Sensing Annual Conference, ASPRS 2013*, 599–604.

Reljić, I., & Dunder, I. (2019). Application of photogrammetry in 3D scanning of physical objects. *TEM Journal*, *8*(1), 94–101. https://doi.org/10.18421/TEM81-13

S. Jain, R., D. Parmar, P., & P. Patel, D. (2017). 3D City Model' through QGIS: A Case Study of GIFT City, Gujarat, India. *ResearchGate*, *11*(4), 70808.

Saran, S., Oberai, K., Wate, P., Konde, A., Dutta, A., Kumar, K., & Senthil Kumar, A. (2018). Utilities of Virtual 3D City Models Based on CityGML: Various Use Cases. *Journal of the Indian Society of Remote Sensing*, *46*(6), 957–972. https://doi.org/10.1007/s12524-018-0755-5

Shoko, M., & Gavu, E. K. (2021). Digital Models for Planning and Disaster Management: Lidar-derived Shack Footprint for the City of Cape Town. *GIM International*. https://www.gim-international.com/content/article/digital-models-for-planning-and-disaster-management?sid=139206&utm_campaign=Data Visualization Weeks %7C Newsletter 3 %7C 04-10-21&utm_medium=email&utm_source=newsletter%3Foutput%3Dpdf?output=pdf

Singh, S. P., Jain, K., & Mandla, V. R. (2013a). Virtual 3D Campus Modeling by Using Close Range Photogrammetry. *American Journal of Civil Engineering and Architecture*, *1*(6), 200–205. https://doi.org/10.12691/ajcea-1-6-9

Singh, S. P., Jain, K., & Mandla, V. R. (2013b). Virtual 3D city modeling: Techniques and Applications. *International Archives of the Photogrammetry, Remote Sensing and Spatial Information Sciences - ISPRS Archives*, *XL-2/W2*(ISPRS 8th 3DGeoInfo Conference & WG II/2 Workshop, Istanbul, Turkey), 73–91. https://doi.org/10.5194/isprsarchives-XL-2-W2-73-2013

Singla, J. G., & Padia, Kirti. (2020). A Novel Approach for Generation and Visualization of Virtual 3D City Model Using Open-Source Libraries. *Journal of the Indian Society of Remote Sensing*, *8*, 3–8. https://doi.org/10.1007/s12524-020-01191-8

Stal, C., Tack, F., Maeyer, P. de, Wulf, A. de, & Goossens, R. (2012). Airborne photogrammetry and LIDAR for DSM extraction and 3D change detection over an urban area – a comparative study. *International Journal of Remote Sensing*, *34*(4), 1087–1110.

Stoter, J., Ohori, K. A., & Noardo, F. (2021). Digital Twins: A Comprehensive Solution or Hopeful Vision? *Gim International-the Worldwide Magazine for Geomatics*, *35*(6), 40-44 WE-Emerging Sources Citation Index (ESCI).

Sulaiman, N. S., Majid, Z., & Setan, H. (2010). DTM GENERATION FROM LiDAR DATA BY USING DIFFERENT FILTERS IN OPEN – SOURCE SOFTWARE. *Geoinformation Science Journal*, *10*(2), 89–109.

Suveg, I., & Vosselman, G. (2004). Reconstruction of 3D building models from aerial images and maps. *ISPRS Journal of Photogrammetry and Remote Sensing*, *58*(3–4), 202–224. https://doi.org/10.1016/j.isprsjprs.2003.09.006

Toschi, I., Nocerino, E., Remondino, F., Revolti, A., Soria, G., & Piffer, S. (2017). Geospatial data processing for 3D city model generation, management and visualization. *International Archives of the Photogrammetry, Remote Sensing and Spatial Information Sciences - ISPRS Archives*, *42*(1W1), 527–534. https://doi.org/10.5194/isprs-archives-XLII-1-W1-527-2017

Toschi, I., Remondino, F., Hauck, T., & Wenzel, K. (2019). When Photogrammetry Meets Lidar: Towards the Airborne Hybrid Era. *GIM International*, *i*, 3–5.

Tunc, E., Karsli, F., & Ayhan, E. (2004). 3D City reconstruction by different technologies to manage and reorganize the current situation. *International Archives of the Photogrammetry, Remote Sensing and Spatial Information Sciences - ISPRS Archives*, *35*.

Uggla, G. (2015). 3D City Models – A Comparative Study of Methods and Datasets List of Figures. *Master Thesis in Geoinformatics*, *June*.

Uyar, A., & Ulugtekin, N. N. (2017). A PROPOSAL for GENERALIZATION of 3D MODELS. *ISPRS Annals of the Photogrammetry, Remote Sensing and Spatial Information Sciences*, *4*(4W4), 389–392. https://doi.org/10.5194/isprs-annals-IV-4-W4-389-2017

van DIERENDONCK, A. J., RUSSELL, S. S., KOPITZKE, E. R., & BIRNBAUM, M. (1978). The GPS Navigation Message. *Navigation*, *25*(2), 147–165. https://doi.org/10.1002/j.2161-4296.1978.tb01326.x

Vermeij, M., & Zlatanova, S. (2001). Semi-automatic 3D building reconstruction using soft plotter. *Proceedings of the International Symposium on Geodetic, Photogrammetric and Satellite Technologies: Development and Integrated Applications*, *November*, 8–9. http://www.tudelft.nl/live/ServeBinary?id=7b70630e-4204-4f71-a29b-e3e75d3b11f6&binary=/doc/MV_SZ_FIG.pdf

Waser, J., Konev, A., & Cornel, D. (2018). On-the-fly Decision Support in Flood Management. *GIM International*, 22–25. https://www.gim-international.com/content/article/on-the-fly-decision-support-in-flood-management

Welter, J. (2021). How 3D Modelling Supports Game- changing Urban Development. *GIM International*, 1–17.

Wiechert, A., Gruber, M., & Ponticelli, M. (2011). Ultracam: The new super-large format digital aerial camera. *American Society for Photogrammetry and Remote Sensing Annual Conference 2011*, 519–525.

Wu, B. (2017). Photogrammetry: 3-D From Imagery. *International Encyclopedia of Geography: People, the Earth, Environment and Technology*, 1–13. https://doi.org/10.1002/9781118786352.wbieg0942

Wu, B. (2021). Photogrammetry for 3D Mapping in Urban Areas. *Urban Book Series*, 401–413. https://doi.org/10.1007/978-981-15-8983-6_23

Xu, H., Badawi, R., Fan, X., Ren, J., & Zhang, Z. (2009). Research for 3D visualization of Digital City based on SketchUp and ArcGIS. *International Symposium on Spatial Analysis, Spatial-Temporal Data Modeling, and Data Mining*, *7492*(October 2009), 74920Z. https://doi.org/10.1117/12.838558

Yalcin, G., & Selcuk, O. (2015). 3D City Modelling with Oblique Photogrammetry Method. *Procedia Technology*, *19*, 424–431. https://doi.org/10.1016/j.protcy.2015.02.060

Yastikli, N., & Cetin, Z. (2017). AUTOMATIC 3D BUILDING MODEL GENERATIONS with AIRBORNE LiDAR DATA. *ISPRS Annals of the Photogrammetry, Remote Sensing and Spatial Information Sciences*, *4*(4W4), 411–414. https://doi.org/10.5194/isprs-annals-IV-4-W4-411-2017

Ying, S., Guo, R., Li, L., & He, B. (2012). Application of 3D GIS to 3D Cadastre in Urban Environment. *Proceedings of the 3rd International Workshop on 3D Cadastres: Developments and Practices*, *October*, 253–272.

Ying, Y., Koeva, M., Kuffer, M., & Asiama, K. (2019). 3D Modelling for Property Valuation in China: A High-resolution Remote Sensing-based Approach. *GIM International*, 2–4. https://research.utwente.nl/en/publications/3d-modelling-for-property-valuation-in-china-a-high-resolution-re

Zheng, Y., Weng, Q., & Zheng, Y. (2017). A hybrid approach for three-dimensional building reconstruction in indianapolis from LiDAR data. *Remote Sensing*, *9*(4). https://doi.org/10.3390/rs9040310

Zhu, Q., Hu, M., Zhang, Y., & Du, Z. (2009). Research and practice in three-dimensional city modeling. *Geo-Spatial Information Science*, *12*(1), 18–24. https://doi.org/10.1007/s11806-009-0195-z

Zomrawi, N., Hussien, M. A., & Mohamed, H. (2013). Accuracy evaluation of digital aerial triangulation. *International Journal of Engineering and Innovative Technology*, *2*(10), 7–11.

# 7 Appendices

**Appendix 1**: Technical specifications of the UltraCam eagle aerial digital camera

| | | Panchromatic Sensor | | Multispectral Sensor | |
|---|---|---|---|---|---|
| Sensor size | long track | 68.016mm | 13080pixel | 68.016mm | 4360pixel |
| | cross track | 104.052mm | 20010pixel | 104.052m | 6670pixel |
| | | | | | |
| Image Extent | | (-34.01, -52.02) mm | | (34.01, 52.02) mm | |
| | | | | | |
| Pixel Size | | 5.200µm*5.200µm | | 15.600µm*15.600µm | |
| | | | | | |
| Focal Length | ck | 100.500 mm ± 0.002mm | | | |
| | | | | | |
| Principal Point (Level 2) | X_ppa | 0.000 mm ± 0.002mm | | | |
| | Y_ppa | 0.000 mm ± 0.002mm | | | |
| | | | | | |
| Lens Distortion | | Remaining Distortion less than 0.002mm | | | |

**Appendix 2**: Flight planning parameters used for the Addis Ababa city photography project

```
Camera: Microsoft Ultracam Eagle 100

Selected lens: 100.5 mm
Sensor dimensions in millimeters
Side parallel to the run: 68
Side perpendicular to the run: 104

Sensor dimensions in pixels
Side parallel to the run: 13080
Side perpendicular to the run: 20010

Pixel size in meter: 0.100000001490116


Scale: 19235
Min scale tolerance: 0
Max scale tolerance: 10
Min scale: 19235
Max scale: 21159
GSR: 0.100
Min GSR: 0.100
Max GSR: 0.110
Footprint along: 1307.98
Footprint across:  2000.44

Sidelap: 60.0
Min sidelap tolerance: 0
Max sidelap tolerance: 10
Min sidelap: 60
Max sidelap: 66
Endlap: 80.0
Min endlap tolerance: 0
Max endlap tolerance: 5
Min endlap: 80
Max endlap: 85
Flying height agl: 6342 feet
```

**Appendix 3**: Aerial Survey flight (acquisition) Report by the flight crew.

## GII AERIAL SURVEY FLIGHT REPORT

| | | |
|---|---|---|
| **Project Name & Block No_: Addis Ababa** | **Flight No: Day_5** | **Flight Date:31/05/21** |
| **Operators: Hailie & Kibret** | **Pilot: Peter** | **Departure: Addis Ababa** |
| **Overlap (%): 80/60** | **GSD (cm): 10** | **Aircraft: caravan (NOCP)** |
| **Navigation System: Applanix-POSTrack** | **Mount: GSM 4000** | **IMU:31** |
| **Camera: UCE f100** | **Serial No_: UCE-1-80810137** | **Focal Length (mm): 100.5** |
| **GPS Data Logging Time: 6:54-8:52** | **Sun Angel: 57** | |
| **Internal POS Data Code: 344-354** | **Aperture: F6.7** | **Shutter Speed:1/125** |
| **ISO: off** | **FMC: On** | **IBD: On** |
| **Engine Start: 6:42** | **Start movement: 7:56** | **Takeoff: 7:06** |
| **Landing: 8:47** | **Stop Movement: 8:50** | **Shutdown: 8:53** |

| Time of entry | Time of End | Turning Time | Run | Heading | Dir. | Photo Numbers | Qty. | Remarks |
|---|---|---|---|---|---|---|---|---|
| 7:21 | 7:28 | - | 12 | 88 | WE | 2633-2743 | 108 | ✓ Aborted due to traffic |
| 7:37 | 7:44 | 9 | 13 | 88 | WE | 2744-2875 | 132 | ✓ |
| 7:55 | 8:03 | 11 | 14 | 88 | WE | 2876-3006 | 131 | ✓ Slightly shadow |
| 8:15 | 8:21 | 12 | 15 | 88 | WE | 3007-3135 | 129 | ✓ Shadow |
| 8:27 | 8:33 | 6 | 16 | 268 | EW | 3136-3262 | 128 | Allowed to start from E |
| 8:37 | - | 4 | 17 | 88 | WE | 3263-3306 | 127 | Aborted due traffic & shadow |

**Appendix 4**: Photogrammetric Project definition window (Inpho, Application Master software)

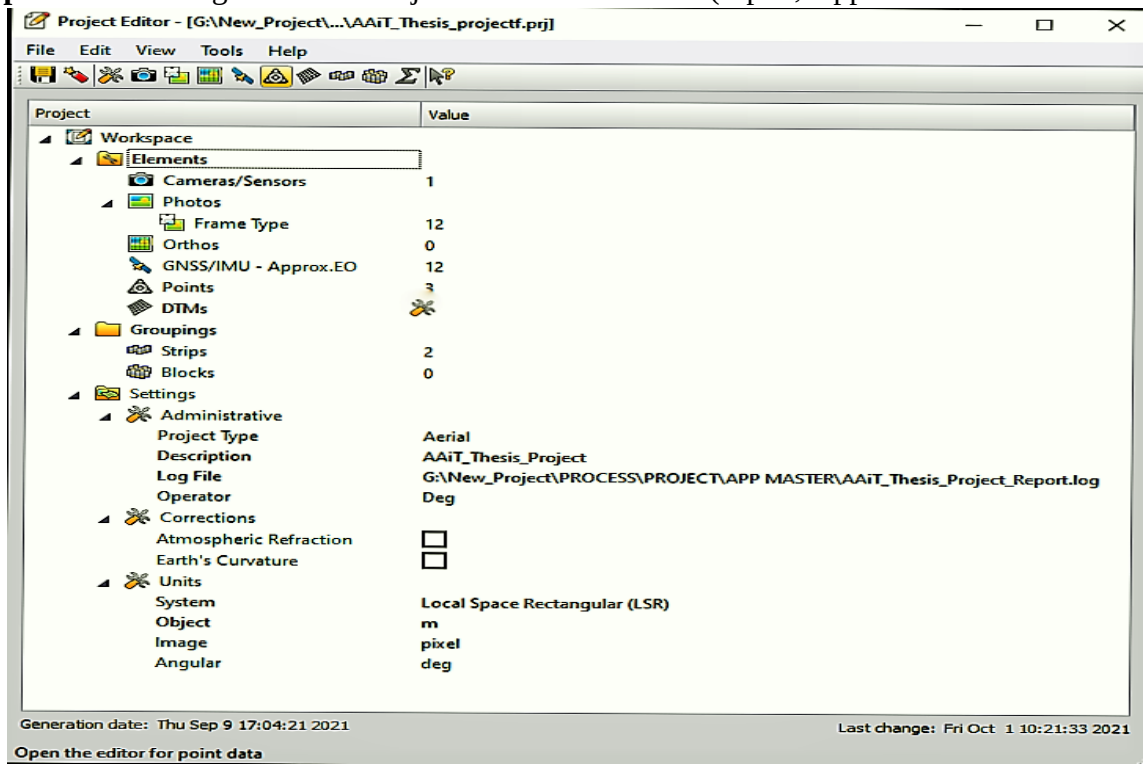

**Appendix 5**: Generated Random Sample points for each building polygon: 321218 random points

**Appendix 6**. Adding nDSM Surface elevation to the generated Random sample point

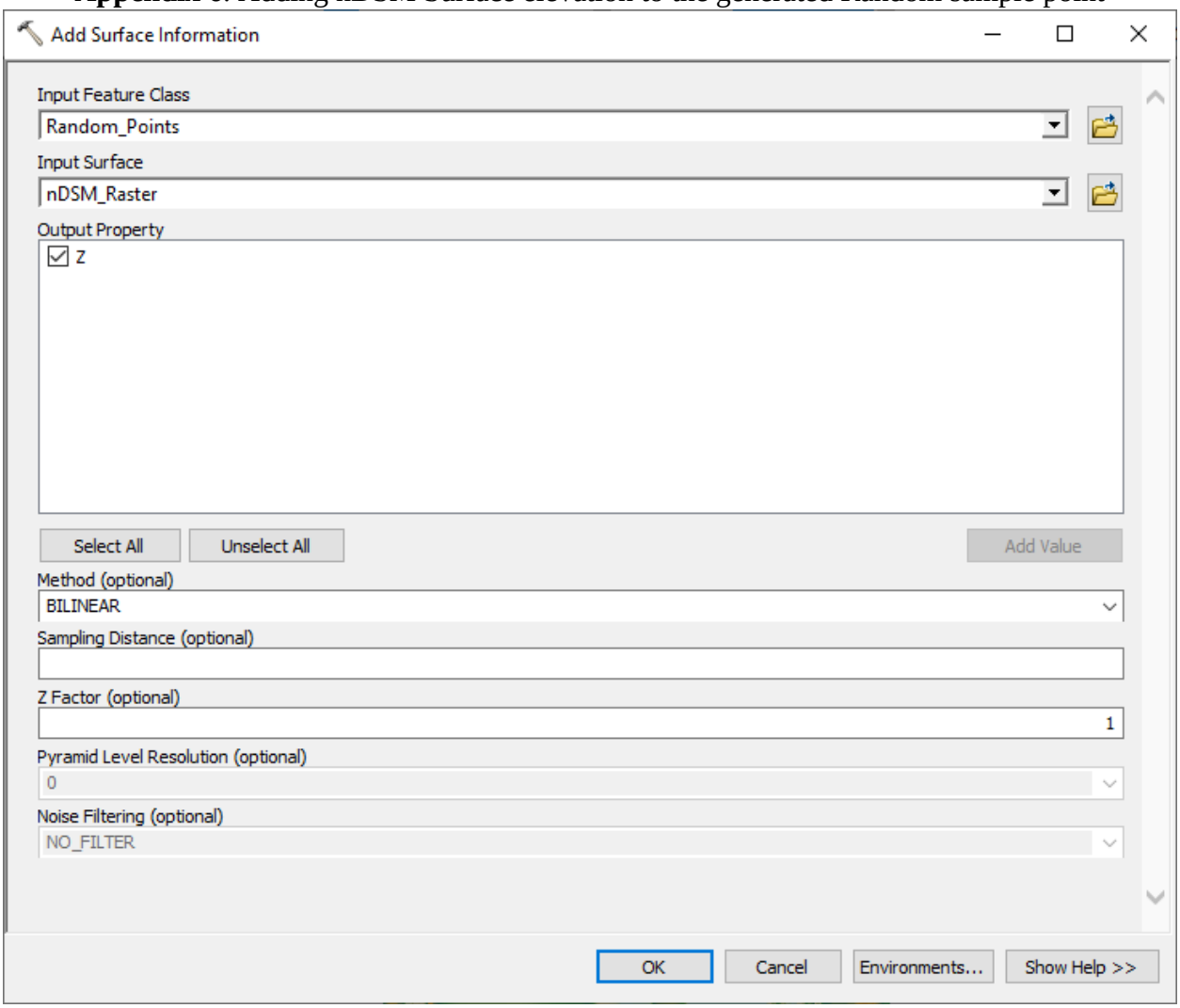

Appendix 7: The Mean Height of Each building feature boundary

| Building_Name | Usage | OID | CID | FREQUENCY | MEAN_Z | SHAPE_Length | SHAPE_Area | Cod |
|---|---|---|---|---|---|---|---|---|
| D-Block | Classrooms and Office | 1 | 1 | 16876 | 16.614668 | 132.702493 | 933.09324 | 4 |
| C-Block | Classrooms and Office | 2 | 2 | 17073 | 16.853614 | 134.270175 | 942.904991 | 3 |
| B-Block | Classrooms and Office | 3 | 3 | 16659 | 15.531695 | 133.547476 | 920.037557 | 2 |
| Security House | Staff Gate | 4 | 4 | 349 | 3.120805 | 17.999418 | 19.634948 | 27 |
| | Electric Power House | 5 | 5 | 661 | 4.319828 | 25.220938 | 36.587565 | 6 |
| | Generator House | 6 | 6 | 649 | 3.224635 | 24.275069 | 36.798398 | 7 |
| Workshop Building | Hydraulic, Civil, and Chemical Workshop | 7 | 7 | 59126 | 6.025387 | 351.665579 | 3271.94365 | 8 |
| Laboratory Building | Highway Lab | 8 | 8 | 16660 | 6.601633 | 122.340177 | 927.735792 | 9 |
| | Water Tanker | 9 | 9 | 800 | 3.378705 | 27.926548 | 44.659087 | 10 |
| Toilet | Male and Femal Toilet | 10 | 10 | 2354 | 4.073469 | 56.746112 | 138.506585 | 11 |
| Security House | exit Check Point | 11 | 11 | 117 | 3.417066 | 11.670128 | 7.355523 | 12 |
| Security House | Entrance Check Point | 12 | 12 | 104 | 2.6721 | 11.643886 | 8.413273 | 13 |
| A-Block | Campus Administartion and Registrar | 13 | 13 | 25521 | 5.293486 | 219.512056 | 1456.622403 | 1 |
| G+10 Building | <Null> | 14 | 14 | 6890 | 35.280424 | 88.221886 | 410.68811 | 14 |
| Sumsung_Building | <Null> | 15 | 15 | 33524 | 13.895168 | 245.621488 | 1869.737959 | 15 |
| E-Block | Classrooms and Office | 16 | 16 | 23376 | 7.018923 | 177.016269 | 1298.879892 | 5 |
| E-Block | By pass roofs | 17 | 17 | 888 | 11.209243 | 44.213116 | 49.614492 | 5 |
| G+2_Building | Classrooms and Office | 18 | 18 | 36354 | 11.3927 | 280.568496 | 2025.388092 | 16 |
| Library Building | All Grade Library Service | 19 | 19 | 17974 | 17.049091 | 132.706316 | 992.624569 | 17 |
| Stair B-C block | Stairs | 20 | 20 | 1996 | 15.331717 | 50.353936 | 110.234664 | 18 |
| Stair C-D block | Stairs | 21 | 21 | 1814 | 15.57443 | 49.729529 | 100.1319 | 19 |
| G+10 Building | <Null> | 22 | 22 | 929 | 11.700966 | 36.087186 | 56.551744 | 14 |
| G+10 Building | <Null> | 23 | 23 | 4647 | 23.863306 | 72.600646 | 259.469074 | 14 |
| Library Building | <Null> | 24 | 24 | 3074 | 7.267485 | 83.755836 | 182.742241 | 17 |
| Library Building | <Null> | 25 | 25 | 8225 | 12.043497 | 87.480724 | 455.124962 | 17 |
| Library Building | <Null> | 26 | 26 | 4411 | 9.764349 | 69.48165 | 244.846213 | 17 |
| Con_steel house | | 27 | 27 | 713 | 3.264832 | 36.16698 | 54.368684 | 26 |
| steel house | Shower and clothing | 28 | 28 | 741 | 3.995876 | 30.048827 | 40.894314 | 20 |
| E-Block | Stairs | 29 | 29 | 38 | 2.851126 | 12.323654 | 8.98587 | 5 |
| Neighbor Home | <Null> | 30 | 30 | 907 | 4.120963 | 41.878039 | 51.848655 | 21 |
| Bothy1 | <Null> | 31 | 31 | 285 | 3.092569 | 16.865658 | 20.315416 | 22 |
| Bothy2 | <Null> | 32 | 32 | 275 | 3.070059 | 17.082259 | 20.866245 | 23 |
| Bothy3 | <Null> | 33 | 33 | 221 | 3.01134 | 16.934596 | 20.475388 | 24 |
| Entrance | Campus Administartion and Registrar | 34 | 34 | 6280 | 5.651901 | 129.905898 | 353.689997 | 25 |
| C-Block | Installation | 35 | 35 | 2039 | 19.320446 | 43.445288 | 112.609791 | 3 |
| D-Block | Installation | 36 | 36 | 2219 | 18.569385 | 44.682644 | 122.546085 | 4 |
| Workshop Building | Installation | 37 | 37 | 365 | 9.679098 | 17.98378 | 20.209967 | 8 |
| Laboratory Building | Installation | 38 | 38 | 513 | 15.63462 | 21.288038 | 28.302339 | 9 |
| G+10 Building | Installation | 39 | 39 | 710 | 36.107284 | 31.066792 | 59.370492 | 14 |

**Appendix 8**: LOD1 Model extrusion command from the Mean height value of building feature

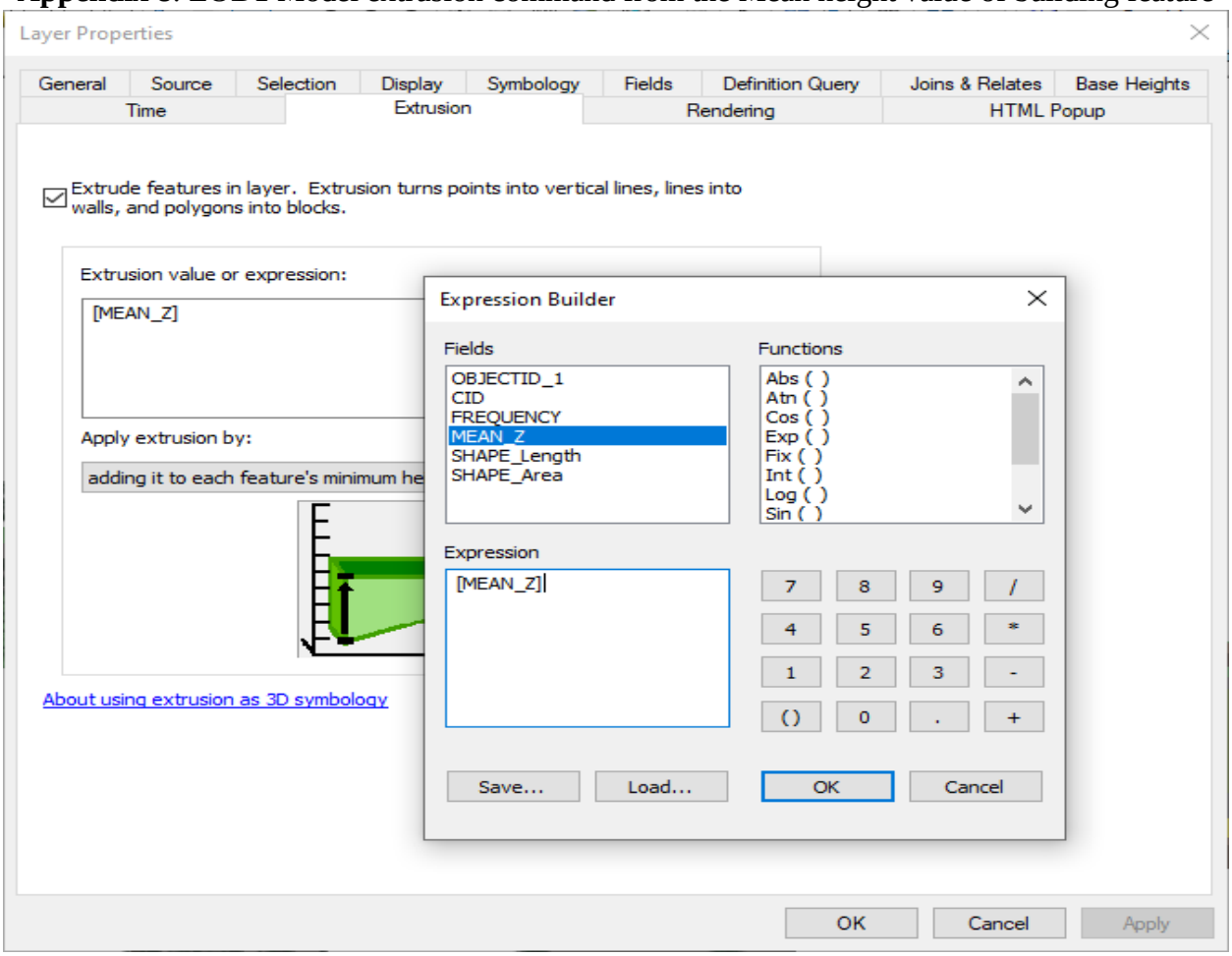


**Appendix 9**: TerraScan Macro command used for classification photogrammetric point clouds

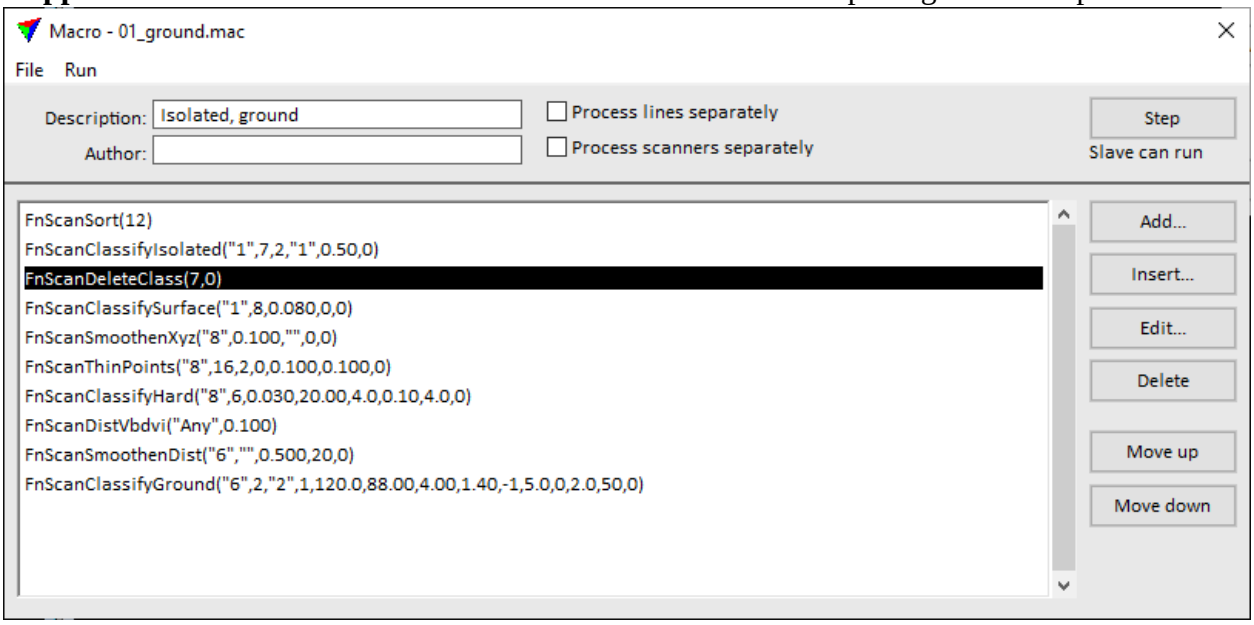

**Appendix 10**: Overlay between reconstructed building model and classified points; Slant view (Top), Section view(bottom)

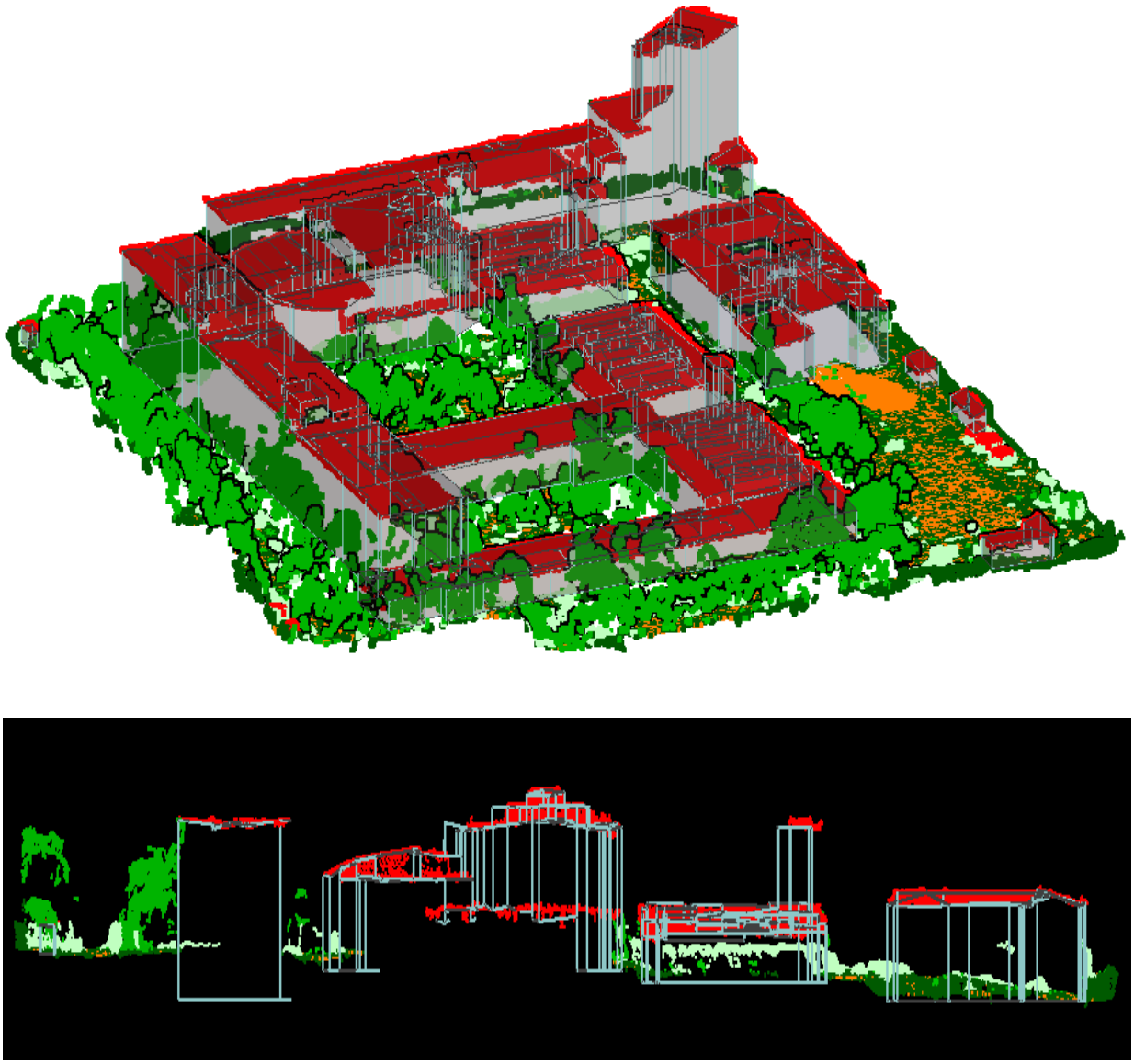

**Appendix 11**: The defined parameters used for building vectorization (Terrascan software)

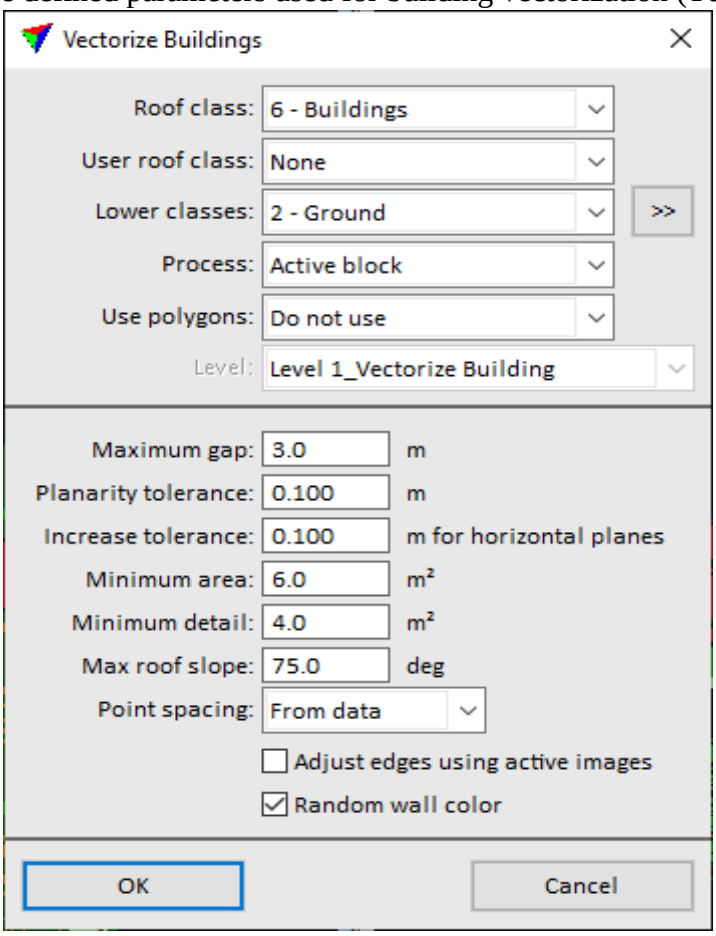

**Appendix 12**: Constituent element of AAiT campus database

**Appendix 13**: Model visualization and information retrieval process